PAUL SCHERRER INSTITUT

PSI

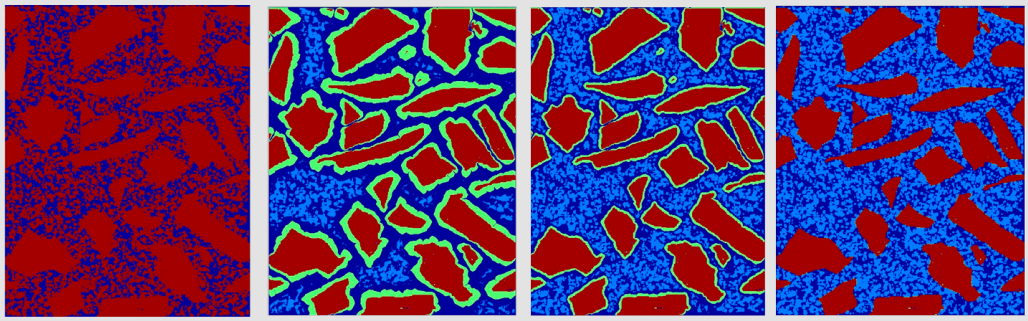

Progress Report 2016

Laboratory for Waste Management :: Nuclear Energy and Safety Department

Cover

Dissolution and precipitation processes at the pore-level explained by combination of lattice Boltzmann method, kinetic rates and classical nucleation theory. The simulations were performed in a 300 mm x 700 mm domain. From left to right: initial system consisting of celestite grains (red) in open porosity (violet); reacted system at different degree of supersaturation SI=3.8, SI=4.0, SI=4.2. In accordance to experiments, the model predicts different proportions of barite precipitated via heterogeneous nucleation (green rims around celestite grains) and homogeneous nucleation (blue domains).

PAUL SCHERRER INSTITUT

PSI

Progress Report 2016

Laboratory for Waste Management
Nuclear Energy and Safety Department

See also our web-page
http://www.psi.ch/les/

Preface

The mission of the Laboratory for Waste Management (LES) is to carry out a comprehensive research and development (R&D) programme in support of Swiss radioactive waste disposal options. In particular, the aim is to be one of the world-leading laboratories in the fields of geochemistry of disposal systems and transport mechanisms of radionuclides, including geochemical retardation and immobilisation.

The laboratory serves an important national role by supporting the Swiss Federal Government and Nagra in their tasks to safely dispose of radioactive wastes from medical, industrial and research applications as well as from nuclear power plants. The research activities cover fundamental aspects of repository geochemistry, chemistry and physics of radionuclides at geological interfaces, and radionuclide transport and retardation in geological and technical barriers. The work performed is a balanced combination of experimental activities in dedicated laboratories for handling radioactive isotopes, field experiments and modelling. The work is directed towards repository implementation and the results find their application in comprehensive performance assessments carried out by Nagra. In particular, a major priority for LES for the next decade will be to contribute to the progress of the Swiss Sectoral Plan for Geological Waste Disposal (Sachplan geologische Tiefen-lagerung).

This report summarises the activities and results achieved in 2016. It gives a detailed overview of research projects, personnel management, national and international collaboration and individual contributions on the work progress achieved in the four research groups.

We gratefully acknowledge the support of our work by the institute's management and by Nagra.

Table of Contents

1 OVERVIEW

S.V. Churakov

1.1 Introduction

The progress made in the Laboratory for Waste Management (LES) over the period from January 1st, 2016 to December 31th, 2016 is summarized in the first part of the report. The detailed descriptions of the main activities carried out in the individual groups are provided in chapters 2 to 5 and are either predominantly "experimental" or predominantly "modelling" in their nature. However, most of the projects are multidisciplinary and require strong interactions between groups and individual group members from both experimental and modelling sides.

1.2 General

The site selection process for geological disposal of radioactive waste in Switzerland, the so called Sectoral Plan (SGT), is ongoing. Potential disposal sites for High (HLW) and Low/Intermediate Level Waste (L/ILW) have been proposed for further investigations. All these regions are located in the Opalinus clay formation. The documentation submitted for Stage 2 of the SGT plan has been under review by the Federal Nuclear Safety Inspectorate (ENSI) since January 2015. Several requests for additional documentation have been formulated by ENSI in 2016. Members of LES have been involved in Nagra working groups answering regulator's requests and providing supplementary documentation. According to the current planning, it is expected that the Federal Government will take a decision on the finalisation of Stage 2 of the SGT by the end of 2017/beginning 2018 and will announce the formal start of Stage 3. The goal of Stage 3 is to select one disposal site for each repository type and to submit a General Licence Application (RBG) for these sites later on.

The research portfolio of LES has been evaluated and adapted for the long-term needs of Stage 3 of the SGT and the following RBG. Main research activities are focused on filling missing gaps in experimental data and models for sorption of redox sensitive elements and experimental confirmation of chemical analogy arguments used in Provisional Safety Analysis (PSA). Experimental diffusion studies and transport modelling are aimed at testing the transferability of the sorption models derived from experiments on dispersed systems to repository conditions, e.g. compacted rocks. Reactive transport simulations and complementary experiments are performed to evaluate the long-term evolution of repository *in situ* conditions and the interaction between repository barriers causing an alteration of their retention and transport properties. Special attention is paid to understanding the role of heterogeneities in a cementitious repository due to spatial and temporal variation of waste reactivity and degradation rates. These aspects have important implications for minimisation of detrimental effects of organics degradation and metal corrosion on repository safety. LES' long-term goal is to maintain state-of-the-art functionality of key models and datasets for safety analysis, including sorption, diffusion and thermodynamics. This can only be achieved by active research in selected strategic areas.

In the last two years the LES team has been particularly successful in attracting competitive funding for PhD and postdoc fellowships from the EU-HORIZON 2020 programme, the Swiss National Science Foundation and other non-Nagra funding agencies. These projects broaden our research competence, bring new expertise, help us to stay competitive with other research groups and last but not least contribute to the knowledge transfer in the field of geological waste disposal. Recruitment of PhD students and postdoctoral fellows is a challenging process, which needs a careful evaluation of candidates. In total, six new PhD and two postdoc positions have become available in 2015-2016. Four PhD positions were successfully filled. One PhD and one postdoc position remain open.

Two new PhD projects have started in 2016 within the EURATOM international research programme "Cement-based materials, properties, evolution, barrier functions (CEBAMA)" (H2020-NFRP-2014/2015, http://www.cebama.eu/). The subprojects hosted at LES will focus on the reactivity of the cementitious barriers in the repository near-field and the retention of dose-determining nuclides in a cement matrix.

LES continues its participation in the Horizon2020 collaborative project "Sustainable network for independent technical expertise (SITEX-II, 2015-2017, www.sitexproject.eu). The overall objective of this project is to ensure a sustainable capability of developing and coordinating joint and harmonized activities related to the independent technical expertise in the field of safety of geological disposal of radioactive waste. Further, LES provides an in-kind contribution to the development of the programme document of the EURATOM Horizon 2020 Joint Programme on Radioactive Waste Disposal (JOPRAD, http://www.joprad.eu).

A collaborative Swiss National Science Foundation (SNSF)-Sinergia project "COTHERM" (Combined hydrological, geochemical and geophysical modelling of geothermal systems) with ETHZ as the leading partner has been successfully completed. The main outcome of the project was the validation of the modelling concepts and thermodynamic data used in simulations for geological disposal against other natural systems. A follow-up project COTHERM-II has been started in 2016. Within the postdoc subproject hosted at LES, a novel reactive transport simulation approach for two-phase fluid transport with volatiles partitioning is being developed for the simulation of boiling geothermal systems. This model could also be applied in future simulations of two-phase fluid transport in a geological repository.

Within the collaborative project funded by the German Ministry of Education and Finances (BMBF) "Thermodynamik und Speziation von Actiniden bei höheren Temperaturen" (ThermAc) a thermodynamic database for actinides at non-ambient temperatures will be developed.

Several SNSF-funded PhD projects have been started in 2016. The project: "Thermodynamic and spectroscopic studies of Fe and S speciation in cement" is aimed at understanding the effect of Fe and S on the stability of C-S-H phases in cement systems (collaboration with B. Lothenbach, EMPA). In the project: "Sorption of thallium to illite and birnessite and its impact on thallium solubility in soils" the applicability of the sorption model for radionuclides developed at LES will be tested in natural systems related to environmental pollution (collaboration with Dr. A. Voegelin, Eawag). An SNSF-funded PhD project "Dissolution, growth and ion uptake at phyllosilicate surfaces: Coupling atomistic interactions at the mineral-water interface with a kinetic Monte Carlo model" aims to describe ion uptake by clay minerals via adsorption and structural incorporation at an atomistic level. Finally, an SNSF project "Transport of sorbed species in clays" will investigate the mobility of ions adsorbed on the surface of clay minerals.

A multi-institutional three year SNSF-project "Effect of aluminum on C-S-H structure, stability and solubility" has been approved (EMPA(Lead)-PSI-EPFL). The postdoc fellow to be hosted by PSI is expected to start in 2018. The goal of the PSI hosted subproject will be to further improve the in-house solid-solution model for calcium silicate hydrates. Within a new SNSF-Sinergia project: "Alkali-silica reaction in concrete." (EMPA(Lead)-PSI-EPFL), a postdoc fellow will work on the development of a synchrotron-based technique for micro-diffraction studies of phases produced by alkali-silica reactions. Such a technique is indispensable for the characterisation of mineral phases formed at cement-clay interfaces at repository relevant conditions.

In the framework of a cross-department initiative supported by the PSI Directorate (CROSS-PSI) a postdoc project "Cryo-microspectroscopy at the microXAS beamline for the investigation of redox- and radiation-sensitive samples"" (R. Dähn, D. Grolimund, A. Voegelin) will develop a cryo-stabilisation approach for the spectroscopic characterisation of redox sensitive elements.

Further two-years funding were secured for the continuation of the "Carbon-14" Swissnuclear Project 2017-2018. Development and testing phase have been accomplished during the past four years and first measurements with the active materials have started in 2016. The collaborative EU FP7 project CAST "Carbon-14 Source Term" is ongoing, and will be finalised in 2017.

LES actively maintains collaboration with national and international research institutes in the field of waste management and environmental research. The main multi- and ateral co-operations with external institutions and universities are summarized in Table 1.1.

Ongoing PhD and postdoc projects hosted at LES are listed below:

Y. Chen (PhD student): "Retardation of low-molecular weight organic compounds in clay". Start date: March 2013 (Funding: Nagra/PSI).

L. Hax Damiani (PhD student): "Modelling transport across reactive interfaces with the Nernst-Planck approach" Start date: January 2016 (Funding: EU).

A. Keri (PhD student): "Shedding light on metal adsorption processes on clay minerals inferred from atomistic simulations and X-ray Absorption Spectroscopy." Start date: January 2015 (Funding: SNSF)

Ph. Krejci (PhD student): "Multispecies cation transport in compacted clays." Start date: December 2016 (Funding: SNSF).

A. Mancini (PhD student): "Thermodynamic and spectroscopic investigations of the Fe and S speciation in anoxic cementitious systems." Start date: April 2016 (Funding: SNSF).

L. Nedyalkova (PhD student): "A structural and thermodynamic study of the intercalation of selenium(IV), selenium(-II), sulfur(-II) and I(-I) in AFm-phases." Start date: January 2016 (Funding: EU).

R. Schliemann (PhD student): "Dissolution, growth and ion uptake at phyllosilicate surfaces: Coupling atomistic interactions at the mineral-water interface with a kinetic Monte Carlo model." Start date: July 2016 (Funding: SNSF).

S. Wick (PhD student): "Sorption of thallium on illite and birnessite and its impact on thallium solubility in soils." Start date: April 2016 (Funding: SNSF).

C. Wigger (PhD student): "Anion accessibility in low porosity argillaceous rocks (ANPOR)" Start date: February 2014 (Funding: NWMO, Canada).

Dr. A. Yapparova (postdoc): "COTHERM2 – Combined hydrological, geochemical and geophysical modelling of geo-THERMal systems II" Start date: April 2016 (Funding: SNSF).

Dr. D. Miron (postdoc): "Thermodynamik und Speziation von Aktiniden bei höheren Temperaturen." Start date: April 2016 (Funding: BMBF, Germany).

Dr. B. Cvetković (postdoc): "Development of C-14 AMS-based analytical methods for the identification and quantification of C-14 labeled dissolved and volatile organic compounds." Start date: November 2013 (Funding: Swissnuclear).

Dr. B. Thien has completed a four years postdoctoral project on "Combined hydrological, geochemical and geophysical modelling of geothermal systems." He moved to ETH-Zurich to continue his research on characterization and modelling of geothermal alteration in Islandic basalts. To maintain the existing collaboration Dr. Thien continued working at LES approximately 1 day per week until the middle of 2016.

Several personnel and organisational changes took place in the reporting year. One of the most experienced chemists, the former leader of the thermodynamic modelling group Dr. Urs Berner has retired after more than 35 years employment at PSI. During all these years he was actively involved in the evaluation of thermodynamic data and the development of thermodynamic models for minerals. Thanks to this work the thermodynamic databases for disposal relevant nuclides have reached a high-quality mature state. One of his latest contributions was the development of a solid-solution model for smectites which could be later extended for the description of illite/smectites mixed layers. This model has become a standard for reactive transport simulations at LES and is currently one of the most advanced models used in the simulations of cement-clay interactions. Future support of thermodynamic data and solubility limits calculations for the SGT will be conducted by Dr. W. Hummel and Dr. T. Thoenen.

Table 1.1: National and international co-operations.

Co-operations
Nagra Major financial contribution Various technical working groups
Multinational 7th EU FP (CAST) EURATOM HORIZON2020 (SITEX-II) EURATOM HORIZON2020 (CEBAMA) Mont Terri Project (Diffusion-Retardation, Clay Cement Interaction)
Universities Bern*, Switzerland (mineralogy, petrography, water chemistry, C-14 AMS) EPFL, Switzerland (cement systems) Dijon, France (molecular modelling) ETHZ*, Switzerland (GEMS) Hiroshima University, Japan (cement-clay interaction) Tokyo Institute of Technology, Japan (clay systems) Xi'an Jiaotong University, China (clay systems)
Research Centres CEA*, France (near- and far-field) EMPA*, Switzerland (cement) IFR, HZDR*, Germany (XAS, TRLFS) INE, KIT*, Germany (near- and far-field TRLFS) SCK/CEN, Belgium (clay systems) UFZ*, Germany (reactive transport, clay systems) *formal co-operation agreements

Future research activities at LES will focus strongly on the long-term geochemical evolution of *in situ* repository conditions. These activities need a close interplay between thermodynamic modelling and system-specific applications. In this context a reorganisation of LES took place by which the "Reactive Transport Modelling" group was enforced with experts in geochemical modelling from the former "Thermodynamics Group" (Dr. Curti and Dr. D.A. Kulik). The cement and clay systems groups were enhanced by a specialist in clay minerals and pore water chemistry (Dr. T. Thoenen) and a specialist in thermodynamic databases (Dr. W. Hummel). The diffusion group was strengthened with a modelling expert (Dr. W. Pfingsten). The new laboratory structure is presented in Fig. 1.1.

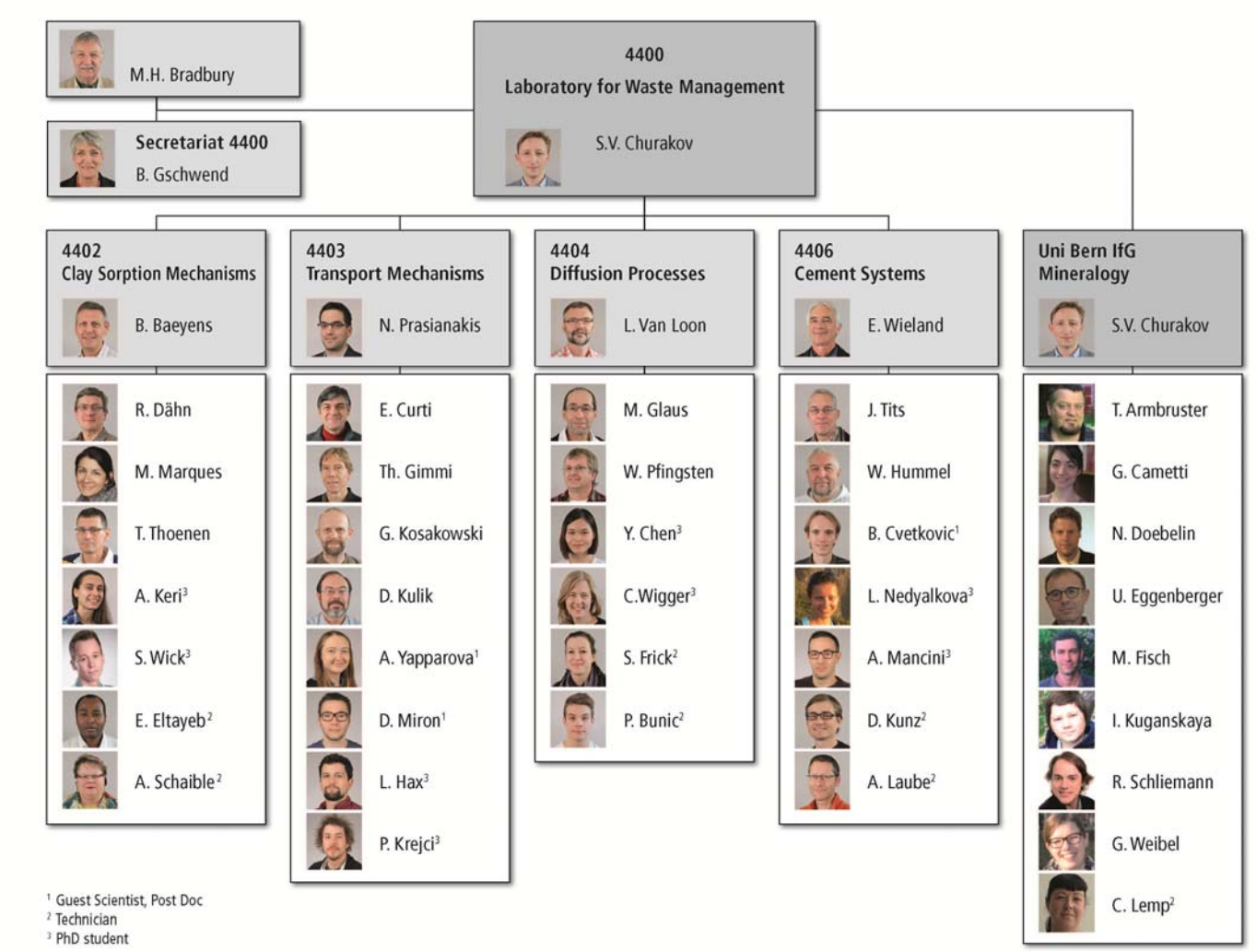

Fig. 1.1: Organisation chart of LES (End 2016).

From July 2016 LES comprises four research groups located at PSI. The fifth research group located at the "Institute for Geological Sciences" strengthens the collaboration with the University of Bern in the field of mineral dissolution kinetics, structural studies of high porous materials and X-ray diffraction based structure characterisation. This expertise nicely complements the LES traditional modelling and experimental capabilities. The group in Bern is also included in the organization chart in Fig. 1.1.

Dr. J. Poonoosamy has successfully defended her PhD thesis "Experimental benchmarks for verification and validation of reactive transport codes" at the University of Bern (Defence date: February 18, 2016). She continues her research carreer at UFZ in Jülich, Germany.

Y. Chen has submitted her PhD thesis "Retardation of low-molecular weight organic compounds in clays" for external review (Prof. Thorsten Schäfer, KIT/University of Berlin). The defence is planned for March 2017 at the University of Bern.

Habilitation of PD. Dr. G. Kosakowski has been accepted at the University of Bern.

1.3 Sectoral plan for deep geological disposal

In the reporting year LES has started the preparation for Stage 3 of the SGT. Main activities include experimental studies and literature reviews aimed at filling remaining gaps in the sorption- and thermodynamic databases (TD-SDB), as well as a better understanding of long-term chemical and transport processes in the repository nearfield. The development of a TD-SDB for montmorillonite and illite has been completed. Two Nagra Technical Reports (NTB) were submitted for peer review. The revised reports are planned to be published in 2017. The methodology for parameter evaluation in SDB for host rocks based on the bottom-up approach was further tested. In particular the approach for a consistent consideration of sorption competition phenomena and variation of pore water chemistry during the long-term repository evolution was revised. A final NTB summarising the effect of competitive

sorption for bentonite MX-80 and Opalinus Clay was submitted for external review. Local heterogeneities in a cementitious repository may have significant impact on the degradation rate of organic matter, metal corrosion and stability of cement phases. Scoping thermodynamic calculations were performed to evaluate the geochemical evolution of a cementitious repository taking into account different waste inventories, cement compositions and overall water content. A Nagra Working Report (NAB) summarising the results was submitted to Nagra. It will provide a basis for the optimisation of waste type partitioning and a more detailed evaluation on the repository evolution. A further state-of-the-art report on transport properties of pure clay minerals was finalised and submitted for external evaluation.

On request of Nagra a literature study was carried out to determine the effect of cementitious materials on the dissolution kinetics of high-level radioactive waste to be disposed of in the planned repositories. The goal was to assess, to which extent the use of cement-based mortars in the vicinity of the waste could reduce its "lifetime" of disposal casks under disposal conditions. This topic is relevant in view of specific requirements by the Swiss authorities concerning the maximum possible depth of a high-level waste repository and possible alternative disposal concepts. This review covered studies both on cement-glass and on cement-spent fuel (SF) interactions. According to the available data, the lifetime of vitrified waste forms in the planned SF/HLW repository would be reduced under the influence of cement materials by 2-3 orders of magnitude. On the other hand, the measured fractional release rates of ^{90}Sr clearly indicate that cement pore waters have no measurable effect on the dissolution kinetics of spent UO_2 fuel.

1.4 Repository near field

1.4.1 Repository chemistry

In the framework of a long-term project on the mobility and chemical speciation of radionuclides in reprocessed high-level radioactive waste (HLW), micro X-ray absorption and micro X-ray fluorescence measurements were carried out systematically at synchrotron facilities on simulated HLW glass leached in aqueous solution during last 12 years. The studies performed in the past included characterisation of Cs, Ni and Ce (as a surrogate of Pu). In the current year the behaviour of Se was investigated. The measured XANES spectra indicate that Se was incorporated as oxidized Se(IV) during glass fabrication in the investigated borosilicate glass. After 12 years of leaching in aqueous solution within a steel vessel, no change in the redox state of Se could be detected; the XANES spectra are nearly identical to those measured in the fresh glass and closely resemble the reference spectrum of Na_2SeO_3. The distribution of Se in the sample is rather heterogeneous. An increase in Se concentration toward the glass-solution interface suggests a mobilization of Se dissolved from the glass (section 2.2.5).

Literature review and evaluation of thermodynamic data for safety relevant nuclides is an on-going activity. The data for ^{36}Cl and ^{108m}Ag were evaluated in 2016. Both ^{36}Cl and ^{108m}Ag are formed by neutron activation of ^{35}Cl and ^{107}Ag. Both parent nuclides have a comparable cross section. The distribution of the isotopes in the waste follows very different patterns, however. While ^{36}Cl is present nearly in each waste form in trace quantities (e.g. in nuclear spent fuel, in reactor steel and other metallic compounds), almost the entire inventory of ^{108m}Ag is concentrated in a single waste form, namely in the control rods of pressurized light-water reactors composed of Ag-In-Cd alloy. The long-term behaviour in a geological repository and upper limits for the solubility of these elements in pore water were evaluated based on the data for the total inventory and the stability of the host phases (4.2.1)

1.4.2 Clay systems

The 2SPNE SC/CE sorption model provides the basis for the evaluation of the TD-SDB in Stage 3 of the SGT. The model is capable of describing the competition effects and has been proven to be successful in "blind predictions" of radionuclide sorption in poly-mineral clay rocks based on reference data for clay minerals. The sorption is described by a set of well-defined parameters such as surface site capacities and complexation reactions. It is further assumed that competing elements are adsorbed at the same sites. The validity of these assumptions and the nature of sorption sites need to be understood by spectroscopic studies and atomistic simulations. The data for some relevant elements (e.g. Pb) are not available and need to be determined experimentally. It also remains unclear whether Fe^{II} is involved in the sorption competition with divalent radionuclides.

To fill the missing gaps in the TD-SDB databases the sorption of Pb on montmorillonite and illite was investigated in batch sorption experiments and the model parameters for the 2SPNE SC/CE were evaluated (section 3.2.1). Further, the applicability of the 2SPNE SC/CE model for Zn sorption on illite was extended to highly acidic conditions pH 2-4. The best description of the full sorption edge was obtained by introducing two cation exchange sites (instead of one) with different affinity and capacity. In this model the high affinity cation exchange sites contribute only 1 % of the CEC. Existence of these sites needs to be

confirmed by spectroscopic investigations (section 3.2.2.1).

The validity of the "bottom-up" modelling methodology was further investigated on Boda Claystone and Opalinus Clay. Zn was used as an analogue for the other divalent elements because of a better signal-to-noise ratio in the Fe-containing clay systems compared to Ni and Co. A good agreement between the measured and the predicted sorption values was found in the lower concentration range. However, the blind predictions clearly underpredict Zn sorption at higher Zn concentrations of the equilibrium solution. The same trend was observed in previous studies with Co and Ni using both rocks types. The analysis of the EXAFS spectra indicates that the deviation between predicted sorption isotherm and measured Zn uptake can be explained by precipitation of Zn layered double hydroxides (LDH) and/or Zn phyllosilicates (section 3.2.2.2).

Sorption studies of Np^{IV}/Np^{V} on montmorillonite in absence and in presence of ferrous iron under reducing conditions are on-going. The experiments performed in electrochemical cells demonstrate that Fe(II) plays an important role in the reduction of Np^{V} to Np^{IV}. EXAFS spectroscopy indicates that Np^{IV} forms strongly bound complexes to the Fe sites in clay. The exact nature of the final surface complex is still not clear. Under reducing conditions and in the presence of ferrous iron NpO_2^+ sorbed on montmorillonite becomes fully reduced to Np^{IV}. Previous Np sorption experiments performed in the presence of dissolved Fe^{II}, yet, under anoxic conditions (without electrochemical control of the redox potential), showed only a partial reduction of Np^{V} (3.2.3).

Thallium (Tl) is a highly toxic trace metal. In a natural environment, Tl exists as a monovalent and trivalent cation. Tl^+ has a similar ionic radius as K^+, and thus can substitute K^+ in a wide range of K-bearing minerals. In soils and sediments, Tl^+ uptake by the clay mineral illite has long been considered to be a key retention mechanism. The experimental and modelling approach developed for studies of radionuclides is now applied to characterize Tl mobility in a natural environment (SNSF-funded project; Collaboration with Dr. A. Voegelin, Eawag). The sorption behaviour of Tl^+ on pure illite (Illite du Puy) is currently being investigated by batch experiments. First results confirm that Tl^+ uptake by illite is highly specific and exhibits similar trends known for Cs^+. Further insight into Tl uptake by illite and Tl speciation in soils will be obtained by a combined analysis of macroscopic sorption experiments and soil extractions, and EXAFS studies. The obtained results and their model based interpretation will contribute to an improved quantitative and mechanistic understanding of the solubility, mobility and bioavailability of Tl in soils. (section 3.2.4).

Atomistic simulations of mineral fluid interfaces provide direct insight into the molecular mechanism of ion adsorption by mineral surfaces and dissolution/precipitation of minerals. Combining such simulations with spectroscopic studies can help to obtain a quantitative interpretation of spectroscopic observations both in terms of structural and compositional information. In the first year of the SNSF founded PhD project "*Detailed understanding of metal adsorption on clay minerals obtained by combining atomistic simulations and X-ray absorption spectroscopy*", the structural environment of Fe^{II} and Fe^{III} incorporated in Milos montmorillonite has successfully been modelled. The theoretical EXAFS and XANES spectra were calculated on the basis of the molecular dynamics trajectories. Comparison with experimental observations indicates that structural iron in montmorillonite is present as Fe^{III} and is equally partitioned between the cis- and trans-octahedral positions (3.3.1).

In the past years, synchrotron-based micro-focused X-ray fluorescence (micro-XRF), X-ray absorption spectroscopy (micro-XAS) and X-ray diffraction (micro-XRD) have become the standard tools for characterisation of trace elements (contaminants and nutrients) in heterogeneous environmental samples such as soils, sediments, rocks or organic materials. A high photon flux density is needed for trace element studies. This may induce radiation damage, including structural changes in host phases or direct changes in the oxidation state of the studied elements. Sample cooling helps to prevent or strongly attenuate such radiation-induced damage. A 2-years research proposal for the development of cryo-spectroscopic techniques for studying redox- and radiation-sensitive samples has been submitted in collaboration with the microXAS beamline of the Swiss Light Source (SLS) and Eawag. The project proposal has received funding from the PSI and Eawag directorates via the PSI CROSS initiative. (section 3.3.2)

1.4.3 Cement systems

The geological repository for low- and intermediate-level waste (L/ILW) will contain large quantities of degradable materials such as cement, gravel (quartz), spent ion exchange resins, low-molecular-weight (LMW) organics, steel, and some plastic and rubber containing materials. These materials are not in equilibrium with cement pore water and will react with different rates depending on the local *in situ* conditions. The degradation of organics results in the

formation of gaseous compounds: CH_4 and CO_2. Metal corrosion leads to the release of H_2. The dissolution of gravel gives rise to the release of $SiO_xH_{y,aq}$ species which react with portlandite to produce calcium silicate hydrates (C-S-H) or with C-S-H phases with high Ca/Si ratios to reduce the Ca/Si ratio. Uptake of alkalis by C-S-H phases reduces the pH of the pore water. The degradation of organics, the dissolution of quartz and the metal corrosion are water-consuming reactions, whereas the carbonation of portlandite and C-S-H are water-releasing reactions. It is therefore important to understand how partitioning of waste materials and local heterogeneities may affect the gas production rates and the evolution of *in situ* conditions in a cementitious repository. In a first step thermodynamic modelling of the temporal evolution of selected waste sorts was carried out using the GEM software. The core thermodynamic data were taken from the Nagra/PSI database and a solid solution based description of the cement system was applied. Several scenarios were considered including possible meta-stability of mineral phases (e.g. zeolites). In all considered simulation scenarios the system was closed for non-volatile components except water whereas gases were allowed to leave the system.

The thermodynamic modelling allows the behaviour and reactivity of the various waste sorts of interest to be predicted over the entire lifetime of the repository. The simulations reveal a very different behaviour of the different waste sorts which strongly depends on the type and amount of materials in the waste sort and the recipe used for the solidifying concrete. The simulations further suggest that the main factors controlling the reaction progress and the reaction rates are the water content and the *in situ* pH condition in the repository.

The repository evolution is mainly controlled by the degradation of organic materials and, as a consequence, continuous production of CH_4 and CO_2. The released CO_2 reacts with C-S-H to form calcite and amorphous silica. Portlandite, which is present in the initial mix, is converted into C-S-H phases due to a continuous reaction with a silica source, i.e. gravel (quartz). In the early ageing phase of the waste sorts, the phase assemblage of the cement matrix is composed of C-S-H phases, Al/Fe-Si hydrogarnet, ettringite, monocarbonate, strätlingite and hydro-talcite. In the long run, however, the cement phases are thermodynamically unstable and calcite, dolomite, magnetite, siderite, pyrite and, in the absence of zeolites, kaolinite and gibbsite are formed. The pH value of the porewater is controlled by the evolution of C-S-H phases or zeolites, respectively, which are the main sink for the alkalis in the system. Simulations predict that pH drops below 10.5 depending on the inventory of the waste sort after a few thousand to a few ten thousand years. At this point, the H_2 production rate due to steel corrosion accelerates by a factor of 100 compared to the high pH ($\geq$ 10.5) conditions. As a consequence, the amount of remaining steel and iron is completely corroded within a few thousand years (section 4.2.2).

The current simulation setup assumes a homogeneous distribution of waste materials and a fast intermixing of the reaction products. These assumptions may not hold locally in a real heterogeneous system resulting in local acceleration or deceleration of the reaction progress and need to be further investigated with reactive transport simulations.

Experimental studies of C-14 release due to corrosion of activated steel demonstrate that C-14 is mainly liberated in form of low molecular weight organic (LMW) molecules. These may be chemically unstable under the hyperalkaline, reducing conditions of a cement-based repository. In case of a complete thermodynamic equilibrium LMW molecules should decompose into the thermodynamically most stable species CO_2 (g), HCO_3^-, CO_3^{2-} and CH_4. Complete thermodynamic equilibrium is rarely achieved in the C-H-O system at moderate temperatures. It is therefore not obvious what kind of organic compounds might predominate in the repository. In a first step the chemical stability of acetate and formate in hyperalkaline, anoxic conditions relevant to a cement-based repository was evaluated. The four month long degradation experiments showed that acetate is stable in alkaline conditions and that the presence of Fe as a catalyst does not increase the decomposition rate at room temperature. The stability tests with ^{13}C labelled formate were performed in pure water at moderately elevated temperatures (150°C – 200°C) to verify decomposition rates published in the literature. Preliminary data from samples taken between 1 day and 2 weeks reaction time do not show decomposition of formate suggesting that the molecule is more stable than expected on the basis of literature data. Thus, the preliminary in-house experimental data indicate that complete thermodynamic equilibrium is not achieved in the C-H-O system under conditions relevant to a cement-based repository (section 4.3.2).

^{79}Se (half-life $3.27 \cdot 10^5$ years) is an important redox-sensitive, dose-determining radionuclide in an L/ILW repository. The selenium speciation under oxidizing conditions is dominated by SeO_4^{2-} and SeO_3^{2-} while in alkaline, reducing conditions, Se(0), HSe^- and poly-selenide species are stable along with SeO_3^{2-}. Sorption data for Se(-II) in a cementitious environment are still lacking. Studies in the framework of the German collaborative project "Immorad" enabled us to gain

valuable insight into Se(-II) retention in cementitious systems. Batch sorption experiments with HSe^- onto various cement phases in the presence of hydrazine (N_2H_4) as a reducing agent showed that the anionic HSe^- species sorbs preferentially onto AFm phases. The study further showed that the affinity of the AFm phases for HSe^- is strongly dependent on the type of interlayer anions. For example, HSe^- was strongly retained by monosulfate (AFm-SO_4) and hemi-carbonate (AFm-OH-CO_3) while a weak retention was observed on Friedel's salt (AFm-Cl_2) and mono-carbonate (AFm-CO_3). XAS investigations further revealed that sorbed HSe^- was mainly intercalated in the AFm interlayers upon sorption onto AFm-OH-CO_3 whereas HSe^- sorbed onto AFm-CO_3 was bound mainly on the positively charged sites of the outer surfaces. In January 2016 a PhD project was started in the framework of the Horizon-2020 EU project "CEBAMA". In this PhD project the thermodynamic stability of AFm phases containing Se, S and I in various redox states and the formation of solid solutions of Se, S and I bearing AFm endmembers with AFm-CO_3 and AFm-OH-CO_3 will be explored. The aim is to develop thermodynamic solid solution models capable of simulating the uptake of Se(IV), Se(-II) and I(-I) by AFm phases (section 4.4)

Application of so called "low pH-cements" is foreseen to reduce an alteration of the host rocks by the pH plume. Such low pH-cements are known to have a higher Al content compared to conventional OPC cements. The influence of Al on the stability of C-S-H and radionuclide retention capacity is purely constrained. The thermodynamic description of Al incorporation in C-S-H is essential for the long-term prediction of the *in situ* condition in the repository. Complementary to the experimental studies the thermodynamics of Al-Si exchange in C-S-H was investigated by theoretical atomistic calculations. Consistent with the spectroscopic observations, the result suggests that Al substitutes in the C-S-H structure for Si in bridging tetrahedral sites. Further, the effect of pH and background electrolyte was evaluated. The theoretically predicted uptake of Al by C-S-H was found to be in good agreement with the experimental data (section 2.5.5)

The parameterisation of the C-S-H multi-site (sub-lattice) solid solution thermodynamic model based on available solubility data is ongoing in collaboration with EMPA. Na and K end-members were included in the model. The results point to the need for considering alternative Ca ion substitutions on the bridging tetrahedral structural sites in C-S-H. This model will be further developed in the framework of a forthcoming SNSF project "Effect of aluminum on C-S-H structure, stability and solubility (CASH-2)"

1.4.4 Interfacial processes

^{14}C is a potentially major contributor to the dose release from a cementitious L/ILW repository. ^{14}C is released into the repository near- and far field by the anoxic corrosion of activated steel. To date the chemical form of ^{14}C-bearing compounds – probably small organic molecules - is only poorly known. The ^{14}C project in LES aims at filling this knowledge-gap. The research programme comprises corrosion experiments with activated steel and subsequent identification and quantification of the ^{14}C-bearing compounds in the gas and liquid phase using compound-specific ^{14}C accelerator mass spectrometry (^{14}C AMS). The project has been started in 2012. One of the major challenges in measuring the ^{14}C release is the low corrosion rates of steel under repository relevant conditions and accordingly the very low concentration of the released ^{14}C-bearing compounds. The typical concentrations are far below the detection limit of conventional off-the-shelf analytical techniques. During the last 4 years an experimental setup and analytical protocols for compound-specific analysis have been developed and tested nearly from scratch. In 2016, further development and testing of a sampling and analytical protocol for gaseous compounds was undertaken. The current system is installed in the Hot Laboratory of PSI. It consists of a gas chromatographic column for the separation of the gaseous organic compounds coupled to a combustion reactor which oxidizes the released organic compounds to CO_2, and a CO_2 sampling system. The sampling process is controlled by a thermal conductivity detector which monitors the CO_2 production in the combustion reactor (section 4.3.1.1).

In May 2016 the corrosion experiment was started with segments of an activated steel nut. Samples were collected after 1, 15, 29, 93 days of reaction time. The samples were analysed to determine short chain carboxylic acids, hydrocarbons and total organic carbon (all ^{12}C compounds). Additionally, the ^{14}C activity of the liquid samples was determined by LSC and accelerator mass spectrometry (^{14}C AMS). Up to now, both the concentrations of the ^{12}C and ^{14}C-bearing compounds are still below or, at best, close to the detection limit of the available analytical techniques. In particular, the concentration of the ^{14}C-containing carboxylic acids is still below the detection limit of the compound-specific ^{14}C AMS method (section 4.3.1.2).

The Cement Interaction (CI) experiment, started nearly a decade ago at the Mont Terri underground laboratory, is dedicated to investigation of mineral reactions and porosity changes at the interface of Opalinus Clay (OPA) with different cements and concretes. Currently available samples provide

information about the cement-clay interaction after 2.2, 5 and 8 years of reaction time. In 2016 we have started reactive transport simulations of the CI experiment with an updated thermodynamic database for cement phases using the OpenGeoSys-GEM framework. Compared to previous simulations updated models for clay minerals and zeolites, improved reaction kinetics and an alternative approach for cation exchange modelling were considered (section 2.2.2).

The 1D radial symmetric modelling domain includes the interface between OPA and Ordinary Portland Cement (OPC), and the interface between OPA and a low pH cement (ESDRED). The model considers the kinetically controlled hydration of clinker phases and the kinetic control of relatively slowly reacting phases like clays and zeolites. The modelling results for the hydration of OPC qualitatively agree with the most experimental findings. The calculated mineralogical profile across the OPC/OPA interface after 5 years of reaction time indicates that small amounts of portlandite and M-S-H precipitated directly at the interface. The modelling further predicts an ettringite precipitation front that extends to about 2 mm from the interface into OPC. This front originates from the in-diffusion of sulphur species from the Opalinus Clay.

The same thermodynamic models were used to simulate the evolution of the ESDRED/OPA interface. However the model failed to reproduce the ESDRED hydration. Experimentally observed reaction fronts could not be matched without increasing the diffusion coefficients to very high values. Possible reasons for the mismatch are missing thermodynamic data and kinetic parameters.

In-house laboratory studies of the cement-montmorillonite interaction clearly demonstrate a drop of the water filled porosity at the interface after 1 year of reaction time, leading to a reduction of the diffusivity by at least one order of magnitude. The precipitation leading to the partial clogging of the interfaces takes place on a sub-millimeter scale or even less, thus making the experimental characterisation of these processes very challenging. In particular we had to apply neutron radiography measurements to monitor the water content across the interface in a nondestructive way. The reactions leading to changes of porosity and transport properties of the interface at such a small scale can't be described accurately with continuum models and need a pore scale description of dissolution/precipitation reactions with an explicit consideration of solids, porosity and mineral-fluid interfaces. To this end we have developed a Lattice-Boltzmann reactive transport model which takes into account the pore scale precipitation by both homogeneous nucleation and epitaxial growth. This model was applied to reproduce the experimental reactive transport benchmark, involving precipitation of $BaSO_4$ in a granular porous medium developed in the framework of the PhD thesis of J. Poonoosamy. The model successfully reproduces the mineral precipitation pattern observed in the experiments. Resulting permeability and diffusivity can be measured at any given time and is directly linked to the change in pore topology. This type of simulations will be further applied to the modelling of cement-clay interaction processes (section 2.3.2).

1.5 Repository far field

Mineral surfaces often exert an electrostatic potential imposed by structural or surface charge due to isomorphic substitutions or protonation/de-protonation of surface –OH groups. This electrostatic potential affects the partitioning and transport of ions in the pore space. Negatively charged surfaces of clay minerals attract cations at the mineral surface and repel anions. These processes are manifested experimentally in an enhanced diffusion of cations and a reduction of the anion accessible porosity. The diffusion of ions is governed by different driving forces, viz. the concentration gradients of the species in the different pore domains and gradients of electrostatic potential maintaining the charge neutrality in the system. The balance between these driving forces and the magnitude of the resulting fluxes in compacted clay systems is not *a priori* clear from theory. The recent work has been devoted to the investigation of the coupled diffusion of charged species in argillaceous media.

As a first step the coupled ion transport across an uncharged diffusion barrier was investigated using a commercial polymeric filtration membrane. A gradient of HNO_3 concentrations was superimposed to two adjacent solution reservoirs containing the same initial concentrations of a background electrolyte (e.g. KCl). The subsequent diffusive flux of HNO_3 and the different mobility of the ions involved (H^+, NO_3^-) induce temporal changes of the concentrations of the background electrolyte in both solution reservoirs. The electrochemical coupling thus causes a diffusive flux of ions against the concentration gradient. These experimental results are used to test the electrochemical coupled code being developed within the CEBAMA project for future investigations of cement-clay interactions. The preliminary results demonstrate that the system behaviour can be accurately described using a Nernst-Planck formalism (section 2.4.5 and 5.2).

For neutral and positively charged chemical species, the whole porosity of a clay rock (ε_{tot}) is available for transport. Anions, however, are partially excluded from the near surface domains and the corresponding transport porosity, i.e. the anion accessible porosity (ε_{an}), is smaller than the total porosity. Ionic strength of the electrolyte solution in charged porous media is the main factor controlling the extent of anion exclusion. In general, increasing the ionic strength of the pore solution leads to an increase in the anion accessible porosity. The effect is ion specific, however. Recent experiments with OPA have shown that Ca^{2+} and Cs^{+} are more effective in shielding the electric charge than Na^{+} (section 5.5)

Sorption measurements in compacted smectites remain an unresolved technical challenge. The membrane-confined type of diffusion cell developed in our laboratory does not withstand the high swelling pressure of montmorillonite confined to bulk-dry densities larger than 1000 kg m^{-3}. Two strategies were followed to find a remedy: (i) the use of a mechanical support for the membrane and (ii) the use of synthetic smectites exhibiting less swelling properties. Test experiments with a mechanically reinforced cell using Co^{2+} in-diffusion in compacted illite demonstrated that the same results were obtained as in setups without the mechanical support (a perforated titanium plate). However, the titanium plate added a further diffusive resistance, which leads to increased uncertainties in the determination of capacity factors from in-diffusion experiments. A limited applicability of this setup has thus to be accepted. For the second option two different synthetic clays from the smectite group are currently under investigation: (i) Barasym SSM-100 Syn-1 available from the Clay Minerals Society, which is characterised by having mostly tetrahedral charges (thus having rather properties of a Beidellite), and (ii) a synthetic iron-free montmorillonite having mostly octahedral charges. Both clays exert weaker swelling pressures than Milos montmorillonite. Through-diffusion experiments using simultaneously HTO, $^{22}Na^{+}$ and $^{36}Cl^{-}$ as tracers were carried out at different concentrations of the background electrolyte ($NaClO_4$), in order to clarify whether these clays exhibit similar surface diffusion properties towards cations and exclusion properties towards anions as Milos montmorillonite. The results showed a clear dependence of the effective diffusion coefficients of the charged tracers on the concentrations of the background electrolyte, while these remained unaffected in the case of HTO. The use of these clays appears to be a promising option. Further, the combined sorption and diffusion studies using strongly sorbing elements such as Eu(III) and Th(IV) were continued. One of the key questions to be resolved in the scope of these experiments is whether the pH dependence of sorption ("sorption edge") in compacted clay minerals is the same as obtained from measurements in dilute suspensions. (section 5.2)

The DR-A field experiment in the Mont Terri Underground Rock Laboratory aims at investigating the effects of an increased ionic strength in solution on transport of sorbing and non-sorbing tracers. An increase of the ionic strength provokes changes in the population of cation adsorbed at different sorption sites (notably on exchange sites) and possibly results in an increase of pore space accessibile for anions. The ion transport in the system was modelled with 3 different setups: 1) Donnan equilibrium between the reservoir (external) solution and the clay pore (internal) solution; 2) cation exchange (where the ions on the exchanger neutralize all surface charges) and 3) combination of both Donnan equilibrium and cation exchange. The simulations were performed for the expected background solution concentrations of the DR-A experiment using a three-site ion exchange model with fixed selectivities and capacities obtained from the literature. The measured quantities available for comparison are the total concentrations of cations (sum of aqueous and sorbed species) in the rock.

The parameter variation study shows that the total ion concentration in the sample depends on the surface charges in a non-linear way and demonstrates that the ion exchange selectivities, which are generally obtained from modelling assuming ion exchange only, should not be applied directly to a mixed ion exchange/Donnan equilibrium. Instead, the ion exchange selectivities must be considered as parameters that are conditional to the type of model used for the data evaluation.

Recent sorption studies indicate that trivalent cations (e.g. Eu, Am, …) not only show competitive sorption behaviour among each other but also compete with divalent cations (e.g. Co, Ni, Zn, …). Such sorption competition can enhance the mobility of cationic radionuclides in the near- and far-field. To evaluate the effect of sorption competition on radionuclide transport, a hypothetical case was used which considers an instantaneous release of the total inventory of trivalent cations in solution at the "canister-bentonite-interface" 10,000 years after repository closure. A general mechanistic sorption model for such a system is still under development and preliminary model parameters were applied in transport simulations. A total source concentration of trivalent cations (Eu, Am, …) was represented by Eu at a constant concentration level (10^{-5} M) entering the bentonite at the interface with the (corroded) canister. The total concentration of competing divalent cations was assumed to be $3 \cdot 10^{-5}$ M. The preliminary simulations suggest that sorption competition leads to

nearly one order of magnitude increase in the concentration of mobile trivalent Eu 0.9 m away from the canister surface. Quantitative predictions of radionuclide transport can only be done after the release of the revised sorption model for di- and trivalent cations (section 2.2.3).

To date, performance assessment is based on the assumption that the transport of ^{14}C-bearing organic compounds occurs without retardation. The uncertainties and conservativism in the dose calculations can be reduced if a weak retardation of ^{14}C-carrying molecules could be robustly demonstrated. The interactions of organic model compounds with clay are still poorly characterized, but are presumed to be rather weak. In 2016 the focus was on the transport behaviour of selected organic molecules in Opalinus Clay and in mockup systems composed of illite and kaolinite mimicking Opalinus Clay. Accompanying experiments with HTO and $^{36}Cl^-$ were used to characterise the porosity and the geometric properties of the media. Similar to the concepts used in the sorption studies of cations, the retardation factors obtained from studies with pure materials could be used to estimate the retardation in a composite material. Such a component additivity approach was tested against various illite-kaolinite mixtures and Opalinus Clay. In the case of anionic tracers such as $^{36}Cl^-$ and aliphatic carboxylates, as well as for all tested alcohols the calculated retardation factor were in agreement with the directly measured values within the experimental uncertainties. In the case of the hydroxylated carboxylates, which show relatively strong retardation via site specific interaction, the predicted retardation values were substantially overestimating the measured ones (section 5.4)

1.6 Model development and code benchmarking

The benchmarking and verification of reactive transport coupled codes is an on-going activity. A benchmarking exercise on the modelling of Cs-diffusion through Opalinus Clay was conducted. The co-operation with the Helmholtz Centre for Environmental Research, UFZ Leipzig in the area of reactive transport (OpenGeosys-GEM coupled code) was focused on the application of a new multi-component, multi-phase solver in radioactive waste packages. With this approach the influence of the availability of water on gas production over time can be estimated.

Within the Sinergia COTHERM-II project (Coordinator: T. Driesner, ETHZ) reactive transport modelling has also been applied in research relevant to geothermal energy. The CSMP++GEM code was used to simulate two phase flow in Icelandic geothermal systems (postdoc A. Yapparova).

The GEM Software (GEMS) development has been continued and a Memorandum on Cooperation between PSI/NES/LES and ETHZ/IG/GEG, was brought forward in 2016. The cooperation aims at improving the GEMS numerical kernel by incorporating the accurate, stable and fast GEM-based numerical algorithms from the Reaktoro code framework for modelling chemically reactive systems. A major progress in that direction has been achieved recently with the implementation of the new xLMA (extended law of mass action) method.

Within the ThermAc project the new software tools ThermoMatch and the ThermoFun library for easily sharing thermodynamic and other data with GEMS and other codes have been developed. Further, an internally consistent thermodynamic database for aqueous species in the Na-K-Al-Si-O-H-Cl was finalised and made available for use.

2 TRANSPORT MECHANISMS

N.I. Prasianakis, S.V. Churakov, E. Curti, Th. Gimmi, A. Jakob, G. Kosakowski, D. Kulik, W. Pfingsten, K. Nakarai (guest professor), J. Poonoosamy (PhD student), A. Shafizadeh (PhD student), D. Miron (postdoc), A. Yapparova (postdoc), L. Hax Damiani, (PhD student), Ph. Krejci (PhD student), J. Fernandes (exchange PhD student), M. Gatchet (master student), A. Ong (bachelor student)

2.1 Introduction

In 2016, the main research activities of the transport mechanisms group were devoted to developing competences for the forthcoming Sectoral Plan for Deep Geological Disposal (SGT) Stage 3. Few selected activities were also related to finalizing documentation for the SGT-Stage 2.

The LES lab and groups have been restructured. Dr. E. Curti will strengthen the Transport Mechanisms Group in the area of pore-level characterization and modelling and will continue research relevant to dissolution of spent fuel and vitrified waste. Dr. D. Kulik joined also the Transport Mechanisms Group and existing synergies will be further strengthened in the area of thermodynamics modelling and coupled codes for predicting the geochemical evolution of the repository. The focus of research was on radionuclide mobility in the near field, on multiscale description and upscaling of transport mechanisms, on benchmarking and application of state-of-the art coupled codes and on thermodynamic modelling and databases tools. Dr. W. Pfingsten has joined the Diffusion Processes Group (Group leader L. Van Loon) to further support the design and modelling of laboratory experimental studies.

To test the models at the field scale, group members are involved in the experimental activities in the Underground Rock Laboratory at Mont Terri test site. The DR-A experiment investigates the effects of chemical perturbations in the porewater on ion's transport in Opalinus Clay. The Cement Interaction experiment at Mont Terri explores the interaction between Opalinus Clay and three different types of concrete. The experiment has been modelled using the OpenGeoSys-GEM coupled code and the first quantitative comparison of mineralogical profiles produced by reactive transport models was conducted.

The diffusion and sorption competition of Eu and other trivalent cations in bentonite has been investigated. The simulations were performed based on the 2SPNE CE/SC sorption model and using simplified a K_D sorption approach to investigate applicability of the simplified system description.

In connection with ENSI's request to Nagra concerning alternative disposal scenarios for high-level waste at a larger depth repository, a literature study was carried out to evaluate the possible effect of cementitious environment on the dissolution kinetics of glassified high-level radioactive waste and spent fuel, to be disposed in the planned repositories.

Transport Mechanisms Group maintains and develops modelling capabilities for multiscale transport simulation from the atomistic scale to the pore-level and to the repository scale. These modelling tools are applied to support experimental data and field observations with well justified physical models based on fundamental process understanding. Incorporation of aluminum in C-S-H phases was investigated by ab initio molecular dynamics. The combination of the characterization of reactive transport experiments along with the application of classical nucleation theory shed light on the pore level mechanisms of precipitation. The model takes into account both homogeneous and heterogeneous precipitation at the pore-level using the lattice Boltzmann framework in diffusive as well as in advective regimes. This level of description allows the direct measurement of the effect of geochemical reactions on the effective diffusivity and permeability of the domain of interest, thus improving the modelling and predictive capability by bridging results across different scales.

Mineralogical and porosity changes at interfaces of technical barriers (cement-clay) have an effect on diffusion processes. The ability of reactive transport codes to predict clogging processes can be enhanced and verified via specifically designed laboratory experiments. Prof. Kenichiro Nakarai from Hiroshima University conducted part of his research at PSI and investigated the effect of admixtures to the clay on porosity reduction with help of neutron radiography measurements.

The benchmarking and verification of reactive transport coupled codes is an on-going activity in the Transport Mechanisms Group. A benchmarking exercise on modelling Cs diffusion through Opalinus clay was conducted. The co-operation with the Center for Environmental Research, UFZ Leipzig in the area of reactive transport (OpenGeosys-GEM coupled code) was focused on the application of a new multi-component, multi-phase solver to radioactive waste packages. The influence of the availability of water on gas production over time could be estimated.

LES participates in the HORIZON 2020 Collaborative Project "Cement-based materials, properties, evolution, barrier functions" (CEBAMA) with 2 PhD projects. In 2016, the PhD project "Modelling

transport across reactive interfaces" (L.H. Damiani) has started. This project aims at improving the modelling of clay-cement interaction taking into account electrochemical diffusion processes in the presence of charged mineral surfaces (Nernst-Planck equations).

Within the postdoc project of A. Yapparova, reactive transport modelling has been also applied in research relevant to geothermal energy. The CSMP++GEM code was used to simulate the two phase flow in Icelandic geothermal systems in the context of Sinergia COTHERM-2 project (Coordinator: T. Driesner, ETHZ).

GEM Software (GEMS) development has been continued and a Memorandum on Cooperation between PSI/NES/LES and ETHZ/IG/GEG, was brought forward in 2016. The cooperation aims at improving the GEMS numerical kernel by incorporating the stable and fast GEM-based numerical algorithms from the Reaktoro code framework for modelling chemically reactive systems (LEAL et al., 2016a,b). A major progress in that direction has been achieved recently with implementation of the new xLMA (extended law of mass action) method (Leal et al., 2016b) into the *IPAction* algorithm, completing the work started at LES in 2015.

In the framework of the ThermAc project (postdoc D. Miron) new software tools ThermoMatch and ThermoFun libraries for sharing thermodynamic and other data with GEMS and other codes have been developed. An internally consistent thermodynamic database for aqueous species in the Na-K-Al-Si-O-H-Cl system was finalized. Further, an internally consistent data set for the (Ba,Sr,Ra)SO_4-H_2O system was obtained for an extended temperature range (0-350^{o}C). The impact of the addition of Sr to barite with respect to Ra retention at various temperatures was investigated.

2.2 Sectoral Plan for Deep Geological Disposal

2.2.1 Sensitivity simulations for the DR-A field experiment in the Mont Terri Underground Rock Laboratory

The DR-A field experiment in the Mont Terri Underground Rock Laboratory aims at investigating the effects of an increased ionic strength in solution on transport of sorbing and non-sorbing tracers. The experiment provided a rich data set that sheds light on the influence of the ionic strength of the pore solution on sorption and coupled diffusion of anions and cations. An increase of the ionic strength provokes changes in the cation populations on the different sorption sites (notably on exchange sites) and possibly increases the accessibility of the pore space to anions. This coupled process was modelled using a modified version of Flotran which includes the model of Donnan equilibrium between the reservoir (external) solution and the clay pore (internal) solution. It was possible to describe the observations considering only ion exchange reactions (where the ions on the exchanger neutralize all surface charges) or only a Donnan distribution of anions and cations (where all surface charges remain ionised), or various intermediate situations.

The measured quantities available from the experiment for simulations are the total concentrations of cations (sum of aqueous and sorbed species) in the rock. The calculations show that, such total cation concentrations depend on the net negative surface charge in a non-linear way. For several species the total concentration shows a minimum between the limiting cases (full ion exchange and full Donnan), as shown in Fig. 2.1. The results were obtained for the expected background solution concentrations of the DR-A experiment using a three-site ion exchange model with fixed selectivities and capacities reported in the literature. Whereas for monovalent cations (and especially for K^+) the total rock concentrations are largest for the full ion exchange equilibrium and smallest for the full Donnan equilibrium, a minimum for an intermediate case is obtained for divalent cations. The reason for this behaviour is the strong increase of divalent cations concentration in the aqueous phase when approaching the full Donnan equilibrium, which more than outweighs the decrease in sorbed concentrations when moving away from ion exchange. In other words, it is related to the difference in "effective" selectivities between an ion exchange and a Donnan equilibrium. This behaviour makes global optimization of the model parameters to experimental data very challenging. Fig. 2.2 shows the sum of the cation and anion contents in the different phases and total concentration in the rock. Clearly, a Donnan representation leads to a lower sum of the cation concentrations per rock, and to the lower sum of the anion concentrations.

These sensitivity studies help to improve the understanding the processes in the experimental system and to determine the parameters that best describe *in situ* conditions in the DR-A experiment. Furthermore, the simulation results make clear that the use of ion exchange selectivities, which are generally obtained from experimental data by assuming ion exchange only, should not be applied directly in models using both ion exchange and Donnan equilibrium approaches. In this sense, ion exchange selectivities must be considered as parameters that are conditional on the type of model used to derive them.

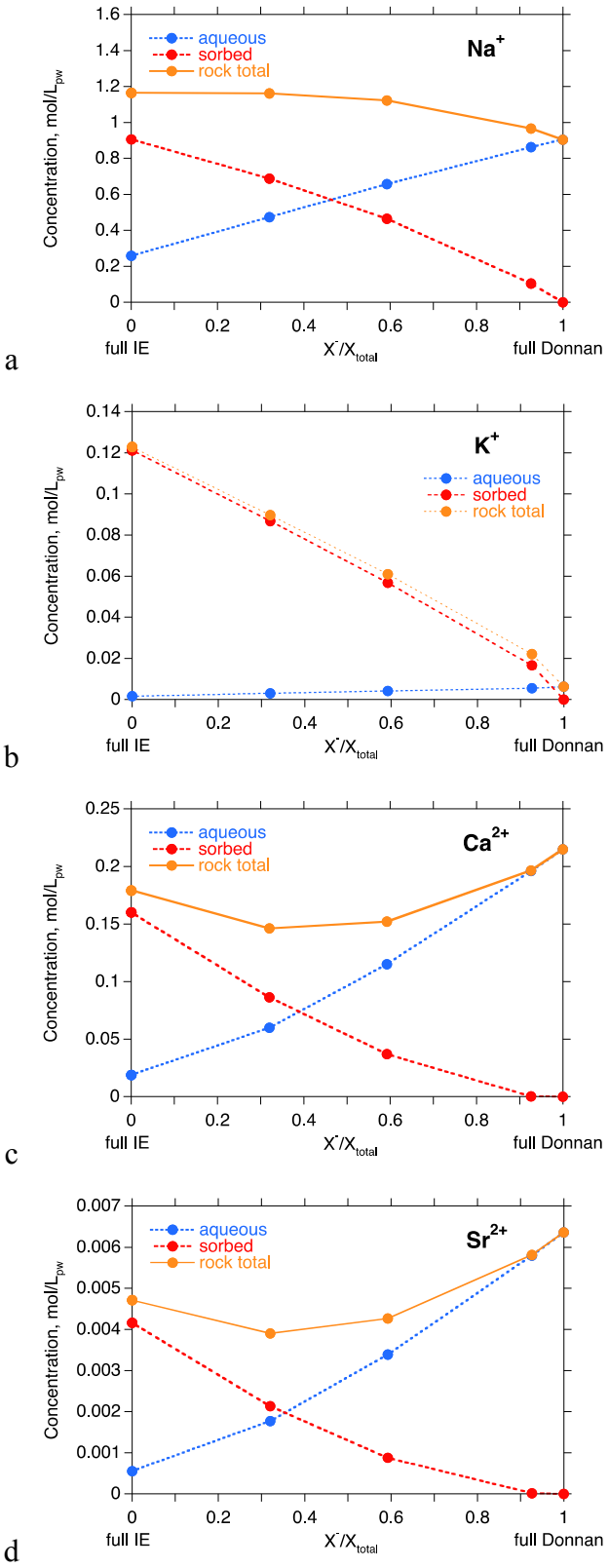

Fig. 2.1: Aqueous concentrations, sorbed concentrations and total concentrations in the rock (all expressed in moles per litre of pore water) for monovalent (a, b) and divalent (c, d) cations as a function of net negative surface charge X^- in simulations considering combined ion exchange and Donnan behaviour.

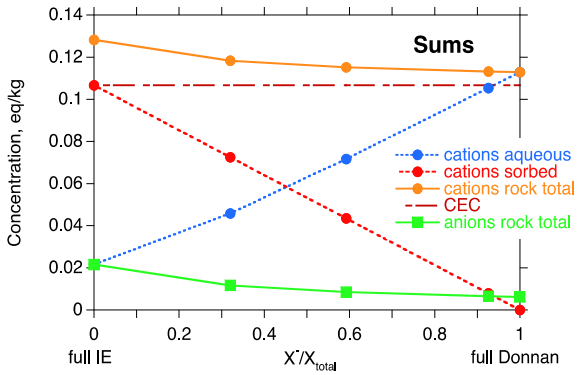

Fig. 2.2: Sum of aqueous cation concentrations, of sorbed cation concentrations, of total cation concentrations in the rock and of total anion concentrations in the rock (in equivalents per kg of solid) as a function of net negative surface charge X^- in simulations considering combined ion exchange and Donnan equilibrium. The cation exchange concentration CEC (= X_{total}) is also shown.

2.2.2 Mont Terri Cement Interaction (CI) Experiment

The ongoing Cement Interaction (CI) experiment is dedicated to investigations of mineral reactions and porosity changes at the interface of Opalinus Clay with different cements and concretes. Two boreholes in the Opalinus Clay formation were filled with sections of three different types of concrete and bentonite. The samples are available after 2.2, 5 and 8 years of interaction. The chemical and mineralogical composition of the reacted interfaces is well characterized (JENNI et al. 2014, DAUZERES et al. 2015) but a thorough quantitative comparison with reactive transport simulations have not been performed so far.

The reactive transport simulations of the CI experiment were started with an updated thermodynamic database for cement phases using OpenGeoSys-GEM framework. Compared to previous simulations updated models for clay minerals and zeolites, improved reaction kinetics and an alternative approach for the description of cation exchange processes were considered. The model domain was represented in form of a 1D radial symmetric model (Fig. 2.3) which takes the center of the borehole as origin and extend to a distance of 1.4 m into the Opalinus Clay.

The modelling setups include the interface between Opalinus Clay (OPA) and Ordinary Portland Cement (OPC), and the interface between OPA and low pH cement (ESDRED). The models consider the kinetically controlled hydration of clinker phases and kinetic control of relatively slowly reacting phases like clays and zeolites.

The models reproduce quite well the hydration of OPC in terms of pore water composition and cement phase assembly as measured by Lothenbach (LOTHENBACH et al, 2011). In addition the OPC model also qualitatively agrees with most experimental findings. A calculated mineralogical profile across the OPC/Opalinus Clay interface after 5 years of reaction time is shown in Fig. 2.4. There are no obvious changes in the Opalinus Clay except minor quantities of portlandite and M-S-H directly at the interface. The main striking feature in the OPC is an ettringite precipitation front that extends to about 2 mm from the interface and originates from in-diffusion of sulphur species from the Opalinus Clay. As a high pH zone extends into the Opalinus Clay, no carbonation in OPC is observed.

The same thermodynamic models were used to simulate the evolution of the ESDRED/OPA interface. It was not possible, however, to reproduce the ESDRED hydration. This might be caused by an inappropriate thermodynamic representation of the low-pH-cement phases. Current modelling work concentrates on testing setups with a new C-S-H model that was designed for blended cements and includes alkali and Al uptake of C-S-H.

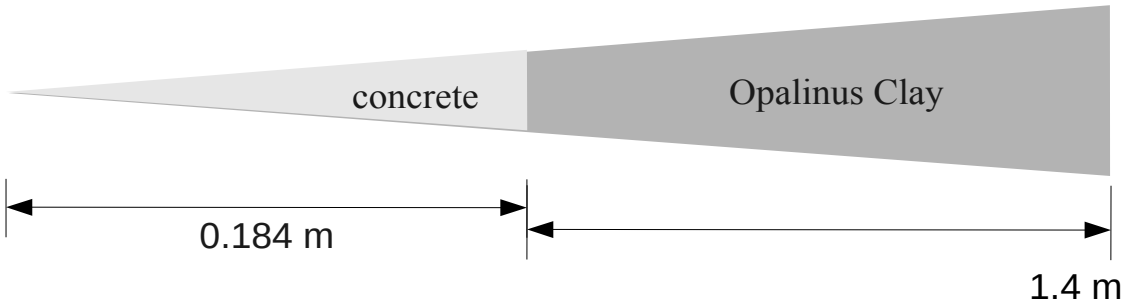

Fig. 2.3: Conceptual 1D radial symmetric representation of the CI Experiment.

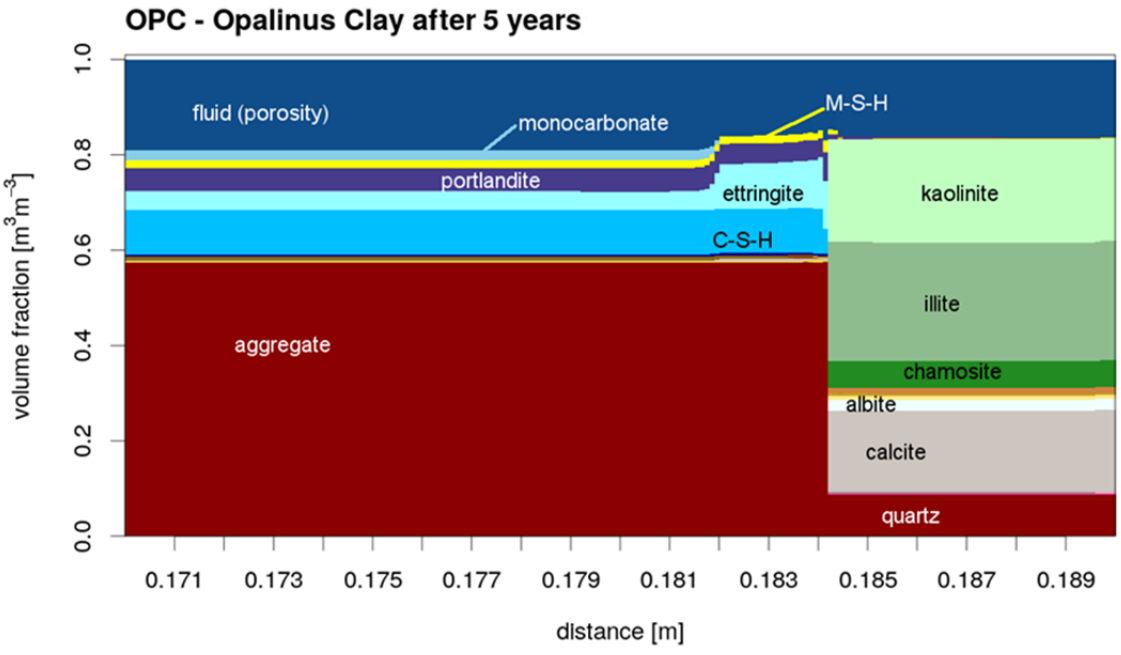

Fig. 2.4: Calculated mineralogical profile across the OPC/Opalinus Clay interface after 5 years of interaction time.

2.2.3 Eu and other trivalent cation diffusion and sorption competition in bentonite

According to recent sorption studies trivalent cations (e.g. Eu, Am, …) may not only show competitive sorption among each other on sorption sites of montmorillonite and clay, but they may also show "partially" competitive sorption with divalent cations (e.g. Co, Ni, Zn, …), (BAEYENS, pers. comm.). This contrasts to previous studies in dispersed systems where only the competition between the ions of the same valence could be observed. In order to assess the possible sorption competition between tri- and divalent cations and to estimate the concentration of trivalent cations transported from canister into the bentonite barrier and the Opalinus Clay, generic calculations have been performed for diffusion/-sorption of tri- and divalent cations through bentonite. A preliminary model setup considers an instantaneous release of total inventory of trivalent cations in solution at the "canister-bentonite-interface" after 10000 years since the repository closure A cumulative concentration of trivalent cations (Eu, Am, …) was represented by Eu at a constant concentration level (10^{-5} M) entering the bentonite at the interface with the (corroded) canister. The total divalent competing cation concentration was assumed to be $3 \cdot 10^{-5}$ M. The calculated breakthrough curves are shown in Fig. 2.5 in comparison to a non-reactive tracer breakthrough and a K_D sorption model approach for Eu. Eu transport and sorption parameters were set according to the 2SPNE SC/CE sorption model and a K_D value for Eu of 2.8 L/kg for the K_D sorption model approach.

As can be seen, the model without sorption competition predicts the concentration of trivalent Eu at 0.9 m away from the canister surface, 10000y after radionuclide release, to be about one order of magnitude lower than the scenario taking into account the competitive sorption. Therefore, sorption competition may also be important for trivalent cations within the bentonite. More accurate quantitative predictions require a refined set of modelling parameters including individual di- and trivalent cation concentrations and their individual transport and sorption parameters.

2.2.4 The effect of cement on the dissolution of high level waste

In the framework of the Swiss Sectoral Plan toward the realization of a geological repository for radioactive waste (SGT-2), a literature study was carried out to determine the effect of cementitious materials on the dissolution kinetics of high-level radioactive waste and spent fuel to be disposed in the planned repositories.

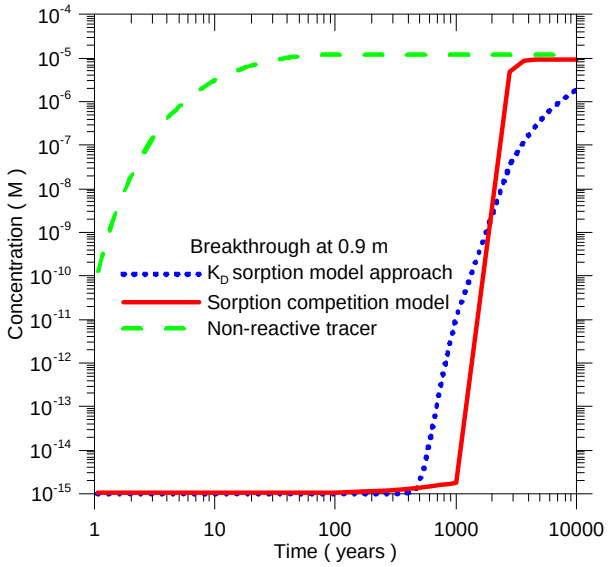

Fig. 2.5: Calculated breakthrough at 0.9 m within bentonite for a trivalent cation represented by Eu using a competitive sorption model approach – sorption competition with divalent cations was assumed - and a K_D sorption model approach. For comparison a non-reactive tracer breakthrough curve is shown.

The goal was to assess, to which extent the use of cement-based mortars in the vicinity of the waste could influence the performance of the multibarrier system. This topic is relevant in view of specific requirements by the Swiss authorities concerning the maximum possible depth of a high-level waste repository and possible alternative disposal scenarios.

2.2.4.1 Glass-cement interactions

In the past few years, several studies focusing on the glass dissolution kinetics in the presence of cement materials and hyperalkaline solution have been published in relation to the disposal programs of U.K., France and particularly Belgium, where high-level waste is foreseen to be encapsulated in a cementitious "supercontainer". The studies were carried out mostly with the same or similar (inactive) reference borosilicate glasses to be used in Switzerland. All experimental data converge, indicating as expected a strong increase in glass dissolution kinetics under highly alkaline conditions. This is not only due to the well-known increase in SiO_2 solubility at high pH, but also due to a change in the composition and transport properties of the amorphous surface layer separating the leaching solution from the non-altered glass surface (GIN et al. 2015). As the pH increases above 11, the passivating surface layer composed of a three-dimensional network of Al and Si tetrahedra dissolves and is replaced by a more permeable layer composed of zeolites and C-S-H phases.

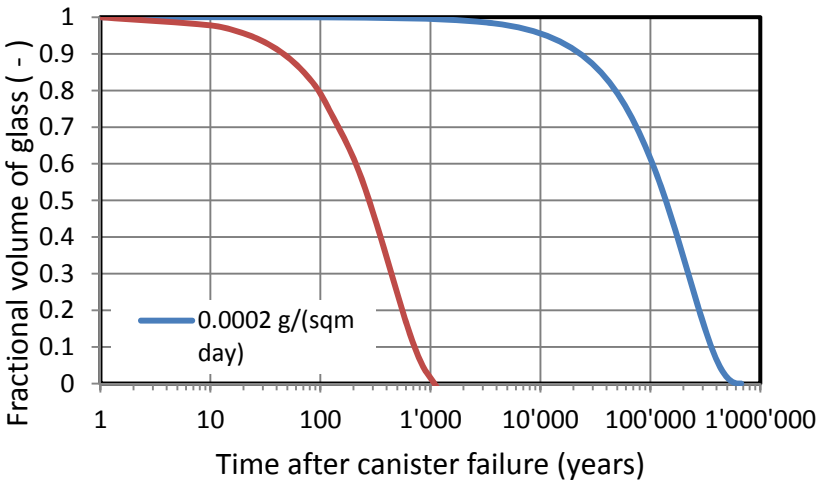

Fig. 2.6: Calculated fractional volumes of AREVA vitrified waste as a function of corrosion time after canister failure, assuming a typical dissolution rate in cement water (red curve, 0.1 g m^{-2} d^{-1}) and in near-neutral reference bentonite pore water (blue curve, 2 x 10^{-4} g m^{-2} d^{-1}).

Based on the available data, the lifetime of vitrified waste forms in the planned SF/HLW repository would be reduced under the influence of cement materials by 2-3 orders of magnitude (Fig. 2.6).

2.2.4.2 Glass spent-fuel interaction

Data on spent fuel dissolution in cement pore water are very scarce and more difficult to interpret than analogous glass corrosion experiments. This is mainly due to the lack of suitable non-sorbing tracer elements (e.g. B and Li in glass), the redox sensitivity of UO_2 dissolution and the technical difficulties when operating with real spent fuel. Careful experiments both under oxidizing and strictly reducing conditions (Ar/H_2 atmosphere) were nevertheless carried out at KIT/INE (e.g. GONZÁLEZ-ROBLES et al. 2015) on spent fuel from the Gösgen nuclear power plant. The measured fractional release rates of ^{90}Sr clearly indicate that cement pore waters have no measurable effect on the dissolution kinetics of spent UO_2 fuel.

2.2.5 Se behavior during aqueous alteration of simulated vitrified HLW

In the framework of a long-lasting project on the mobility and chemical speciation of radionuclides in reprocessed radioactive high-level waste (HLW), micro X-ray absorption and micro X-ray fluorescence measurements are carried out systematically at synchrotron facilities on simulated HLW glass leached in aqueous solution during 12 years. After the investigations of Cs, Ni and Ce (as a surrogate of Pu), the behavior of Se was investigated this year during a beam time granted at the microXAS beamline (SLS). The measured XANES spectra indicate that Se was incorporated as oxidized Se(IV) during glass fabrication in the investigated borosilicate glass (MW glass, from BNFL). After 12 years of leaching in aqueous solution within a steel vessel, no change in the redox state of Se could be detected; the XANES spectra are practically identical to those measured in the fresh glass and closely resemble the reference spectrum of $Na_2Se(IV)O_3$ (Fig. 2.7a).

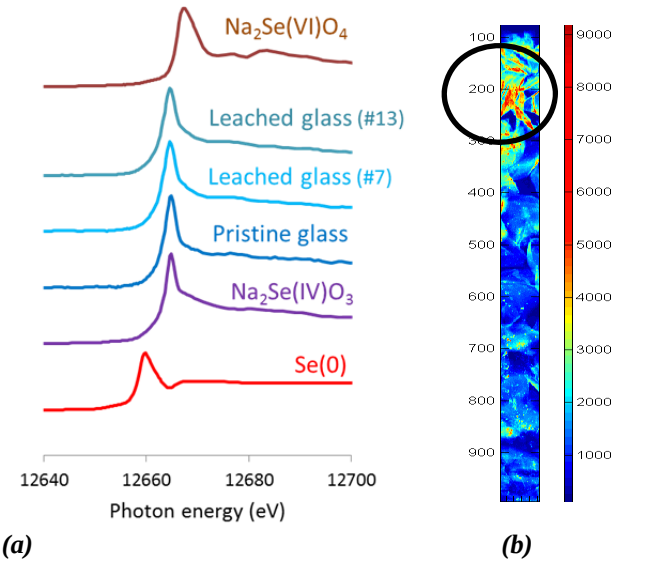

Fig. 2.7: (a) XANES spectra of pristine and leached MW glass compared to spectra of Se(0), Se(IV) and Se(VI) reference compounds. (b) XRF map showing the Se distribution in the leached MW powder sample on a vertical profile ranging from the floor of the vessel (bottom) to the sample-bulk solution interface (top). The left scale gives the position away from bulk solution in µm, the right scale the intensity of Se-K_a fluorescence (detector counts).

A high-resolution Se map encompassing the entire thickness of the powdered glass sample (from the bottom of the vessel to the interface with bulk aqueous solution on the top) shows a quite heterogeneous distribution (with a "hot spot" indicated by the circle) with an increase in Se concentration toward the glass sample-bulk solution interface (Fig. 2.7b). These features suggest a mobilization of Se dissolved from the glass via diffusion toward the bulk solution. The concentration gradient and hot spots are possibly the result of the precipitation of soluble Se(IV) released during the alteration process caused by sample drying.

2.3 Fundamental understanding of transport and sorption mechanisms

2.3.1 Pore-level fundamental understanding of precipitation mechanisms

The mechanisms leading to mineral precipitation in aqueous solution are heavily debated. According to recent studies (GEBAUER et al. 2014) the precipitation of carbonate minerals is initiated through the formation of so-called pre-nucleation clusters, following mechanisms incompatible with those developed earlier in the framework of classical nucleation theory (CNT). In particular, pre-nucleation clusters may have a molecular structure differing from that of the final precipitate. Nevertheless, in a recent publication PRIETO (2014) claimed that the objections put forward by GEBAUER et al. are not valid for sulphate minerals, and provided evidence that CNT is successful in predicting induction times and growth mechanisms for barite in porous media. Specifically, Prieto's model is able to explain the inhibition of precipitation from strongly supersaturated solution when the pore size in the medium decreases.

Based on these arguments, a CNT model was applied to interpret the results of reactive transport experiments performed in our laboratory, in which celestite dissolution and replacement by barite was induced by supplying moderately concentrated $BaCl_2$ solution (0.3 M) into a confined porous medium consisting of a strip of celestite powder embedded in quartz sand (POONOSAMY et al. 2015, 2016). The aim was to predict time and sequence of the observed barite precipitation events and to compare the predictions with the experimental results. Induction times for homogeneous and heterogeneous barite precipitation as a function of pore size, obtained in our model on the basis of CNT are summarized in Fig. 2.8.

For the average pore size of 100 µm the induction times of about 2 minutes and 9 hours were predicted for heterogeneous and homogeneous barite nucleation, respectively (at the upstream celestite-quartz boundary, where a saturation index of ~ 4.0 is calculated).

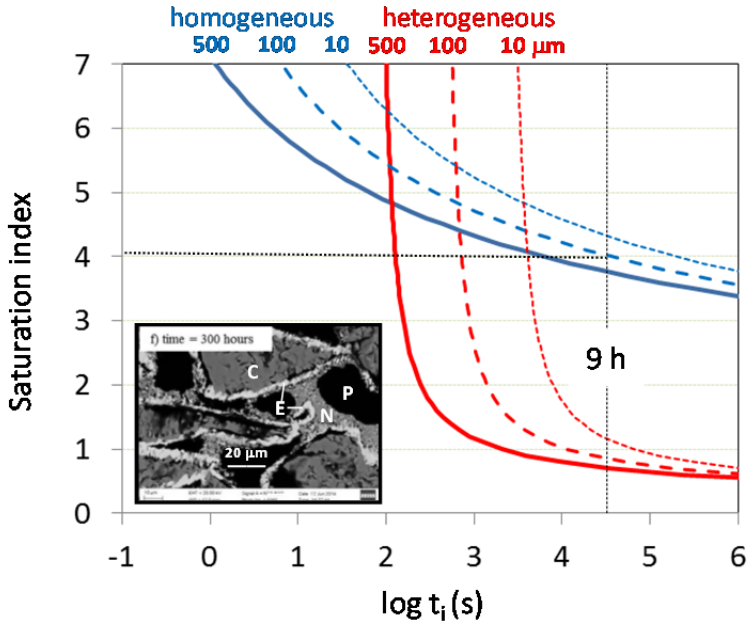

Fig. 2.8: Calculated induction times for homogeneous and heterogeneous barite nucleation as a function of pore size. The dotted black lines indicate the onset of homogeneous nucleation for a solution with saturation index 4 in 100 µm pores at 9 hours. The insert (Fig. 3f in Poonosamy et al. 2016) shows a typical SEM image of the reactive celestite zone 300 h after start of the experiment (C= celestite, N= homogeneously nucleated nano-barite, E= heterogeneously nucleated epitaxial barite, P = unfilled pores).

Whereas the predicted onset of homogeneous nucleation was found to agree with microscopic observations, epitaxially grown barite formed via heterogeneous nucleation (in the form of thin rims coating the celestite grains) apparently started later, in contrast to CNT predictions. This apparent inconsistency was explained by arguing that the detection of the onset of heterogeneous precipitation may have been missed due to the limited resolution of the images. The thickness of the epitaxial rims will be initially in the sub nanometer range and thus not visible in the early stages of rim formation. Moreover, we found independent evidence that heterogeneous barite nucleation preceded homogeneous nucleation of nano-barite: The SEM image shown as insert in Fig. 3.8, taken at 300 h reaction time, clearly shows that the white rim of epitaxial barite (E) surrounding the celestite grains (C) must have formed prior to formation of nano-barite (N) formed via homogeneous nucleation, which partially fills the pores (P).

2.3.2 Pore-level lattice Boltzmann modelling of precipitation processes

The porosity and mineralogical evolution of the technical barriers and their respective interfaces, plays a key role in the performance assessment of a radioactive waste repository. The porosity alterations, due to geochemical reactions, directly affect important processes such as re-saturation times, corrosion rates, or the gas pressure build up within the barriers. At the same time, local transport properties at mineralogical interfaces can be altered, which in turn can affect the intermediate and longer time evolution of the entire barriers. The reactive transport experiment by POONOOSAMY et al. (2015a) in the barite-celestite system highlights the importance of pore scale processes for the geochemical evolution of the system. To tackle the reactive transport phenomena at pore scale we have coupled heterogeneous nucleation and homogeneous nucleation precipitation with mass transport description within the Lattice Boltzmann framework. Classical nucleation theory allowed modelling the sub-micrometer scales and the critical nuclei's formation rate in the bulk solution. The importance of competition between homogeneous and heterogeneous nucleation and the influence of the Saturation Index (SI) are demonstrated in Fig. 2.9. Initial system setup contains a distribution of large and small celestite crystals similar to the reactive transport experiments. Evolution of the system was investigated in a 300x700 µm domain. The results for the barite precipitation in a system with diffusion controlled transport at SI values of 3.8, 4.0 (experimental conditions) and 4.2 are plotted. Green color represents the epitaxially grown barite and light blue the nano-crystalline barite. Thickness of the rims depends on the saturation index. Resulting permeability and diffusivity can be measured at any given state of the evolved system and are directly linked to the change in pore topology.

2.3.3 Modelling of cation transport in clays

The need for a multi-site multi-mobility model for the description of cation transport in clays (e.g., diffuse layer, interlayer, outer-sphere complex, inner-sphere complex, strong site, weak site) is outcome of several laboratory cation diffusion data in various clay samples. A PhD project (Philipp Krejci) on modelling multispecies cation transport in compacted clays has been approved by SNSF. The project started in December 2016 and the capabilities of existing transport codes will be expanded by taking into account variable mobility of sorbed species on different sorption sites.

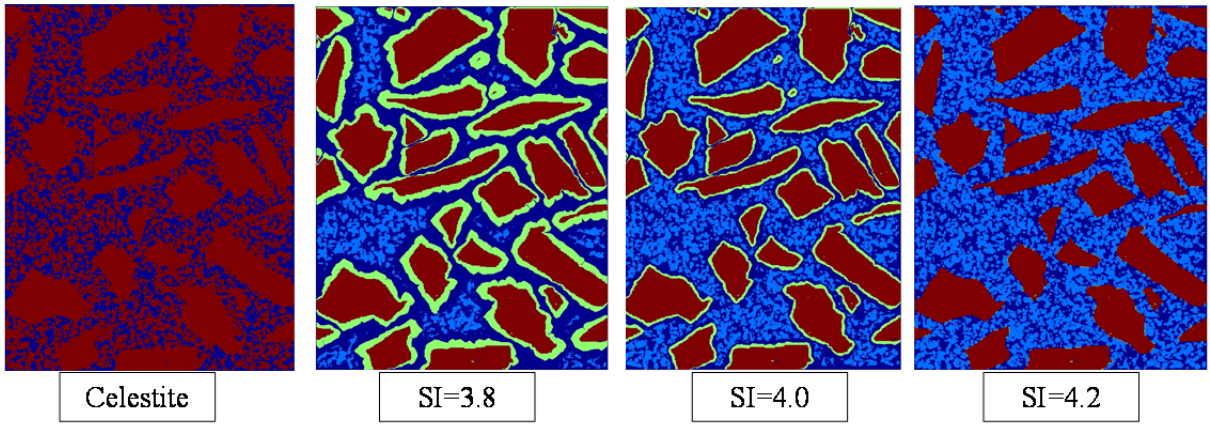

Fig. 2.9: Four plots from left to right represent: a) the initial porous structure of a 300x700 µm domain with large and small celestite crystals, b) the evolved system at SI=3.8, c) the evolved system at SI=4.0 (reactive transport experiment conditions), d) SI=4.2.

2.3.4 Porosity evolution at Clay – Cement interfaces using neutron radiography

Porosity changes at interfaces of technical barriers have an effect on mass transport at the interface. The ability of reactive transport codes to predict clogging processes can be enhanced and verified via specifically designed laboratory experiments. Prof. Kenichiro Nakarai from Hiroshima University is visiting PSI until end of 2017, thanks to a mobility grant from the JSPS (Japan Society for the Promotion of Science) on international scientific cooperation in the field of waste management research. His research project is aimed at experimental and modelling studies of clay/cement interaction. To speedup chemical transformation at the interface, which typically occurs over long time scale due to slow mass transport and kinetics admixtures are added to the clay in order to enhance clogging. The data obtained in this project will serve as experimental benchmark for reactive transport simulations in repository near conditions.

2.4 Benchmarking, validation and application of coupled codes

The benchmarking and verification of reactive transport coupled codes is an on-going activity in the Transport Mechanisms Group. This activity is important to support the credibility of numerical simulations and is essential for advancing the modelling and description of complex geochemical interactions and/or radionuclide migration in the vicinity of a nuclear waste repository or in laboratory experiments. Comparison of output results among different codes in LES, as well as the participation in international benchmarks ensures correctness, guarantees the quality of results and keeps the pace with the international scientific community.

2.4.1 Diffusion transport including ion exchange

Within the DR-A project, simulations including cation exchange reactions (among other processes) were run. Partly different formulations of the basic equations for heterovalent exchange are used in different codes, which then require the use of corresponding selectivity coefficients. To test the consistency of ion exchange simulations between codes, a simple 1D Benchmark case including diffusion and a single ion exchange reaction was run with MCOTAC, Flotran and PHREEQC (the last two are finite difference codes). Constant boundary concentrations were implied, and the solute concentrations at different locations were compared. The results show a very good agreement between the three codes for the studied case of diffusion across a 1cm plug, with Cs-Na and Ca-Na ion exchange on a single site according to the Gaines-Thomas convention (Fig. 2.10).

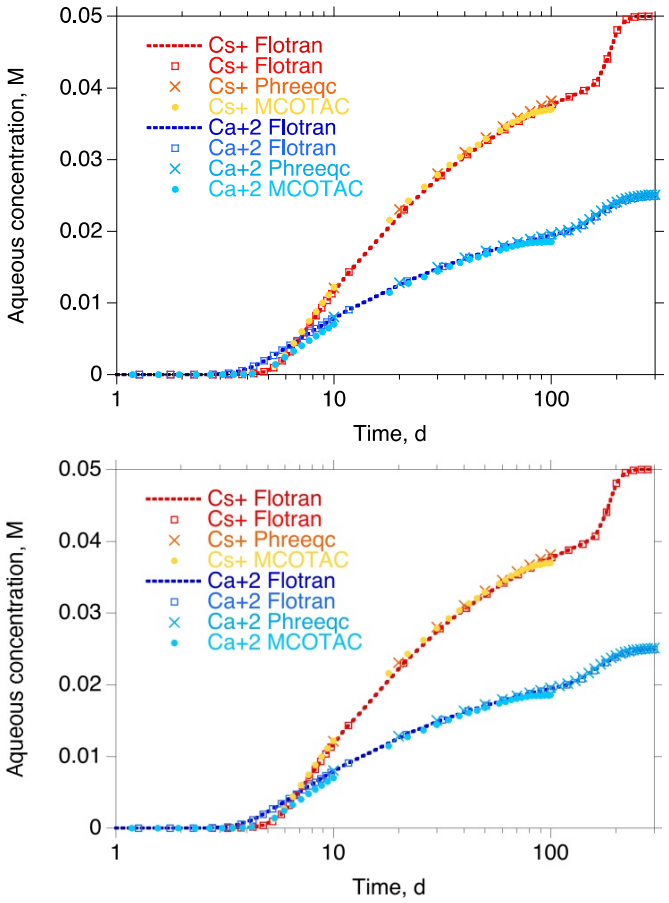

Fig. 2.10: Concentration increases for Cs-Na exchange and Ca-Na exchange at x = 0.0019 m obtained by the codes Flotran (two models), PHREEQC and the LES in-house code MCOTAC.

Only minor deviations occur at early times. These deviations are very likely related to differences in discretization and the way of solution of the transport equations.

2.4.2 Benchmarking of radionuclide transport codes

Within the SeS (Subsurface Environmental Simulation) Benchmarking Group a set of benchmarks describing Cs diffusion into Opalinus Clay with increasing complexity of sorption and transport coupling has been formulated. In a first model, the single species Cs transport has been modelled in 1D geometry using a nonlinear sorption isotherm in a tabulated form. Three different transport codes, COMSOL Multiphysics, MCOTAC and CORE^{2D} were benchmarked. In a second model, Cs sorption was taken into account using the 2SPNE SC/CE sorption model of BRADBURY & BAEYENS (2000) and a multispecies transport was considered. Results obtained with MCOTAC and CORE^{2D} are compared in Fig. 2.11. The agreement for calculated Cs breakthrough curves at different locations within the Opalinus Clay is very good for the whole range of Cs

concentrations at the boundaries. Concentrations ranging from 10^{-7} to 10^{-3} M are assumed at the model boundary and nonlinear sorption behavior of Cs is considered (see Fig. 2.11). Small differences for the calculated early Cs breakthroughs are explained by differences in mesh discretization used by the codes (50 vs 100 nodes).

2.4.3 Multi-phase mass transport in radioactive waste packages

The collaboration with the Department Environmental Informatics (Prof. O. Kolditz) at the Helmholtz Centre for Environmental Research (UFZ, Leipzig, Germany), on extending the modelling capabilities of the OpenGeoSys-GEM code is ongoing. In 2016, the collaboration was focused on the application of a new multi-component multi-phase solver which was developed by Y. Huang and H. Shao (UFZ, Leipzig, Germany), to simulation of *in situ* conditions in a generic waste package in a low-level waste repository coupling two phase mass transport and chemical reactions. The modelling setup takes into account spatial heterogeneity inside the waste package and can be compared, e.g. in terms of gas release with time, to the commonly used "mixing tank approach".

The model setup includes

- gas (H_2, CO_2, CH_4, H_2O vapor) and water transport, equilibration between water in gas and liquid phase,
- gas generation (H_2, CO_2, CH_4) and water consumption by metal corrosion or microbial degradation of organic wastes,
- water consumption (or release) by degradation of concrete due to carbonation or alkali-silica reactions,
- feedback of water availability and concrete degradation state on (bio)chemical reactions.

The modelling parameters for feedback between transport and chemical processes were finetuned. A sensitivity study was carried out to evaluate the influence of water availability in closed and open waste packages on gas production over time. In Fig. 2.12 a first implementation of feedback of chemistry on transport for a generic waste package where cement degradation, degradation of organic material and metal corrosion are taken into account is presented. Gas saturation distribution after 1000 years is plotted.

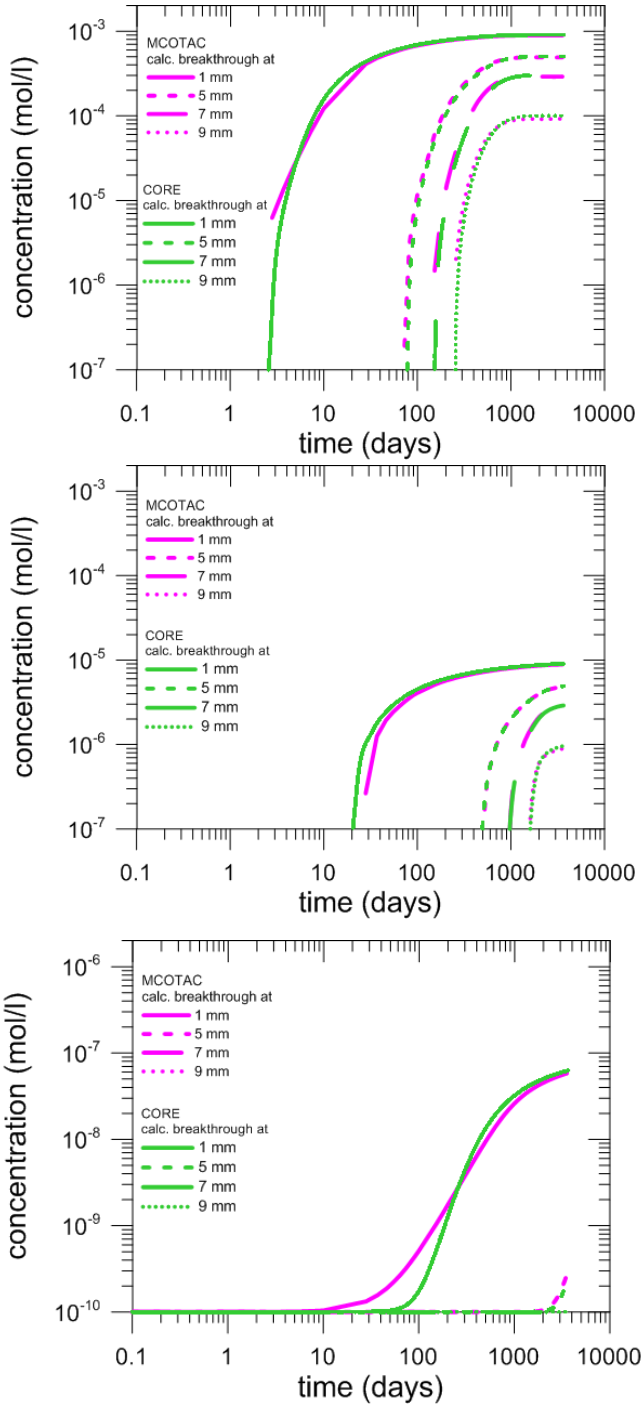

Fig. 2.11: Calculated Cs breakthrough at different locations in the Opalinus Clay sample using the reactive transport codes CORE^{2D} and MCOTAC. The Cs concentration at the "high" concentration boundary was assumed to be 10^{-3} mol/L (top), 10^{-5} mol/L (middle) and 10^{-7} mol/L (bottom).

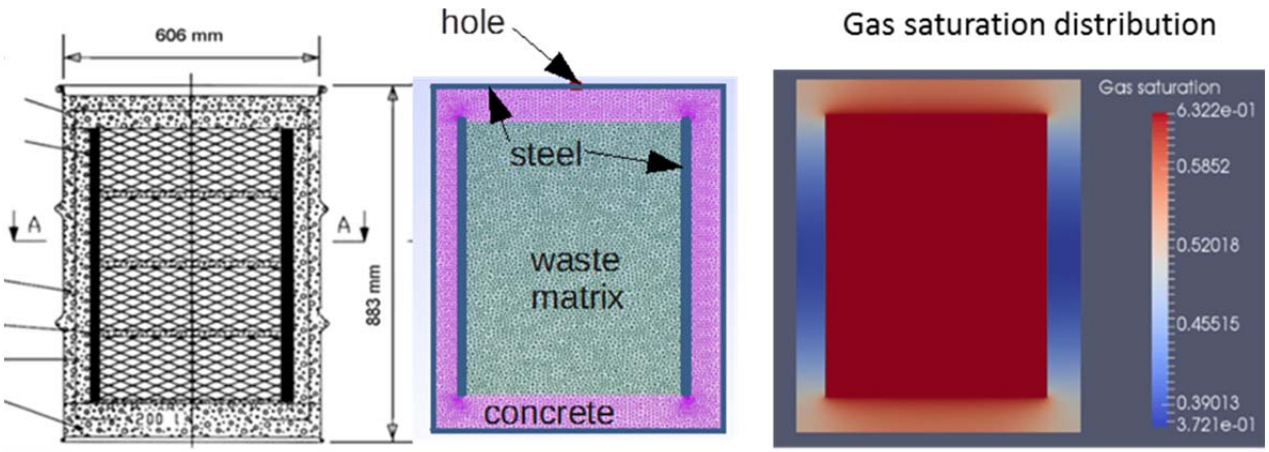

Fig. 2.12: Multiphase mass transport modelling of the evolution of a radioactive waste package. From left to right: The schematic of waste package, the discretized domain, and gas saturation distribution after 1000 years are presented. Cement and organic material degradation along with metal corrosion is taken into account.

2.4.4 Modelling electrochemical diffusion processes in the presence of charged mineral surfaces

LES participates in the HORIZON 2020 Collaborative Project "Cement-based materials, properties, evolution, barrier functions (CEBAMA) with 2 PhD projects. The PhD project "Modelling transport across reactive interfaces" (L. Hax Damiani) will support the interpretation of results and prediction of the long-term evolution of the major transport characteristics such as porosity, permeability and diffusion parameters, especially at the interface between cement based materials and the engineered and natural barriers. In such systems the ion transport in small pores is strongly influenced by the electrostatic interaction with the charged surfaces of mineral phases. These phenomena can be described by the Nernst-Planck transport model. In the first stage of the project an open source numerical code solving the Nernst-Planck equations (FEniCs (LOGG et al. 2012)) is linked to in-house chemical solver (GEMS4K). FEniCs is a scientific tool for solving partial differential equations with several finite elements (FE) based numerical methods. The Nernst-Planck based transport models are computationally intensive and the application of these models to the experiments will require the use of high performance computing. The FEniCs open source library is particularly suitable for the efficient implementation of the transport code at HPC systems

Numerical implementation was first verified against analytical solutions for salt diffusion, and several well-established benchmarks (RASOULI et al. 2015). Fig. 2.13 shows the initial distribution of chemical species (H^+, NO^{3-}, Na^+ and Cl^-) in a typical benchmark setup. In the model HNO_3 diffuses from a low pH solution (pH = 4, right side) to a higher pH solution (pH = 6, left side). A fixed concentration boundary condition is imposed at the left side, while the right boundary condition is a zero-gradient boundary condition. Both solutions contain the same elevated NaCl concentrations. The simulation results are compared to the reference values in Fig. 2.14. As expected an increase in Na^+ and a decrease in Cl^- concentrations is observed which is caused by coupling between diffusive and electrochemical fluxes. Such coupled electrochemical behavior cannot be modelled with simple Fickian diffusion models. A very good agreement between the current implementation and the reference solution is observed.

The current implementation of the code includes coupling to the Reaktoro (LEAL et al. 2014), GEMS4K (KULIK et al. 2013) and PHREEQC (PARKHURST et al. 1999) chemical solvers. Within the next step the Donnan equilibrium concept will be implemented to describe ion partitioning between pores. This will allow to take into account the effects of double-layers at charged mineral surfaces on water composition and to better describe effects like anion-diffusion or surface diffusion in e.g. clay minerals.

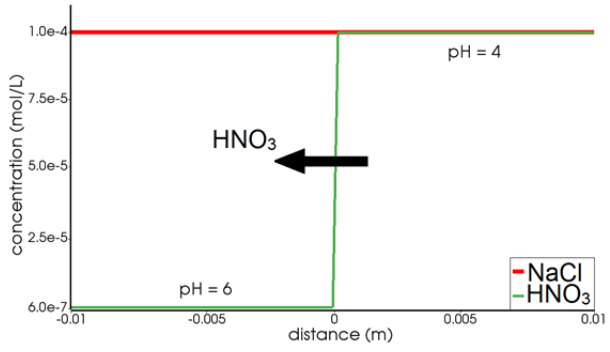

Fig. 2.13: Initial condition of Rasouli's benchmark 1 with indications of expected ion fluxes due to initial and boundary conditions.

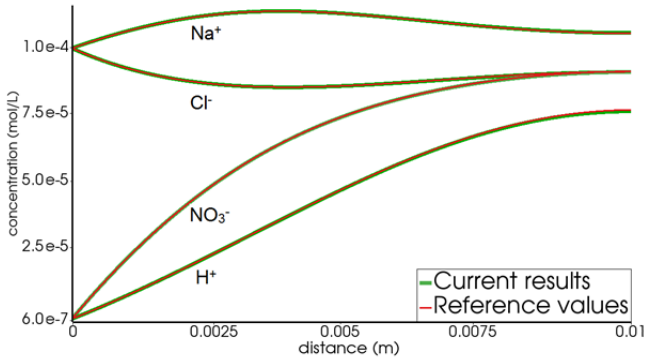

Fig. 2.14: Comparison between Rasouli's benchmark reference values and our results after 1h diffusion time.

2.4.5 Reactive transport studies of two-phase flow in Icelandic geothermal systems

Magma-driven, high enthalpy geothermal systems (see Fig. 2.15) are currently the only type of geothermal reservoirs that is routinely utilized for electrical power generation. The transient evolution of geochemical processes in the subsurface of these systems has remained elusive because direct observation is hampered by the extreme conditions in the boiling reservoir and the difficulties of undisturbed, *in situ* sampling in a producing geothermal field. Numerical reactive transport simulation is, therefore, the tool of choice to study these processes and, combined with sampling, can lead to well-constrained models of chemical reservoir processes. In the context of Sinergia COTHERM-2 project - COmbined hydrological, geochemical and geophysical modelling of geotTHERMal systems (Coordinator: T.Driesner, ETHZ), SP2 (Sub-project 2) "Geochemical reactive transport modelling of fluid-rock interaction" (Co-PIs D. Kulik, G. Kosakowski, Postdoc A. Yapparova), a novel reactive transport simulator CSMP++GEM (YAPPAROVA et al. 2016) that allows simulating reactive transport under boiling conditions on unstructured meshes has been developed. Two-phase transport with partitioning of volatiles between water and steam was implemented in the first working prototype.

Chemical fluid-rock interaction and boiling modify the chemical composition of geothermal fluids and obscure their origin. Geologically constrained simulations allow unraveling the influence of these processes and quantifying the paths that fluids follow, thus providing new insights into the mechanisms of heat and mass transfer. At the same time, a practical interest arises from the fact that the chemical composition of fluids controls factors such as corrosive behavior or heat extraction efficiency that operators like to control to optimize production.

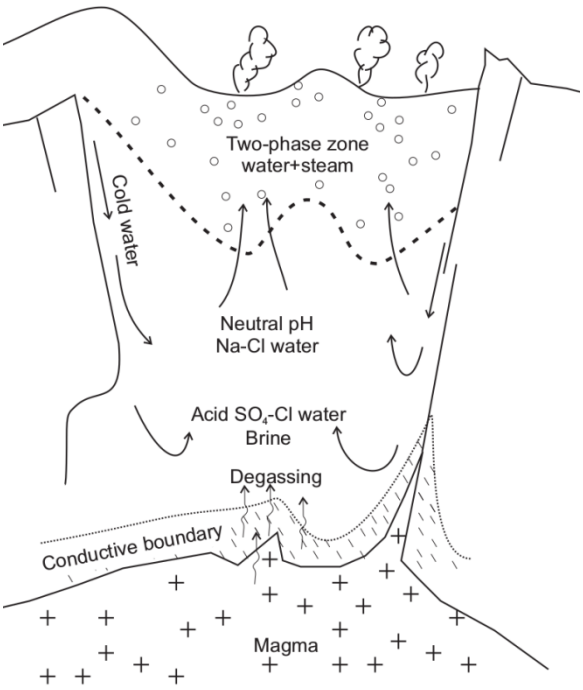

Fig. 2.15: Schematic section of a volcanic geothermal system depicting the origin, interaction, and possible evolution of fluids. (ARNORSSON et al. 2007)

The combination of CSMP++ and GEMS3K provides a unique feature set within a single reactive transport code. Namely, the combination of unstructured meshes with reactive transport in a boiling system has so far not been realized in any other tool, and allow us to perform simulations on "geologically realistic" geometries. The code employs the control volume finite element method (CVFEM) to solve PDEs for two-phase flow and heat transport in terms of pressure, enthalpy and salinity (WEIS et al. 2014). Equation of state for a H_2O-NaCl system (DRIESNER & HEINRICH 2007; DRIESNER 2007) provides an accurate thermodynamic representation of fluid properties. The sequential Non-Iterative Approach (SNIA) that is used for transport-chemistry coupling allows fast reactive transport calculations (compared to Sequential Iterative Approach (SIA) and fully implicit methods). Chemical equilibrium calculations are performed using the Gibbs energy minimization method (GEM), implemented within the GEMS3K standalone library. As Gibbs free energy on the boiling curve is the same for liquid water and vapor, additional constraints on the amount of vapor are necessary to calculate phase partitioning of gases (CO_2 , H_2S, H_2 ,CH_4) in GEMS. These constraints are provided from the CSMP++ part. Liquid water and steam properties are taken from the Haar-Gallagher-Kerr (HGK) equation of state and an ideal mixture of gases with properties calculated from the Peng-Robinson equation of state is used. The calculation of metastable water properties was newly implemented in GEMS.

The model describes a 2 km long 1D flow path in a boiling geothermal reservoir. Aquifer fluid composition was calculated from the liquid and steam sample analysis of the K-14 well from the Krafla geothermal field. Hot 300°C vapor is injected from the left into the 200°C warm liquid, A boiling zone develops in the middle part of the model and volatiles partition between the liquid and vapor phases. Simulation results after 500 years are shown in Fig. 2.16. Curve shapes reflect the fact that species concentrations in liquid and vapor phases depend on the distribution coefficients and on the masses of liquid and vapor along the flow path, including concentration changes due to condensation and boiling.

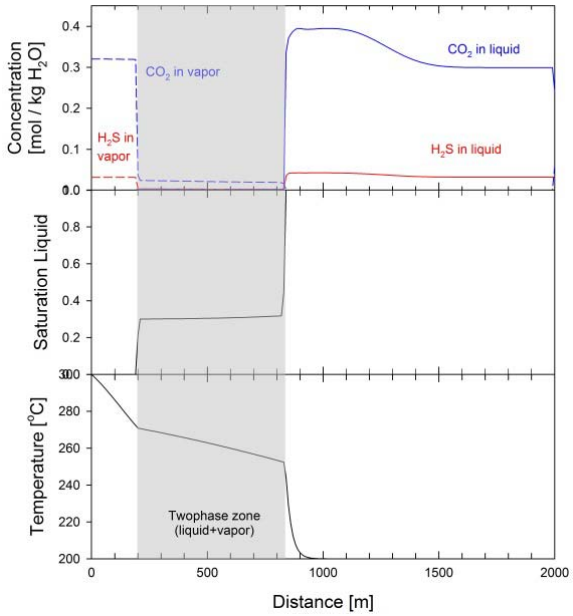

Fig. 2.16: CO_2 and H_2S concentrations in the vapor and liquid phases, saturation of liquid and temperature distribution.

The model developed within the project was able to accurately describe two phase flow coupled with chemical reactions and successfully predict the dynamic behavior of key chemical components in a dynamic geothermal system.

2.5 Thermodynamic modelling framework and thermodynamic databases

The GEM Software (GEMS) code collection has been developed at LES PSI since 2000 by a community team led by Dr. D. Kulik. The advanced features and unique capabilities of the software are described in detail at the GEMS project web site http://gems.web.psi.ch. The software comes with an adapted version of the PSI/Nagra Chemical Thermodynamic Database 12/07 (www.psi.ch/les/-database) for applications to low-temperature aquatic systems related to geological radioactive waste disposal. The imported SUPCRT98 database is also provided for generic geochemical applications. Third-party databases for hydrated cement systems (www.empa.ch/cemdata), nuclear materials (www.psi.ch/heracles/gems-specific-heracles-database), and hydrothermal geochemistry (http://tdb.mines.edu) are available as well from their maintainers.

2.5.1 ThermAc3 project

In the framework of the joint project on Thermodynamics of Actinides (ThermAc3), the new software tools ThermoMatch and ThermoFun have been developed to facilitate the sharing of thermodynamic data with the GEMS package and external software. These tools are implemented using modern IT solutions which allow the use of import filters to feed the available data from GEMS, old PMATCHC, foreign TDBs, etc. for elements, substances, reactions and data source references into the ThermoHub NoSQL graph database.

Based on the property graph database paradigm, ThermoHub is designed to serve as a hub for delivering thermodynamic data to speciation codes via the ThermoFun application programming interface (API), and also to maintain searching and editing the data for elements, substances, reactions, interaction parameters, and phases-solutions.

The database is implemented keeping in mind a complete traceability of data modification and bibliography. Currently, the THERMOMATCH database includes the data for chemical elements and substances available in the GEM-Selektor default and third-party databases (e.g SUPCRT, PSI-Nagra, HERACLES).

ThermoFun is a newly-developed C++ library (compatible with both GEMS and Reaktoro framework) for correcting standard state thermodynamic properties of chemical substances and reactions from reference temperature (298.15 K) and pressure (1 bar = 10^5 Pa) to temperature and pressure of interest. This library was implemented by merging/adapting various methods for temperature-pressure correction of standard thermodynamic functions from the GEM-Selektor code. The library has a simple to use API and GUI (graphical user interface) and can be easily called from any C++ code for chemical thermodynamic calculations.

Structured data (SD) formats greatly facilitate processing, exchange and storage of complex data in a NoSQL database, at the same time dramatically reducing the costs of development due to the usage of efficient, stable open-source software. Thermo-dynamic entities such as reactions, interaction

parameters, phases, LMA reaction sets, GEM thermodynamic data sets and data source references can all be represented, efficiently traversed, extracted and processed. The ThermoFun GUI interface helps the user to select a list of substances, temperature and pressure intervals, and thermodynamic properties to be calculated and to export the results in a convenient file format. The cornerstone architecture of the software integration and connection with external codes and databases is schematically represented in Fig. 2.17

ThermoFun supports several popular Equations of State (EOS) and temperature and pressure correction models for substances. These include the IAWPS95 (WAGNER & PRUSS 2002) and ZHANG & DUAN (2005) EOS for water. The latter, together with the newly implemented model for calculating the dielectric properties of H_2O and the revised HKF model (SVERJENSKY et al. 2014) allows for calculating the properties of aqueous ions and complexes at pressures beyond the previous 5 kbar limit of the HKF model (TANGER & HELGESON 1988). The library allows different combinations of the available models for correcting standard state thermodynamic properties. For example, it is possible to combine the standard state properties of H_2O calculated with the IAWPS95 EOS, the dielectric permittivity calculated using the empirical fit of SVERJENSKY et al. (2014), and the revised parameters for the HKF model (SVERJENSKY et al. 2014), to calculate the reference properties of ions and aqueous species at a given temperature and pressure.

ThermoFun uses the automatic differentiation scheme developed in Reaktoro (http://reaktoro.org) for some of the implemented models. This means that, besides the calculated values of the respective thermodynamic properties, the library API can provide their first- and second-order derivatives with respect to temperature and pressure. This can significantly accelerate calculations of equilibria in (geo-) chemical systems using the Reaktoro algorithms (LEAL et al. 2016a; LEAL et al. 2016b).

The main expected future benefit of ThermoHub consists in creating an unmatched opportunity for exploring and improving the mutual consistency of different thermodynamic datasets by keeping them in the same graph database, connected to a global optimization tool that uses a database of experimental (solubility, conductivity, spectroscopy etc.) data. First attempts of this kind have already commenced (MIRON et al. 2016), revealing the need for tighter software integration.

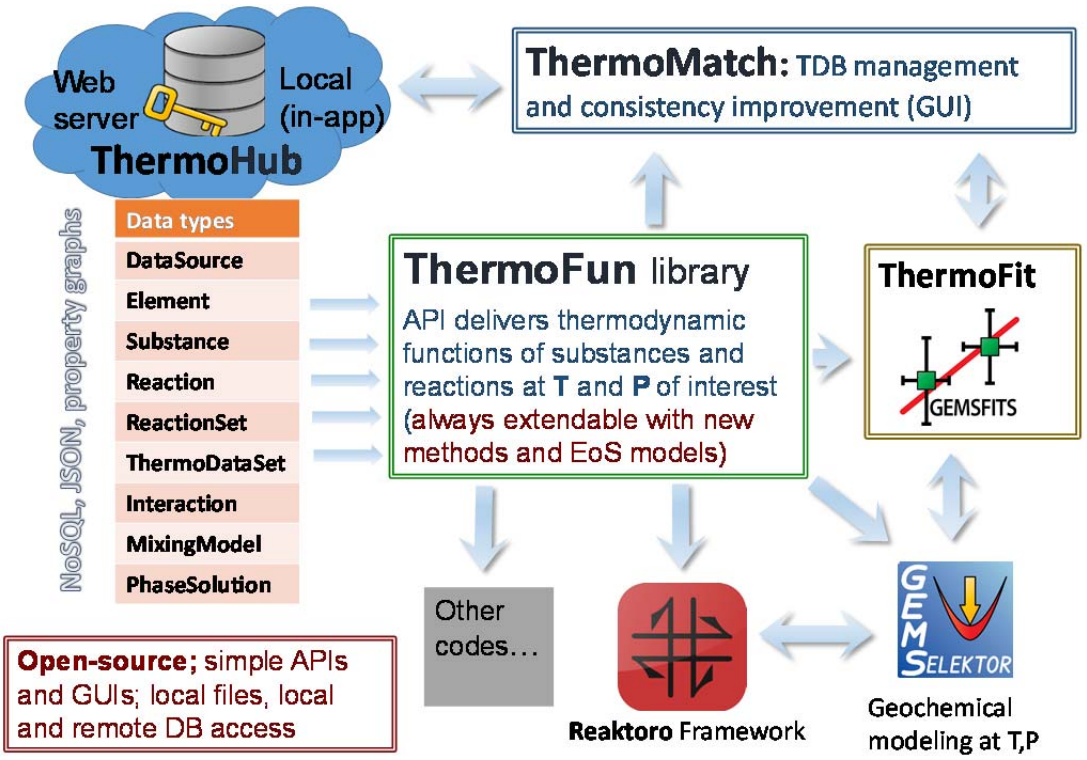

Fig. 2.17: Data-centric integration of the GEMs software around the ThermoHub TDB and the ThermoFun (formerly TCorrPT) library. Arrows show the directions of data flow.

2.5.2 Extension of the internally consistent thermodynamic database

The extension of the previous work on developing an internally consistent database for aqueous species in the system Na-K-Al-Si-O-H-Cl (MIRON et al. 2016) was finalized with the addition of substances containing Ca, Mg and C. The thermodynamic dataset now covers all of the most important elements, thus becoming highly relevant for geochemical applications. A large set of solubility experiments over a wide range of temperature, pressure and composition was critically assessed and used in the global optimization procedure. We took the thermodynamic data for minerals from the database of HOLLAND & POWELL (1998) and simultaneously refined the standard state Gibbs energy of the aqueous ions and complexes against a large collection of solubility experiments. The new thermodynamic dataset is shown to largely reproduce the available fluid-mineral phase equilibria and mineral solubility data with good accuracy and precision over wide ranges in temperature, pressure and composition (25 to 800°C; 1 bar to 5 kbar; salt concentrations up to 5 M).

2.5.3 Project GEMS-Reaktoro, xLMA methodology

This project, initiated at LES in 2014, now continues in collaboration with Dr. A. Leal and Prof. Dr. M. Saar (ETHZ) on the basis of the Memorandum on Cooperation between PSI NES LES and ETHZ IG GEG, signed in September 2016. The project is aimed at improving the GEMS numerical kernel by incorporating the accurate, stable and fast GEM-based numerical algorithms from the Reaktoro code framework for modelling chemically reactive systems (www.reaktoro.org; LEAL et al. 2016a, 2016b, 2016c).

A major progress in developing Reaktoro algorithms has been achieved recently with the implementation of the new xLMA (extended law of mass action) method (LEAL et al. 2016b) into the *IPAction* algorithm, completing the work started at LES in 2015.

The GEMS competitors – popular conventional LMA speciation codes such as GWB, OLI, PHREEQC, MINEQL, MINTEQ, CHESS (MOREL & MORGAN 1972; REED 1982; BETHKE 2007) – all consider chemical species taken as master (primary) and product (secondary). A *product species* is defined by the LMA expression of its reaction from *master species* (for example, for the calcite end member $CaCO_3 + H^+ = Ca^{2+} + HCO_3^-$) with the equilibrium constant $K_{CaCO_3} = \frac{a_{Ca^{2+}} \cdot a_{HCO_3^-}}{a_{H^+} \cdot a_{CaCO_3}}$, where *a* denotes the species activity - a function of phase composition, temperature and pressure. The standard state thermodynamic data for master species (usually aqueous ions) are typically ignored. Equilibrium speciation methods based on the conventional LMA approach directly minimize the mass balance residuals using the LMA expressions as boundary conditions. In multiphase systems, they may require the tentative addition and removal of phases to/from the mass balance so that the system of LMA equations is always valid (REED 1982). These widely used conventional LMA methods are simple and efficient, if certain aspects of the chemical system are known in advance (e.g., aqueous phase is always present, minerals are added/removed according to their saturation indices). Some LMA algorithms are limited to ideal gaseous, liquid or solid solutions; some extended to binary non-ideal solutions (PHREEQC); and some cannot process solid solutions or gas mixtures at all (GWB).

The xLMA expressions were formally derived from the general Gibbs energy minimization (GEM) problem with the following conditions of optimality (Leal et al. 2016a):

$$\mu(n) - A^T y - z = 0, \quad An = b,$$
$$n_i z_i = 0 \ \ (i = 1, \dots, N), \quad n_i \geq 0, z_i \geq 0,$$

where n is the vector of sought-for amounts of chemical species; N is the number of species; A is their elemental stoichiometry matrix; b is the vector of bulk elemental composition of the system; y is the vector of Lagrange multipliers conjugate to b (i.e. chemical potentials of elements); z is the vector of Lagrange multipliers conjugate to n (species stability indices); and $\mu(n)$ is the vector of primal chemical potentials of species, defined as $\mu_i = \mu_i^o + RT \ln a_i$, via the standard chemical potential μ_i^o and the activity a_i which is a function of concentration and activity coefficient, i.e. a function of system speciation n.

By representing activities of species via the LMA expressions of the reactions (LEAL et al. 2016b), one can eliminate Lagrange multipliers y and finally arrive at the *extended mass action* expressions $K_m = \prod_{i=1}^{N} (a_i \omega_i)^{\nu_{mi}}$, where $\omega_i = exp\left(^{-z_i}/_{RT}\right)$ is the *stability factor* obtained from the same species stability index z_i (Lagrange multiplier conjugate to n_i) as that involved in the above GEM optimality conditions. The product $a_i \omega_i$ can be called the *extended activity* (of i-th chemical species), in which the stability factor ω_i, which is missing from all conventional LMA codes (compare eqs 3 and 1), now renders the xLMA algorithm the full power and generality of GEM methods.

Rigorous accounting for stability factors ω_i (or stability indices z_i) enables the xLMA method to determine in one run all stable phases without

presuming their types (e.g., aqueous, gaseous) or their presence in the equilibrium state. Any additional technique that tentatively adds or removes reactions based on phase stability indices (e.g., saturation indices for minerals) becomes obsolete, since the xLMA expressions are valid even when unstable species are involved in them.

The proposed method was implemented as *IPAction* algorithm in the Reaktoro framework, and successfully tested on reactive transport modelling examples, where PHREEQC and GEMS were used as alternative "back-ends" for the calculation of equilibrium constants of reactions, standard chemical potentials of species, concentrations, and activity coefficients (LEAL et al. 2016b). Tests showed that our algorithm is efficient and robust for demanding applications, such as reactive transport modelling, where it converges within 1–3 iterations in most cases. This opens up new perspectives in geochemical and reactive transport modelling, including the re-use of numerous past applications of conventional LMA chemical solvers.

2.5.4 Thermodynamics of (Ba,Sr,Ra)SO_4 – H_2O system

In the first part of this work (collaboration with V. Vinograd, FZJ under ThermAc3 project), literature data and several prediction and correlation methods were used to obtain an internally consistent thermodynamic dataset for the solids $BaSO_4$,cr (barite), $SrSO_4$,cr (celestite) and $RaSO_4$,cr, compatible with the PSI/Nagra 12/07 database (THOENEN et al. 2014), and valid for temperature corrections in the range 0 to 350 °C. In the second part of this study (VINOGRAD, KULIK, BRANDT et al, 2016), atomistic methods were used to re-evaluate parameters of mixing in the ternary (Sr,Ba,Ra)SO_4 solid solution system, leading to a regular model of mixing with binary interaction parameters and no ternary parameter. This model of mixing, together with the "tCp" thermodynamic dataset and the PSI/Nagra database, was used in GEM-Selektor simulations of SS-AS systems involving a binary (Ba,Ra)SO_4 phase to test temperature trends of radium retention in barite (a widely recognized repository-relevant issue).

Furthermore, a ternary (Sr,Ba,Ra)SO_4 phase was employed to investigate the impact of addition of Sr to barite onto retention of radium at various temperatures. This scenario is of interest because natural barites, e.g. such as found in Opalinus clay, have various contents of Sr, and the porewater in clayrock appears to be saturated with respect to celestite. Process simulations were conducted using parent systems composed of 1 kg of H_2O, 0.1 mol of NaCl, 5E-6 mol $RaCl_2$, 0.1 g of dry air, and either 0.5 g or 5.0 g $BaSO_4$ initially. The SUPCRT extended Debye-Hückel aqueous activity model was used.

Overall, it is clear that the most efficient immobilization of radium in solid solution with barite happens at lower temperatures and higher S/W ratios – the latter produces a stronger "dilution effect" for Ra in solid solution. At 125 °C, the mobility of radium will be ca. 10 times higher than at 25 °C (at all other conditions kept constant). The Ra-Ba fractionation coefficient in the solid decreases with temperature by two orders of magnitude.

In systems with the ternary solid solution, the same initial recipes were used as before (at S/W = 0.5 g/kg or 5.0 g/kg $BaSO_4$). In the process, the composition of solid solution was changed by a stepwise addition of $SrSO_4$ (starting from 1e-6 mol) and subtraction of $BaSO_4$ such that the mass of the solid phase remains constant at given S/W ratio. Simulations were performed at several temperatures, as shown in Fig. 2.18. At both S/W ratios, the addition of $SrSO_4$ to barite results in a much stronger retention of radium, especially at low temperatures, the strongest at 7-10% of the Sr end member.

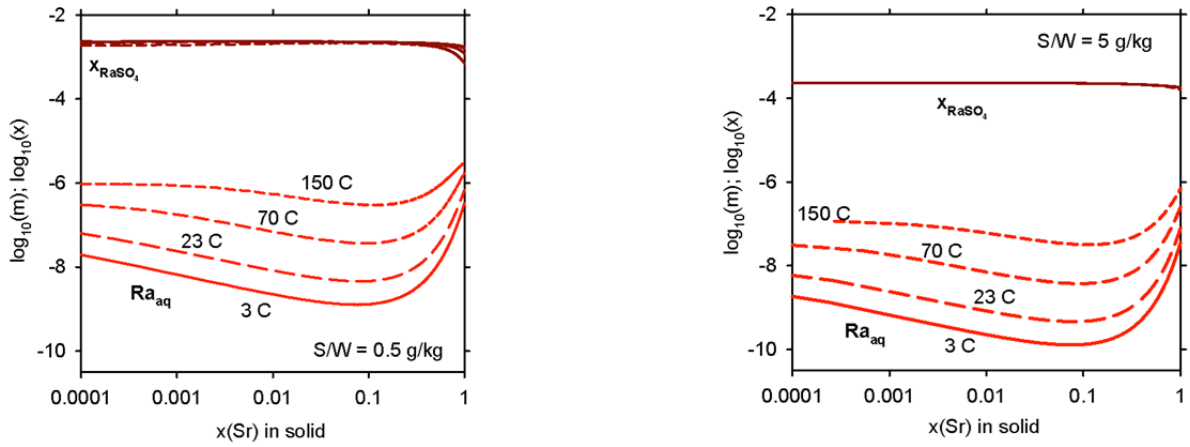

Fig. 2.18: The impact of Sr content in ternary non-ideal (Sr,Ba,Ra)SO_4 solid solution at 5e-6 m $RaCl_2$, constant S/W mass ratios, and different temperatures (150 °C at saturated vapour pressure).

In comparison with the binary $(Ba,Ra)SO_4$ – H_2O system at the same S/W ratio, the addition of 5-10% Sr results in an about 9-11 times lower aqueous Ra_{aq} concentration; this effect becomes much weaker at increasing temperature. In the Opalinus clayrock, natural diagenetic Ba-Sr sulphate cements contain 22% to 90% Sr and fibrolytic barite along shear planes 2 to 12 % Sr (LEROUGE et al. 2014). In the Callovo-Oxfordian clayrock, rare diagenetic barite contains up to 19% Sr and more abundant celestite contains 7 to 16% Ba (LEROUGE et al. 2011). In both clayrocks, the porewater is assumed saturated with respect to celestite. Such predictions of equilibrium Ra retention in non-ideal ternary $(Ba,Sr,Ra)SO_4$ solid solutions can only be calculated using GEM algorithms (advanced LMA codes can only solve speciation involving binary or ideal solid solutions (REED 1982)). Indeed, our results are more realistic than those involving pure (Sr-free) barite, hence comprising a more general and favourable case for considering in safety assessments.

2.5.5 Thermodynamic equilibrium in C-A-S-H system

The influence of Al on the stability of calcium silicate hydrates (C-S-H) is purely constrained. The thermodynamic description of Al incorporation in C-S-H is essential for long-term prediction of the *in situ* condition in the repository. The thermodynamic stability of Al rich phases is being evaluated by molecular and macroscopic thermodynamic modelling. Free energy of Al-Si exchange between C-S-H and aqueous solution was evaluated using quantum mechanical calculations.

Consistent with the spectroscopic observations, the result suggest that Al substitutes in the C-S-H structure for Si in bridging tetrahedral sites. It was further observed that the substitutions in the neighbouring bridging sites is less favourable by about 5 kcal/mol (PEGADO et. al. 2014). These data were used to simulate the effect of pH and $[Al(OH)_4^-]_{aq}/[Si(OH)_3O^-]_{aq}$ concentration in aqueous solution on the equilibrium [Al]/[Si] ratio in C-S-H based on Grand Canonical Monte Carlo simulations (GCMC) using the so called primitive model for electrolyte solutions. A good agreement between the simulations and the available experimental data were obtained (CHURAKOV & LABBEZ 2017). The results suggest that Al affinity to C-S-H has a maximum at pH ~ 11, which is related to the concentration maxima of the singly protonated bridging sites $\equiv Si(OH)O^-$ at the C-S-H surface (Fig. 2.19).

The parameterization of the C-S-H multi-site (sublattice) solid solution thermodynamic model based on available solubility data is ongoing in collaboration with B. Lothenbach (EMPA). Na and K end-members were included in the model. The results point to the need for considering alternative Ca ion substitutions on the bridging tetrahedral structural sites in C-S-H. Recently a new SNF project proposal "Effect of aluminum on C-S-H structure, stability and solubility (C-A-S-H-2)" by B. Lothenbach, D. Kulik has been approved. The project will start in January 2017. It is expected that first experimental data will be available in 2018. These data will be particularly valuable for further parameterisation of the solid-solution model for cement phases.

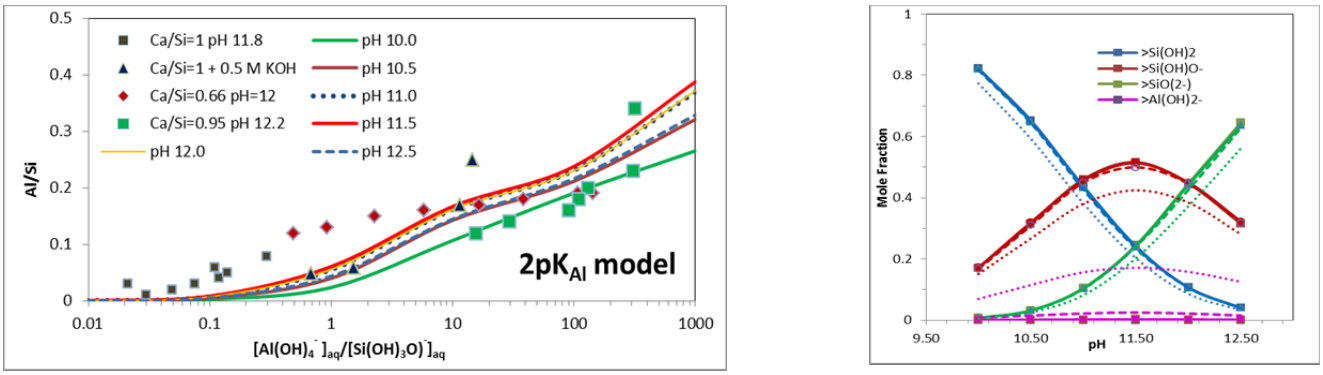

Fig. 2.19: Left: Experimental [Al]/[Si] ratio in solid C-(A)-S-H versus $[Al(OH)_4^-]$ $[Si(OH)_3O^-]$ ratio in solution, obtained at pH > 11 in various experimental conditions (points) (Lothenbach & Nonat 2015) experimental data are compared with the results of GCMC simulation in 1mM $CaCl_2$ solution at different pH controlled by NaOH. Right:Speciation of C-A-S-H surface as function of pH obtained by GCMC simulation for $[Al(OH)_4^-]/[Si(OH)_3O^-]_{aq}$ equal to 0.01, 0.1 and 1 are shown by solid, dashed and dotted lines respectively. The results to Al-free system are shown by symbols symbols. Note that at $[Al(OH)_4^-]_{aq}/[Si(OH)_3O^-]_{aq}$ the lines representing concentrations of $[Al(OH)_2^-]$and $[Si(OH)O^-]$ species overlap.

2.5.6 References

ARNORSSON S., STEFANSSON A., BJARNASON J.O. (2007)
Fluid-Fluid interactions in geothermal systems. Rev. Mineral. Geochem. 65, 259-312.

BETHKE C.M. (2007)
Geochemical and biogeochemical reaction modelling. Cambridge University Press.

BRADBURY M.H., BAEYENS B. (2000).
A generalised sorption model for the concentration dependent uptake of caesium by argillaceous rocks. J. Contam. Hydr., 42(2-4): 141-163.

CHURAKOV S.V., LAPPEZ CH. (2017)
Thermodynamics and molecular mechanism of Al incorporation in calcium silicate hydrates. J. Phys. Chem. C, 121, 4412-4419.

DAUZERES A., ACHIEDO G., NIED D., BERNARD E., ALAHRACHE S., LOTHENBACH B. (2015)
Magnesium perturbation in low-pH concretes placed in clayey environment—solid characterizations and modelling. Cem. Concr. Res. 79, 137–150.

DRIESNER T. (2007)
The system H_2O–NaCl. Part II: Correlations for molar volume, enthalpy, and isobaric heat capacity from 0 to 1000 °C, 1 to 5000 bar, and 0 to 1 X_{NaCl}. Geochim. Cosmochim. Acta 71, 4902 – 4919.

DRIESNER T., HEINRICH C.A. (2007)
The system H2O–NaCl. Part I: Correlation formulae for phase relations in temperature–pressure–composition space from 0 to 1000 °C, 0 to 5000 bar, and 0 to 1 X_{NaCl}. Geochim. Cosmochim. Acta 71, 4880 – 4901

GEBAUER D., KELLERMEIER M., GALE J.D., BERGSTRÖM L., CÖLFEN H. (2014)
Pre-nucleation clusters as solute precursors in crystallization. Chem. Soc. Rev. 43, 2348–2371.

GIN S., JOLLIVET P., FOURNIER M., BERTHON C., ZHAOYING W., MITROSHKOV A., ZHU Z., RYAN J.V. (2015)
The fate of silicon during glass corrosion under alkaline conditions: A mechanistic and kinetic study with the International Simple Glass, Geochim. Cosmochim. Acta 151, 68-85.

GONZÁLEZ-ROBLES et al. (2015)
Dissolution experiments of commercial PWR (52 MWd/kgU) and BWR (53 MWd/kgU) spent nuclear fuel cladded segments in bicarbonate water under oxidizing conditions. Experimental determination of matrix and instant release fraction. J. Nucl. Mat. 465, 63-70.

HOLLAND T.J.B., POWELL R. (1998)
An internally consistent thermodynamic data set for phases of petrological interest. J. Metam. Geol. 16, 309-343.

JENNI A., MÄDER U., LEROUGE C., GABOREAU S., SCHWYN B. (2014)
In situ interaction between different concretes and Opalinus Clay. Phys. Chem. Earth 70–71, 71–83.

KULIK D.A., WAGNER T., DMYTRIEVA S.V., KOSAKOWSKI G., HINGERL F.F., CHUDNENKO K.V., BERNER U. (2013)
GEM-Selektor geochemical modelling package: revised algorithm and GEMS3K numerical kernel for coupled simulation codes. Computat. Geosci. 17, 1-24.

LEAL A.M.M., BLUNT M.J., LAFORCE T.C. (2014)
Efficient chemical equilibrium calculations for geochemical speciation and reactive transport modelling. Geochim. Cosmochim. Acta 131, 301–322.

LEAL A.M.M., KULIK D.A., KOSAKOWSKI G. (2016a)
Computational methods for reactive transport modelling: A Gibbs energy minimization approach for multiphase equilibrium calculations. Adv. Water Res. 88, 231-240.

LEAL A.M.M., KULIK D.A., SAAR M.O. (2016b)
Enabling Gibbs energy minimization algorithms to use equilibrium constants of reactions in multiphase equilibrium calculations. Chem. Geol. 437, 170-181.

Leal A.M.M., Kulik D.A., Kosakowski G., Saar M.O. (2016c)
Computational methods for reactive transport modelling: An extended law of mass-action, xLMA, method for multiphase equilibrium calculations. Adv. Water Res. 96, 405-422.

LEROUGE C., GRANGEON S., GAUCHER E.C., TOURNASSAT C., AGRINIER P., GUERROT C., WIDORY D., FLEHOC C., WILLE G., RAMBOZ C., VINSOT A., BUSCHAERT S. (2011).
Mineralogical and isotopic record of biotic and abiotic diagenesis of the Callovian–Oxfordian clayey formation of Bure (France). Geochim. Cosmochim. Acta 75, 2633–2663.

LEROUGE C., GRANGEON S., CLARET F., GAUCHER E. C., BLANC PH., GUERROT C., FLEHOC CHR., WILLE G., MAZUREK M. (2014)
Mineralogical and isotopic record of diagenesis from the Opalinus Clay formation at Benken, Switzerland: Implications for the modelling of pore-water chemistry in a clay formation. Clays Clay Miner., 62(4), 286-312.

LOGG A., MARDAL K.-A., WELLS G.N. et al. (2012). Automated Solution of Differential Equations by the Finite Element Method, *Springer*.

LOTHENBACH B. (2011)
CI experiment: Hydration experiments of OPC, LAC and ESDRED cements: 1h to 3.5 years. Mont Terri Project Technical Note 2010-75, EMPA, Dübendorf, Switzerland.

LOTHENBACH B., NONAT A. (2015)
Calcium silicate hydrates: Solid and liquid phase composition. Cem. Concr. Res. 78: 57-70.

MOREL F.,, MORGAN J. (1972)
Numerical method for computing equilibriums in aqueous chemical systems. Environ. Sci. Tech., 6(1), 58-67.

MIRON G.D., WAGNER T., KULIK D.A. & HEINRICH C.A. (2016). Internally consistent thermodynamic data for aqueous species in the system Na-K-Al-Si-O-H-Cl. Geochim. Cosmochim. Acta 187, 41-78.

PARKHURST D., APPELO C. (1999)
User's guide to PHREEQC (Version 2)—A computer program for speciation, batch-reaction, one-dimensional transport, and inverse geochemical calculations. USGS Water Res. Investigations Report 99, 326.

PEGADO L., LABBEZ CH. CHURAKOV S.V. (2014)
Mechanism of aluminium incorporation in C-S-H from ab initio calculations. J. Mater. Chem. A2, 3477-3483.

PFINGSTEN W., JAKOB A. (2014)
Benchmark for nonlinear sorption processes of Cs migration through Opalinus Clay using a single species (COMSOL) and a multi-species (MCOTAC) reactive transport model. Workshop TRePro III - Transport and Reaction Processes, 5-7 March 2014, Karlsruhe, Germany.

PFINGSTEN W. (2002)
Experimental and modelling indications for self-sealing of a cementitious low- and intermediate-level waste repository by calcite precipitation. Nucl. Techn., 140, 63 – 82.

POONOOSAMY J., KOSAKOWSKI G., VAN LOON L.R., MÄDER U. (2015)
Dissolution-precipitation processes in tank experiments for testing numerical models for reactive transport calculations: experiments and modelling. J. Contam. Hydrol. 177–178, 1–17.

POONOOSAMY J., CURTI E., KOSAKOWSKI G., GROLIMUND D., VAN LOON L.R., MÄDER U. (2016)
Barite precipitation following celestite dissolution in a porous medium: A SEM/BSE and μ-XRD/XRF study. Geochim. Cosmochim. Acta 182, 131–144.

PRIETO M. (2014)
Nucleation and supersaturation in porous media (revisited). Mineral. Mag., 78(6), 1437–1447.

REED M.H. (1982)
Calculation of multicomponent chemical equilibria and reaction processes in systems involving minerals, gases and an aqueous phase. Geochim. Cosmochim. Acta 46, 513-528.

SAMPER J., XU T., YANG C. (2009)
A sequential partly iterative approach for multicomponent reactive transport with CORE^{2D}. Comput. Geosci., 13:301–316.

SVERJENSKY D.A., HARRISON B., AZZOLINI D. (2014)
Water in the deep Earth: The dielectric constant and the solubilities of quartz and corundum to 60 kb and 1200 °C. Geochim. Cosmochim. Acta 129, 125-145.

TANGER J.C., HELGESON H.C. (1988)
Calculation of the thermodynamic and transport properties of aqueous species at high pressures and temperatures; revised equations of state for the standard partial molal properties of ions and electrolytes. Am. J. Sci. 288, 19-98.

THOENEN T., HUMMEL W., BERNER U., CURTI E. (2014)
The PSI/Nagra Chemical Thermodynamic Database 12/07. PSI Bericht Nr. 14-04, ISSN 1019-0643.

VINOGRAD V.L., KULIK D.A., BRANDT F., KLINKENBERG M., WINKLER B., BOSBACH D. (2016)
Thermodynamics of the solid solution - aqueous solution system $(Ba,Sr,Ra)SO_4 + H_2O$. 70 p., to be submitted

WAGNER W., PRUSS A. (2002)
The IAPWS formulation 1995 for the thermodynamic properties of ordinary water substance for general and scientific use. J. Phys. Chem. Ref. Data, 31(2), 387–535.

WEIS P., DRIESNER T., COUMOU D., GEIGER, S. (2014)
Hydrothermal, multiphase convection of H2O-NaCl fluids from ambient to magmatic temperatures: a new numerical scheme and benchmarks for code comparison. Geofluids 14, 347–371

YAPPAROVA A., GABELLONE T., WHITAKER F., KULIK D.A., MATTHAI S. (2016)
Reactive transport modelling of dolomitisation using the new CSMP+ +GEM coupled code: governing equations, solution method and benchmarking results. Transport in Porous Media (in revision)

ZHANG Z., DUAN Z. (2002)
Prediction of the PVT properties of water over wide range of temperatures and pressures from molecular dynamics simulation. Phys. Earth Planet. Inter. 149, 335-354.

Comsol Multiphysics: http://www.comsol.com

Fenics Modelling Platform http://fenicsproject.org/

Geochemical Modelling Software GEMS
http://gems.web.psi.ch

Nanocem Research Network:
http://www.nanocem.org

PHREEQC Algorithm: http://www.hydrochemistry.eu

Reaktoro Framework: http://www.reaktoro.org

3 CLAY SORPTION MECHANISMS

B. Baeyens, R. Dähn, M. Marques Fernandes, T. Thoenen, A. Schaible, E. Eltayeb, A. Kéri (PhD student), S. Wick (PhD student)

3.1 Introduction

The research activities in 2016 were focused on resolving open questions in sorption behaviour of selected nuclides and preparing thermodynamic sorption data bases (TD-SDB) for the safety analyses to be carried out in Stage 3 of the Sectoral Plan (SGT-E3). The development of TD-SDBs for mont-morillonite and illite has been completed (BAEYENS & BRADBURY 2017; BRADBURY & BAEYENS 2017). The TD-SDB was derived from the 2 Site Protolysis Non Electrostatic Surface Complexation and Cation Exchange (2SPNE SC/CE) sorption model which relies on well-defined structural and thermodynamic parameters such as sorption site types, site capacities, selectivity coefficients and surface complexation constants. In addition, the influence of competitive sorption on the solid liquid distribution ratios (K_d values), used for the provisional safety analyses for SGT-E2 for MX-80 and Opalinus Clay, was evaluated and summarized in a final report (BRADBURY et al. 2017). The reports on these topics are currently under external peer review.

The main activities in 2016 were devoted to the mechanistic sorption investigations on clay minerals and the topics studied are listed below:

- The sorption of Pb on montmorillonite and illite was investigated by batch sorption experiments and modelling using the 2SPNE SC/CE sorption model.
- Zn sorption studies on illite and the application of the bottom up approach on Boda Clay and Opalinus Clay.
- Np^V sorption studies on montmorillonite in the absence and presence of ferrous iron under electrochemically reducing conditions are on-going.
- In the framework of the PhD project of S. Wick (in collaboration with Eawag) sorption measure-ments and modelling of Tl on illite have started.
- Spectroscopic and atomistic studies on structural Fe in montmorillonite have continued in the 2nd year of the PhD project of A. Kéri.

A research proposal on cryo-microspectroscopy at the microXAS beamline for the investigation of redox- and radiation-sensitive samples has been prepared in collaboration with SYN/microXAS and Eawag. The proposed project has successfully passed the evaluation in the framework of the PSI-CROSS initiative and was approved for funding.

3.2 Mechanistic sorption studies

3.2.1 Sorption of Pb on montmorillonite and illite

Pb is one of few key radionuclides missing in the TD-SDBs so far, due to the absence of reliable experimental data. Sorption edges and isotherms of Pb on homoionic Na forms of montmorillonite (SWy-2) and illite du Puy (IdP) were determined. The experimental results for one edge and one isotherm on both clays are shown in Fig. 3.1. The data have been modelled using the 2SPNE SC/CE sorption model (BRADBURY & BAEYENS 1997, 2009) and the model parameters given in Table 3.1. The experimental results could be quantitatively well described. The uptake of Pb on illite is more pronounced as on montmorillonite. The cation exchange selectivity coefficients and the surface complexation constants summarized in Table 3.1 are important basic data and will be used in future safety analyses in SGT-E3.

Table 3.1: Surface complexation constants on strong and weak sites and selectivity coefficients for Pb sorption on Na-SWy-2 and Na-IdP.

Surface complexation reactions	SWy-2	IdP
Strong sites	log ^{S}K	
$\equiv S^{S}OH + Pb^{2+} \Leftrightarrow \equiv S^{S}OPb^{+} + H^{+}$	1.1	2.7
$\equiv S^{S}OH + Pb^{2+} + H_2O \Leftrightarrow \equiv S^{S}OPbOH^{0} + 2H^{+}$	-7.6	-5.0
$\equiv S^{S}OH + Pb^{2+} + 2H_2O \Leftrightarrow \equiv S^{S}OPb(OH)_2^{-} + 3H^{+}$	-17.0	-
Weak sites	log ^{W1}K	
$\equiv S^{W1}OH + Pb^{2+} \Leftrightarrow \equiv S^{W1}OPb^{+} + H^{+}$	-1.5	0.3
Cation exchange	K_c	
$2\ Na^{+}$-clay + $Pb^{2+} \Leftrightarrow Pb^{2+}$-clay + $2Na^{+}$	11.0	20.0

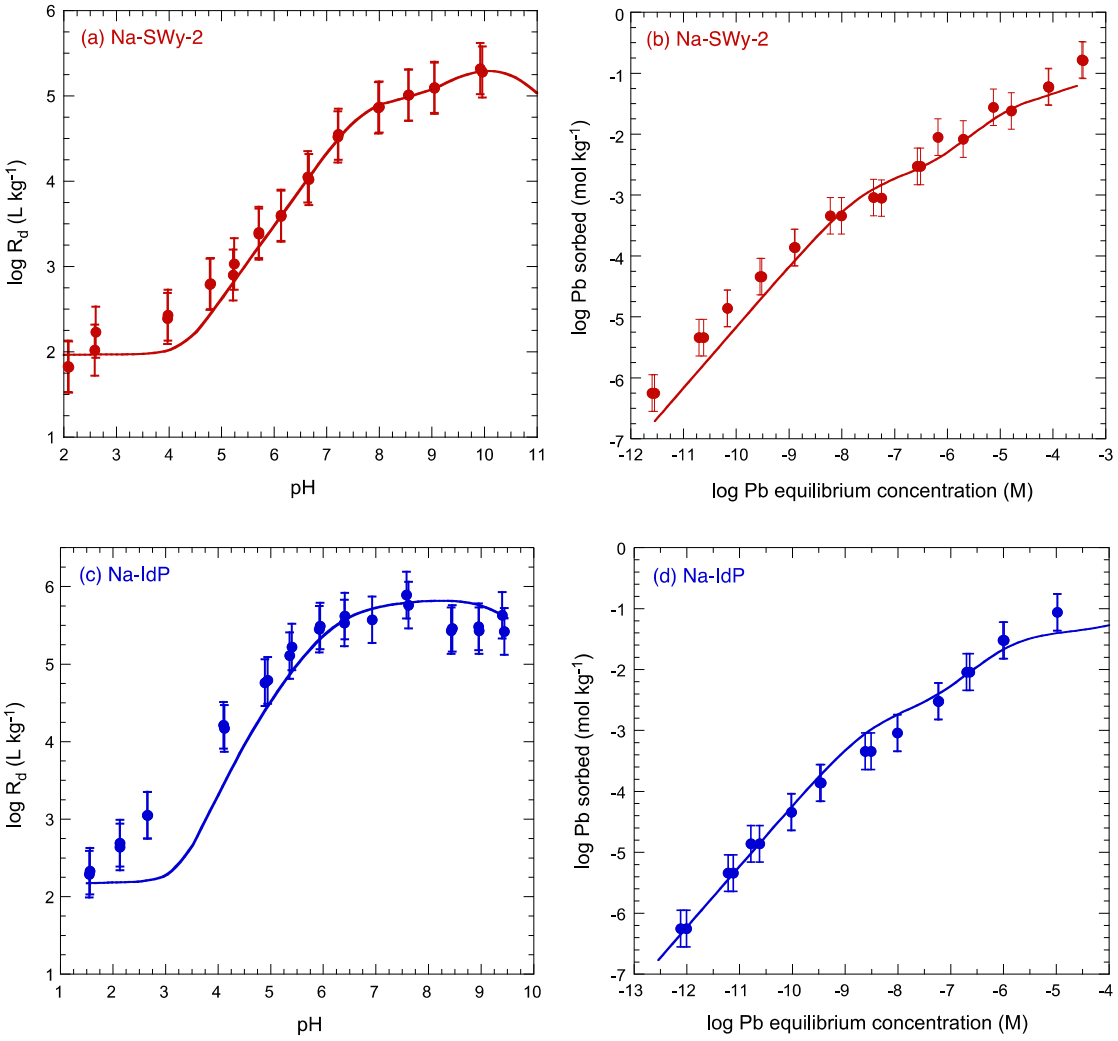

Fig. 3.1: Pb sorption data and modelling on Na-SWy-2 and Na-IdP in 0.1 M $NaClO_4$. Sorption edges (a,c) and sorption isotherms at pH= 6.9 and (b) pH = 7.0 (d).

3.2.2 Zn sorption on illite and argillaceous rocks

3.2.2.1 Experimental, modelling and spectroscopic studies of Zn sorption on illite

Zn sorption edges on Na- and K-IdP and an isotherm at pH 7.2 on Na-IdP were measured. The data were modelled with the 2SPNE SC/CE sorption model for illite with the cation exchange and surface complexation constants given in Table 3.2. The experimental data and the modelling results are shown in Fig. 3.2. The broken and coloured curves in Fig. 3.2 are the calculated contributions of the various surface species to the overall sorption represented by the black continuous lines.

Table 3.2: Surface complexation constants on strong and weak sites and selectivity coefficients for Zn uptake on Na-IdP.

Surface complexation reactions on strong sites	log ^{S}K
$\equiv S^{S}OH + Zn^{2+} \Leftrightarrow \equiv S^{S}OZn^{+} + H^{+}$	2.3
$\equiv S^{S}OH + Zn^{2+} + H_2O \Leftrightarrow \equiv S^{S}OZnOH^{0} + 2H^{+}$	-6.4
$\equiv S^{S}OH + Zn^{2+} + 2H_2O \Leftrightarrow \equiv S^{S}OZn(OH)_2^{-} + 3H^{+}$	-14.9
Surface complexation reaction on weak sites	log ^{W1}K
$\equiv S^{W1}OH + Zn^{2+} \Leftrightarrow \equiv S^{W1}OZn^{+} + H^{+}$	-1.0
Cation exchange reaction on planar sites	log K_c
$2\ Na^{+}\text{-PS} + Zn^{2+} \Leftrightarrow Zn^{2+}\text{-PS} + 2Na^{+}$	0.6
$2\ Na^{+}\text{-HA} + Zn^{2+} \Leftrightarrow Zn^{2+}\text{-HA} + 2Na^{+}$	4.2

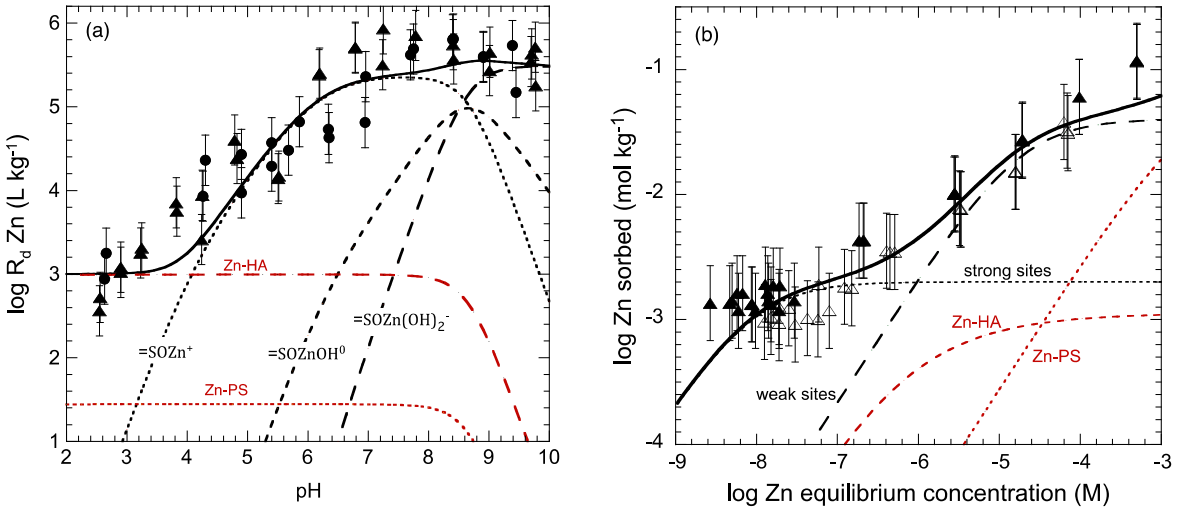

Fig. 3.2: Zn sorption on IdP: (a) edges on Na-IdP in 0.1 M $NaClO_4$ (●) and on K-IdP in 0.1 M KNO_3 (▲) and (b) sorption isotherm at pH 7.2 in 0.1 M $NaClO_4$. Experimental data and modelling.

The sorption behaviour of Zn on illite resembles the uptake of other transition metals such as Ni and Co (BRADBURY & BAEYENS 2009) with the exception that in the pH region from 2 to 4 the sorption of trace Zn is much higher and could not be fitted with the Zn-Na selectivity coefficient (K_c) equal to 4 on the planar sites (PS) of illite (LES PROGRESS REPORT 2015). A high affinity (HA) exchange site had to be introduced to reproduce the full edge. The site capacity of this HA site was taken to be 1 % of the CEC. The structural nature of these HA sites is not yet understood and further investigations are necessary to confirm this preliminary model assumption.

EXAFS was used to provide additional information on the Zn sorption processes occurring along the isotherm at the molecular level. The EXAFS measurements were performed at the Beamline 11-2 at the Stanford Linear Accelerator Center (SLAC, USA) in fluorescence mode using a 100-element solid state Ge detector. Samples with increasing Zn loadings (Zn1 to Zn4) equilibrated for 7 days (Zn1,4-7d) and 2 years (Zn1,4-2y) as well as the clay itself (intrinsic available Zn) were measured.

The k^3 weighted K-edge EXAFS spectra obtained for Zn intrinsically incorporated in pure illite (Zn-inc.), Zn1-7d and Zn1-2y illite samples are very similar (Fig. 3.3a). This indicates that the amount of 2.1 mmol kg^{-1} Zn taken up is located on edge positions which have a very similar coordination environment as Zn atoms incorporated in the structure. With increasing metal loading small changes are visible, *e.g.* the amplitude of the peaks at $R+\Delta R$ = 3.0 and 3.8 Å decreases (Figs. 3.3b + c).

Data analysis showed that the illite intrinsic Zn is surrounded by one O shell at 2.07 Å, one Al Shell at 3.02 Å and one Si shell at 3.25 Å. This local structure is characteristic of octahedral Zn in a 2:1 phyllosilicate environment (Dähn et al. 2011). Further, the analysis showed that Zn is surrounded by 2.5(9) Al at 3.02(3) Å and 4.4(9) Si2 at 3.25(1) Å. The fact that Zn appears to be surrounded by ~3 Al, and not 6, in illite further indicates that Zn substitutes for Al and does not fill an empty site from the dioctahedral aluminium sheet.

Data analysis for the Zn samples after 7 reaction days indicates that $CN_{Zn\text{-}Al}$ and $CN_{Zn\text{-}Si}$ are decreasing with increasing loading ($CN_{Zn1\text{-}Al}$ = 2.0(6) vs. $CN_{Zn4\text{-}Al}$ = 1.5(5), and $CN_{Zn1\text{-}Si}$ = 4.0(7)) vs. $CN_{Zn4\text{-}Si}$ = 2.3(5)). In addition a slight decrease of $R_{Zn\text{-}Al}$ and $R_{Zn\text{-}Si}$ with increasing loading was observed ($R_{Zn1\text{-}Al}$ = 3.02(3) Å vs. $R_{Zn4\text{-}Al}$ = 3.06(3) Å, and $R_{Zn1\text{-}Si}$ = 3.24(1) Å vs. $R_{Zn1\text{-}Si}$ = 3.27(2) Å).

The decrease of coordination numbers of Zn-Al/Si backscattering pairs and increase of Zn-Al and Zn-Si distances in the samples for a reaction time of two years were less pronounced ($CN_{Zn1\text{-}Al}$ = 2.1(5)) vs. $CN_{Zn4\text{-}Al}$ = 2.0(5), and $CN_{Zn1\text{-}Si}$ = 3.6(5)) vs. $CN_{Zn4\text{-}Si}$ = 3.0(5), and $R_{Zn1\text{-}Al}$ = 3.03(2) Å vs. $R_{Zn4\text{-}Al}$ = 3.03(1) Å, and $R_{Zn1\text{-}Si}$ = 3.24(1) Å vs. $R_{Zn1\text{-}Si}$ = 3.27(1) Å)).

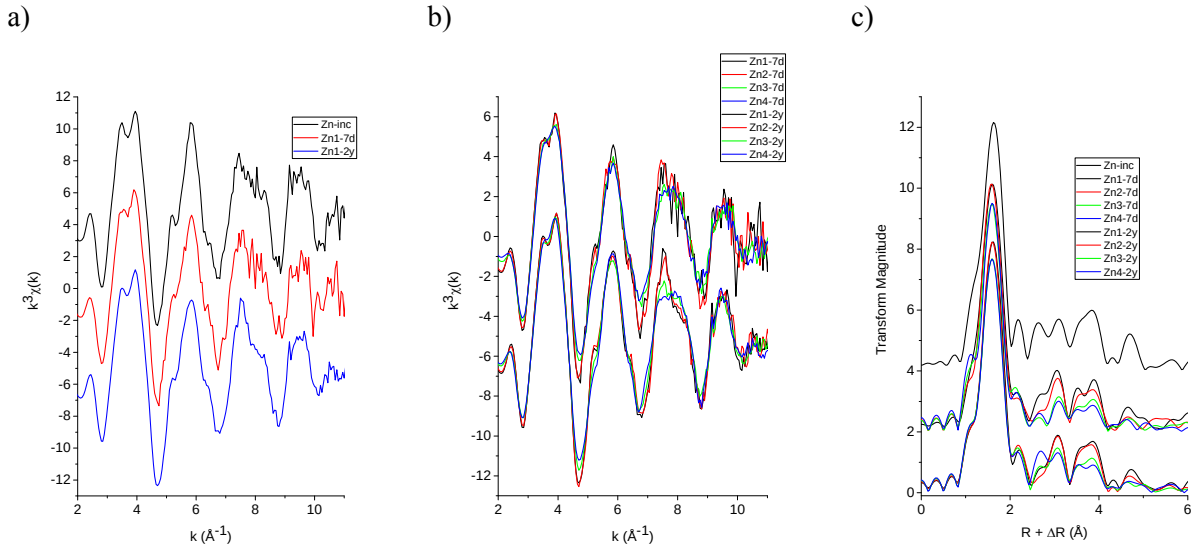

Fig. 3.3: Comparison of the k^3-weighted Zn K-edge EXAFS spectra of a) pure illite, Zn1-7d and Zn1-2y, b) of the Zn treated illite samples, and c) the corresponding RSFs.

3.2.2.2 Testing the bottom up approach for Zn uptake on Boda Clay and Opalinus Clay

In the framework of the RaWaDi project the validity of the "bottom-up" modelling methodology on Boda Clay and Opalinus Clay was investigated for a number of radionuclides (MARQUES FERNANDES et al. 2015). In this project the transition element Zn was also studied because EXAFS spectra for Zn yield lower detection limits and subsequently a better signal to noise ratio in the Fe-rich rock matrix than Ni and Co.

The "bottom-up" modelling approach is based on the premise that Zn uptake in complex mineral/ groundwater systems can be quantitatively described from the sorption model developed for illite (see section 3.2.2.1). Here the 2SPNE SC/CE sorption model was used to make blind predictions of the Zn sorption isotherms on both argillaceous rocks.

Sorption isotherms for Zn were measured on Boda Clay and Opalinus Clay in their respective synthetic porewaters (MARQUES FERNANDES et al. 2015). The sorption predictions were then carried out using the sorption model developed for illite and the results were scaled over the illite and illite/smectite weight content in the sample. A good agreement between the measured data and the predicted values was found for the lower concentration range of the isotherms, see Fig. 3.4. However, the blind predictions clearly underpredict Zn sorption at higher Zn equilibrium concentrations. The same trend was observed for the sorption of Co and Ni on both rocks (MARQUES FERNANDES et al. 2015).

EXAFS measurements were performed at the Beam-line 11-2 at the SSRL. The k^3-weighted K-edge of Zn-EXAFS spectra for both argillaceous rocks are shown in Fig. 3.5. Additionally, the EXAFS spectra of the Zn intrinsically available in these rocks (~ 2 mmol kg^{-1} in Boda Clay and 4 mmol kg^{-1} in Opalinus Clay) was measured (see Fig. 3.5). The spectral features of this intrinsic Zn are typical for structurally incorporated Zn in 2:1 phyllosilicates (DÄHN et al. 2011).

EXAFS spectra of the low loaded Zn Boda Clay and Opalinus Clay samples exhibit mixed spectral features of incorporated and/or sorbed species (Figs. 3.5). Thus, based on this similarity, and the absence of any characteristic features of Zn precipitation, it can be concluded that at these low metal loadings inner-sphere complexation is the predominant uptake mode.

Consequently, in the isotherm region where prediction and measurement coincide, sorption through inner sphere complexation seems to be the main uptake mechanism.

The splitting of the EXAFS oscillation at $k \sim 8$ $Å^{-1}$ in the higher loaded Zn Boda Clay and Opalinus Clay samples is characteristic for Zn-Zn backscattering pairs, indicating the precipitation of Zn solid phases, even though the initial Zn concentrations were below the solubility limits of Zn-hydroxide. These EXAFS results clearly show precipitation as an additional process in the isotherm region where prediction and measurement deviate, and is probably the reason for the mismatch between the modelling and the experimental data (Fig. 3.4). The similarity of the spectra with those of Zn layered double hydroxides (LDH) and Zn phyllosilicates supports this hypothesis (see Fig. 3.5).

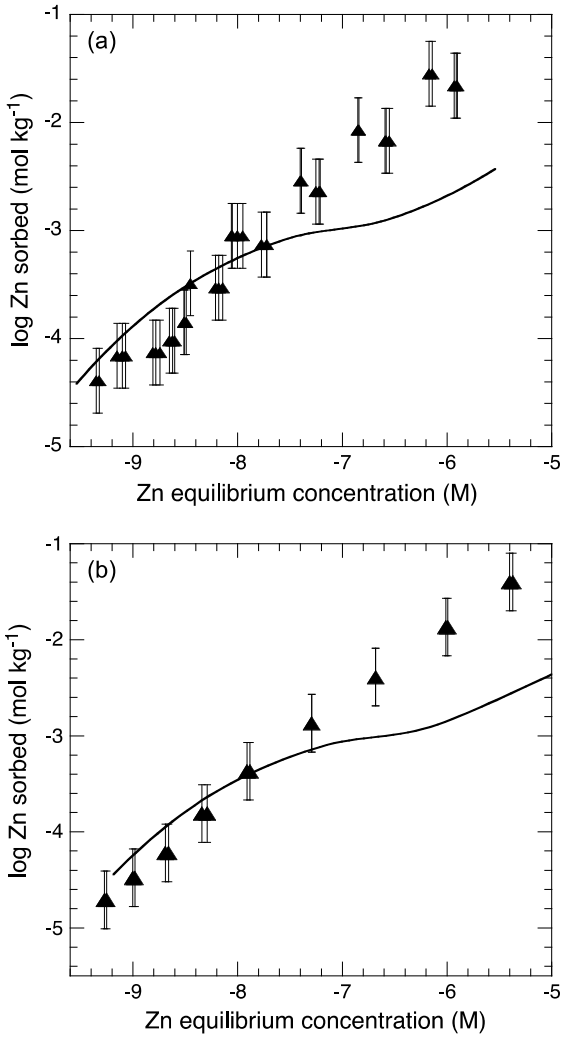

Fig. 3.4: Zn sorption isotherms on a) Boda Clay (Ib-4) at pH 8.1 and b) Opalinus Clay (SLA-938) at pH 8.0: Experimental results (symbols) and blind predictions (continuous line).

3.2.3 Sorption of NpO_2^+ onto montmorillonite under electrochemically reducing conditions in the presence and absence of dissolved Fe^{II}

The sorption of NpO_2^+ on montmorillonite (Na-STx-1) was measured in 0.1 NaCl (initial Np concentration: $[Np]_{in} = 2.5 \cdot 10^{-5}$ M; S:L ratio ~$4.3 \cdot 10^{-3}$ kg·L^{-1}) in the absence and presence of ferrous iron under reducing conditions to simulate repository relevant conditions. The experiments were carried out in a bulk electrolysis cell composed of a three electrode system (i) a glassy carbon working electrode, (ii) an Ag/AgCl reference electrode, and (iii) a coiled platinum wire auxiliary electrode at a fixed redox potential, E_h = −291 mV vs SHE. In both experiments the initial pH was set to 7.8 and the NpO_2^+ montmorillonite system was first let to equilibrate under anoxic conditions (log R_d ~ 1.8 L·kg^{-1}).

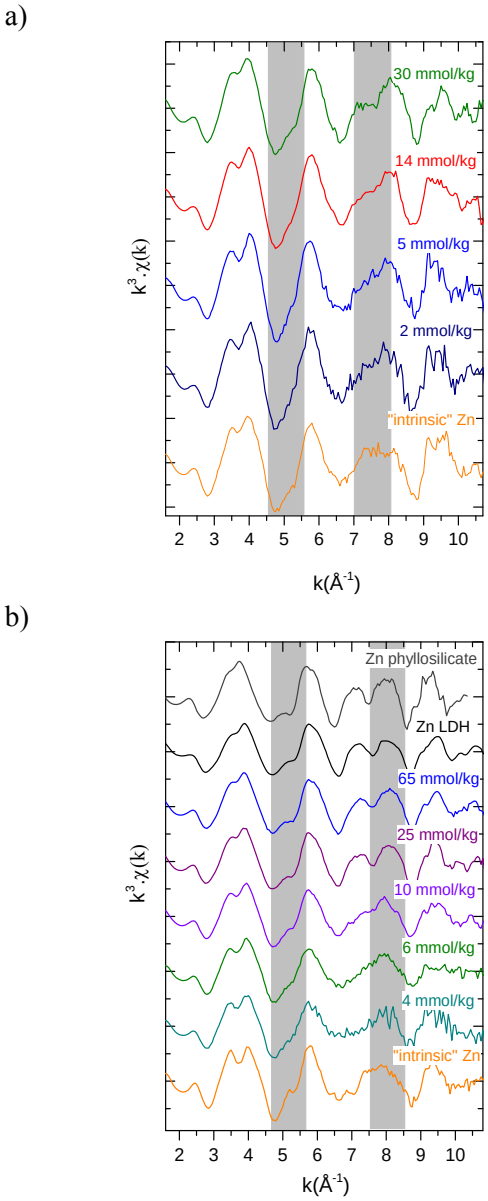

Fig. 3.5: k^3-weighted K-edge Zn-EXAFS spectra a) Opalinus Clay and b) for Boda Clay at different Zn loadings and 2 reference spectra (Zn-phyllosilicate and Zn-LDH).

After three days the electrochemical potentials were set to -291 mV in both cells. In one cell ferrous iron was additionally admixed ($[Fe^{II}]_{in}$=$2.1 \cdot 10^{-4}$ M). Sampling at regular intervals during 14 days allowed following the evolution of the sorption under reducing conditions in the absence and presence of Fe^{II} as shown in Fig. 3.6a. In the cell without ferrous iron, the sorption of NpO_2^+ remained nearly constant and no noticeable increase of sorption compared to anoxic conditions could be observed. The NpO_2^+ concentration was probably too low to be electroactive, even so UO_2^{2+}sorption experiments on STx carried out under similar experimental conditions lead to complete reduction of U(VI) to U(IV) (see LES PROGRESS REPORT 2015).

In the presence of ferrous iron, the sorption of NpO_2^+ steadily increased, and reached a plateau (log R_d ~ 3.8 $L \cdot kg^{-1}$) after 14 days (see Fig. 3.6a). $[Fe^{II}]_{eq}$ of $8.1 \cdot 10^{-6}$ M was determined by UV/Vis spectroscopy using the 1,10-phenantroline method, corresponding to an Fe loading of ~ 44 $mmol \cdot kg^{-1}$. The pH value increased during the experiment from ~ 7.7 up to ~8.8. A light reddish shading of the clay paste was observed suggesting the presence of some ferric iron (Fe^{III}) at the clay surface.

The increase of sorption under the electrochemically reducing conditions suggests the reduction of Np^V to Np^{IV}. Evidence for the oxidation state and type of surface complex formed was obtained from spectroscopy. EXAFS spectroscopy was performed on both Np-montmorillonite samples. The measurements were carried out at the Np L_{III} edge in fluorescence mode at the ROBL Beamline, ESRF in Grenoble.

Figs. 3.6b and c clearly evidence that under reducing conditions and in the presence of ferrous iron NpO_2^+ sorbed on montmorillonite becomes fully reduced to Np^{IV}. Previous Np sorption experiments performed in the presence of dissolved Fe^{II}, yet, under anoxic conditions showed only a partial reduction of Np^V (see LES PROGRESS REPORT 2015). The derived structural parameters confirm that NpO_2^+ is reduced to Np^{IV} (7 O at 2.3 Å) and suggest a strong association to Fe (3 Fe at ~3.38 Å). The exact nature of the final surface product is still not clear. The precipitation of the solubility limiting NpO_2 solid phase was not observed. Experiments with lower initial Fe^{II} concentrations are planned.

3.2.4 Sorption of thallium on illite

Thallium (Tl) is a highly toxic trace metal. In the environment, Tl occurs in the monovalent and trivalent oxidation state. Tl^+ exhibits both chalcophilic and lithophilic character. Because Tl^+ has a similar ionic radius as K^+, it can substitute K^+ in a wide range of K-bearing minerals. In soils and sediments, Tl^I uptake by the clay mineral illite has long been considered to be a key retention mechanism. Direct evidence for Tl uptake by illite in soils was provided by a recent spectroscopic study on geogenically Tl-rich soils (VOEGELIN et al. 2015). To date, however, data on Tl sorption by illite and its effect on Tl solubility in soils are lacking.

The sorption behaviour of Tl^+ on pure illite (IdP) is currently being investigated by batch experiments.

First results confirm that Tl^+ uptake by illite is highly specific and exhibits similar trends as known for Cs^+. This is illustrated in Fig. 3.7 by a sorption isotherm of Tl on Na-IdP in 0.1 M NaCl at pH 6.6.

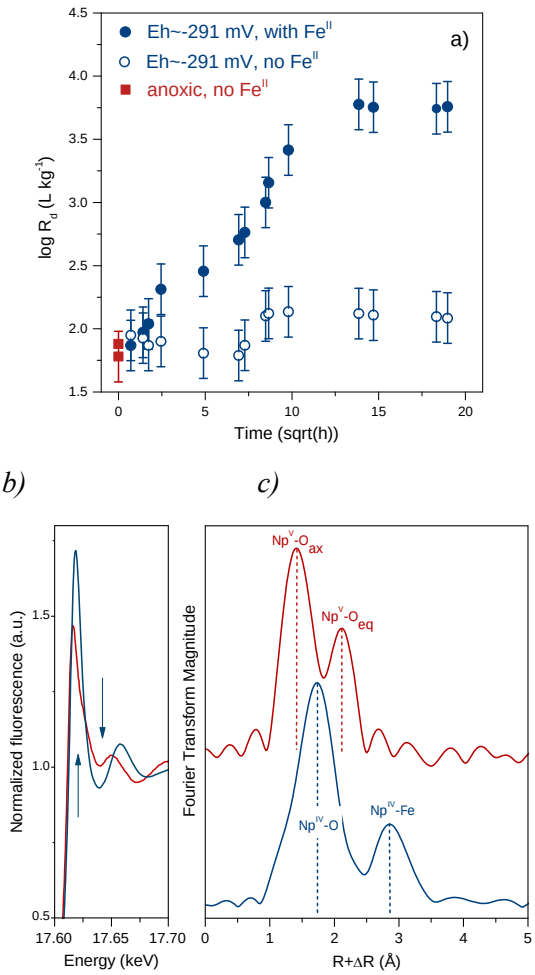

Fig. 3.6: a) Evolution of the sorption of NpO2+ on Na-STx under anoxic conditions (red symbols) and under reducing conditions (-291 mV vs. SHE) in the absence of FeII (blue open symbols) and in the presence of FeII (blue closed symbols). Np-LIII edge XAFS spectra of Np sorbed to STx under reducing conditions in the absence (red) and presence of FeII (blue): b) XANES spectra and c) Fourier transforms (FTs).

The isotherm of Tl^+ on illite could be quantitatively described with a similar sorption model as developed for Rb^+ and Cs^+ uptake on ilite (BROUWER et al. 1983; POINSSOT et al. 1999). The site capacities and selectivity coefficients used for the modelling are summarized in Table 3.3. The measurement and modelling of sorption edges and isotherms on Na- and K-illites are ongoing.

Further insight into Tl uptake by illite and Tl speciation in soils will be obtained by combined analysis of macroscopic sorption experiments, soil extractions and EXAFS studies. The obtained results and their model based interpretation will contribute to an improved quantitative and mechanistic understanding of the solubility, mobility and bioavailability of Tl in soils.

Table 3.3: Summary of the parameters derived from the fitting of Tl sorption on Na-IdP.

Site type	Site capacity	Cation exchange reaction	Selectivity coefficient values
Frayed edge site	0.56 meq kg^{-1}	Na-FES + Tl^+ ⇔ Tl-FES + Na^+	$\log {}^{Tl}_{Na}K_c^{FES} = 6.3$
Type II site	45 meq kg^{-1}	Na-II + Tl^+ ⇔ Tl-II + Na^+	$\log {}^{Tl}_{Na}K_c^{II} = 3.5$

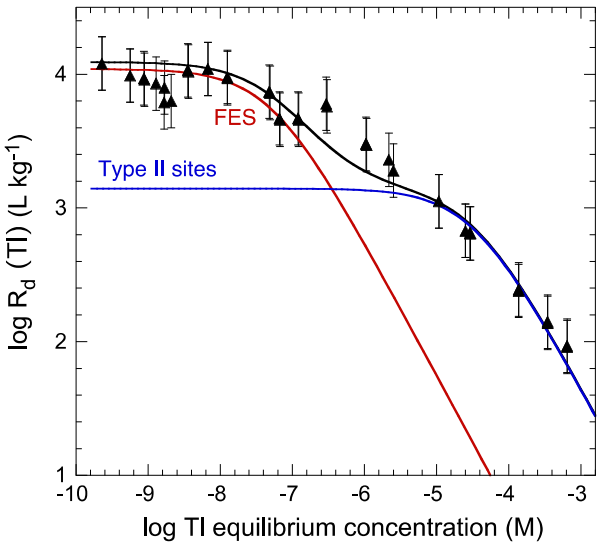

Fig. 3.7: Tl sorption on conditioned Na IdP as a function of Tl concentration in 0.1 M NaCl at pH 6.6. The continuous curve is a fit to the data using the parameter values given in Table 3.3. The red and blue lines are the contributions by FES and type II sites to the overall sorption of Tl, respectively.

3.3 Mechanistic understanding of sorption processes

3.3.1 Atomistic modelling of $Fe^{II/III}$ uptake by clay minerals

Atomistic simulations of mineral fluid interfaces provide direct insight into the molecular mechanism of ion adsorption by mineral surfaces. Combining such simulations with spectroscopic studies can help to obtain quantitative interpretation of spectroscopic observation both in terms of structural and compositional information. To this aim it is essential to develop a reliable method for the simulations of XAS spectra. In the first year of the SNF funded PhD project "*Detailed understanding of metal adsorption on clay minerals obtained by combining atomistic simulations and X-ray absorption spectroscopy*", the structural environment of Fe^{II} and Fe^{III} incorporated in Milos montmorillonite has successfully been modelled. On the basis of the molecular dynamics trajectories, the theoretical EXAFS and XANES spectra were calculated (Fig. 3.8). The calculations were used to identify the preferential structural position and the oxidation state of Fe in Milos montmorillonite. The interpretation of spectroscopic data indicate that iron is present in montmorillonite in Fe^{III} oxidation state while the ions are equally distributed between the cis- and trans- octahedral positions in the octahedral layer of the montmorillonite (Fig. 3.8). The draft of the manuscript summarizing the simulation results is being prepared for submission (KÉRI et al. 2017).

The investigation of Fe incorporated in the bulk montmorillonite served a well-defined benchmark which allowed us to verify the modelling parameters and the simulation setup. Currently, (in the second project year) the trajectories of Fe adsorbed on the surface sites of montmorillonite are being evaluated. The molecular dynamics trajectories used to calculate theoretical spectra of inner- and outer-sphere surface complexes and to interpret the experimental observations.

3.3.2 Development of cryo-microspectroscopic techniques for redox- and radiation-sensitive samples

In the past years, synchrotron-based micro-focused X-ray fluorescence (micro-XRF), X-ray absorption spectroscopy (micro-XAS) and X-ray diffraction (micro-XRD) have developed into powerful tools for spatially resolved micro-scale investigations of the speciation of trace elements (contaminants, nutrients) in heterogeneous environmental samples such as soils, sediments, rocks or organic materials. However, it has also become increasingly evident that the high photon flux density at 3rd-generation synchrotron sources may induce radiation damage, including structural changes in host phases of trace elements such as metal oxides or natural organic matter or direct changes in the oxidation state and speciation of trace elements. Sample cooling helps to prevent or strongly attenuate radiation-induced damage. Therefore, a research proposal on cryo-microspectroscopy at the microXAS beamline for the investigation of redox- and radiation-sensitive samples has been prepared in collaboration with SYN/microXAS and Eawag. The proposed project has successfully passed the evaluation within the framework of the PSI-CROSS initiative.

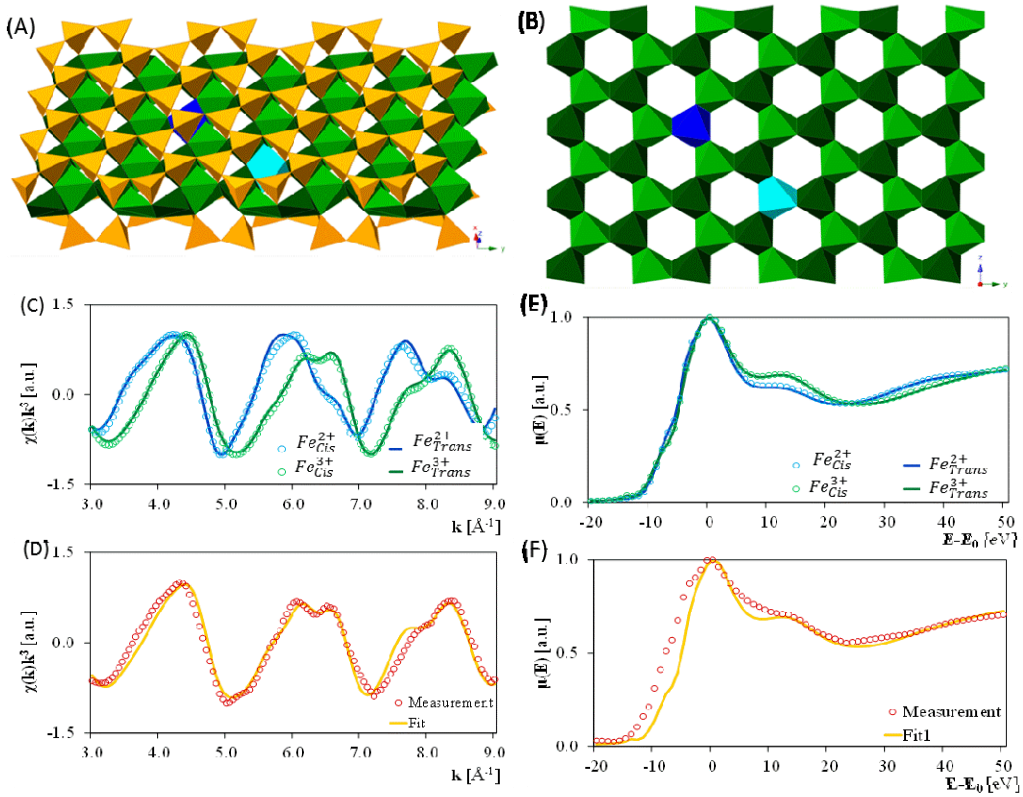

Fig. 3.8: Modelling approach to assess the mechanism of Fe incorporation in Milos montmorillonite (A). Insert (B) shows the octahedral layer of the same system setup presented in insert (A). Yellow color represents Si tetrahedral, Al octahedral are shown with green color while Fe incorporation is marked with blue color. Light colors in the octahedral layer represent cis while dark colors show trans occupational sites in respect to the relative positions of the hydroxyl groups. The system setup used in this study contained about 600 atoms. The calculated EXAFS and XANES spectra of Fe substitution in the bulk montmorillonite for ferrous and ferric ions are shown in insert (C) and (E), respectively. The linear combination fits of the calculated EXAFS and XANES spectra to the measured one are represented in insert (D) and (F), respectively.

A two years postdoc position and the investment funds for He/N_2-cryostates were granted. The project is aimed at the development of the infrastructure at the microXAS beamline for the analysis of radiation-sensitive samples at temperatures of 10-80 K and to perform exemplarily microspectroscopic studies on Tl in soils to advance our mechanistic understanding of key Tl retention mechanisms.

3.4 References

BAEYENS B., BRADBURY M.H. (2017)
The development of a thermodynamic sorption data base (TD-SDB) for montmorillonite and the application to bentonite: Nagra Technical Report, (in prep.).

BRADBURY M.H., BAEYENS B. (1997)
A mechanistic description of Ni and Zn sorption on Na-montmorillonite Part II: modelling: J. Contam. Hydrol. 27, 3–4, 223-248.

BRADBURY M.H., BAEYENS B. (2009)
Sorption modelling on illite Part I: Titration measurements and the sorption of Ni, Co, Eu and Sn: Geochim. Cosmochim. Acta 73, 4, 990-1003.

BRADBURY M.H., BAEYENS B. (2017)
The development of a thermodynamic sorption data base (TD-SDB) for illite and the application to argillaceous rocks: Nagra Technical Report, (in prep.).

BRADBURY M.H., MARQUES FERNANDES, M., BAEYENS B. (2017)
Estimates of the influence of radionuclide solubility limits and sorption competition on the sorption values in the SDBs of MX-80 bentonite and Opalinus Clay: Nagra Technical Report, (in prep.).

BROUWER E., BAEYENS B., MAES A., CREMERS A. (1983)
Cesium and rubidium ion equilibria in illite clay: J. Phys. Chem., 87, 1213-1219.

DÄHN R., BAEYENS B., BRADBURY M.H. (2011)
Investigation of the different binding edge sites for Zn on montmorillonite using P-EXAFS – The strong/weak site concept in the 2SPNE SC/CE sorption model: Geochim. Cosmochim. Acta, 75, 5154-5168.

KÉRI A., DÄHN R., KRACK M., CHURAKOV S.V. (2017)
Combined XAFS spectroscopy and ab initio study on the characterization of iron incorporation by montmorillonite: In preparation.

MARQUES FERNANDES M., VÉR N., BAEYENS B. (2015)
Predicting the uptake of Cs, Co, Ni, Eu, Th and U on argillaceous rocks using sorption models for illite: Appl. Geochem. 59, 189-199.

POINSSOT C., BAEYENS B., BRADBURY M.H. (1999)
Experimental and modelling studies of caesium sorption on illite: Geochim. Cosmochim. Acta, 63, 3217-3227.

VOEGELIN A., PFENNINGER N., PETRIKIS J., MAJZLAN J., PLÖTZE M., SENN A.C., MANGOLD S., STEININGER R., GÖTTLICHER J. (2015)
Thallium speciation and extractability in a thallium- and arsenic-rich soil developed from mineralized carbonate rock: Environ. Sci. Technol. 49, 5390-5398.

4 CEMENT SYSTEMS

E. Wieland, J. Tits, L. Nedyalkova (PhD student), A. Mancini (PhD student), A. Laube, D. Kunz, W. Hummel, B.Z. Cvetković (post doc)

4.1 Introduction

The group "Cement Systems" carries out research in connection with the long-term assessment of the behaviour of important waste components and on radionuclide-cement interactions in the near field of the deep geological repositories for low-level and short-lived intermediate-level (L/ILW) and long-lived intermediate-level (ILW) radioactive waste in Switzerland.

In 2016 the main activities focused on i) a review of the origin and chemistry of selected safety-relevant radionuclides, ii) modelling the chemical processes in selected waste sorts in conjunction with long-term predictions of the evolution of the heterogeneity in the cementitious near field, iii) the development of compound-specific ^{14}C AMS (accelerator mass spectrometry) for the detection of ^{14}C-bearing compounds at very low ^{14}C concentrations, iv) measurements of the low molecular weight (LMW) organics produced during the anoxic corrosion of non-activated and activated steel, v) the development of a methodology suitable to investigate the chemical stability of LMW organics under conditions relevant to a cement-based near field, and vi) mechanistic sorption studies with redox-sensitive, dose-determining Se(IV/-II) anions on hardened cement paste (HCP) and cement phases.

The ^{14}C project comprises work on LMW organic corrosion products and the development of a very sensitive ^{14}C AMS-based analytical method for the determination of ^{14}C-bearing compounds. This research is partially funded by swissnuclear (Project title: "Investigation of the chemical speciation of ^{14}C released from activated steel") and by the EU FP7 collaborative project "CAST" (CArbon Source Term). Specific tasks within this project have been developed in co-operation with PD Dr. S. Szidat and Dr. G. Salazar (Department of Chemistry & Biochemistry at the University of Bern, Switzerland), and Brechbühler AG (Schlieren, Switzerland), the commercial partner in the project.

An EU-funded PhD project carried out jointly with Empa (Dr. B. Lothenbach) was started in 2016 focussing on the interaction of Se with cementitious materials under reducing conditions. L. Nedyalkova joined Empa on January 1st, 2016, for this project and from 2017 on she will perform her research on the subject at both institutes. The project is carried out in collaboration with Dr. A. Scheinost (Rossendorf (ROBL) beamline at the ESRF) and funded by the EU Horizon 2020 collaborative project "CEBAMA" (CEment-BAsed MAterials, properties, evolution, barrier functions).

A second PhD study was started in 2016 focusing on the speciation of Fe and S in reducing cementitious systems. A. Mancini joined LES on April 1st, 2016. The project is funded by the Swiss National Science Foundation (SNF grant No. 200021_162342/1).

PD Dr. W. Hummel joined the group on July 1st, 2016, due to a LES internal reorganization. Progress in his research will be documented in the following section.

4.2 Activities in support of the Sectoral Plan

The two main activities undertaken in 2016 to support assessments required in connection with the Sectoral Plan comprise i) a review of the origin and chemistry of selected safety-relevant radionuclides, and ii) long-term predictions of the evolution of the chemical conditions in selected waste sorts using thermodynamic modelling.

4.2.1 Chemistry of selected safety-relevant radionuclides

The origin and the chemistry of selected safety-relevant radionuclides have been reviewed. The selected nuclides are ^{36}Cl, ^{79}Se, ^{108m}Ag and ^{129}I. In a nuclear reactor ^{79}Se and ^{129}I are produced by fission of ^{235}U and ^{239}Pu, while ^{36}Cl and ^{108m}Ag are neutron activation products. The original distribution in waste forms and the chemistry of ^{36}Cl and ^{108m}Ag is briefly compared here.

^{36}Cl and ^{108m}Ag are produced by neutron capture of inactive nuclides: $^{35}Cl + {}^{1}n \rightarrow {}^{36}Cl + \gamma$ and $^{107}Ag + {}^{1}n \rightarrow {}^{108m}Ag + \gamma$. Both ^{35}Cl and ^{107m}Ag have comparably high cross sections of 43.63 and 37.64 barn, respectively. Therefore, the production rate per amount of inactive nuclides, at the same neutron flux, is expected to be similar. Nevertheless, the distribution of the activation products in different waste forms was found to have very different patterns (Fig. 4.1). While ^{36}Cl occurs in many different waste forms in trace quantities, 98.2% of ^{108m}Ag is concentrated in one single waste form. This single waste form comprises control rods of pressurized light-water reactors consisting of a Ag-In-Cd alloy with about 80% metallic Ag. In contrast, ^{35}Cl is a trace impurity in nuclear fuel, in reactor steel and

other metallic compounds. This different origin of ^{36}Cl and ^{108m}Ag provides boundary conditions to their long-term behaviour in a geological repository.

More than 98% of ^{108m}Ag is contained in chunks of metallic Ag. From the known total amounts of silver in this waste form and the amount of activated silver the mole fraction $^{108m}Ag/Ag(total)$ is determined to be 0.0034. This is the "primary isotopic dilution" of ^{108m}Ag. If the metal container and the chunks of metallic Ag corrode, a strongly reducing environment will develop. Silver dissolves then in redox state zero, $Ag(s) \Leftrightarrow Ag(aq)$, with a pH independent solubility of about $3 \cdot 10^{-7}$ mol/L Ag(aq) (KOZLOV & KHODAKOVSKIY 1983). Considering the primary isotopic dilution factor 0.0034, a concentration of $1 \cdot 10^{-9}$ mol/L $^{108m}Ag(aq)$ in the pore water of the corroding waste is expected, corresponding to $3.2 \cdot 10^{4}$ Bq/L or 0.07 mSv/L. If Ag(aq) is oxidized somewhere on its migration pathway it will form AgCl(aq) or $AgCl_2^-$ complexes, depending on the concentration of the Cl^- ubiquitous in pore waters. None of these anionic species is expected to sorb significantly on mineral surfaces.

^{36}Cl is present everywhere in trace quantities, but whenever it is released into pore water it is reduced to $^{36}Cl^-$. In the case of spent fuel, the anion Cl^- will not sorb on clay minerals and it will not be incorporated in any solid phase of the bentonite backfill or the host rock. Weak interactions with cement phases, especially some incorporation in Friedel's salt, $Ca_2Al(OH)_6(Cl,OH) \cdot 2H_2O$, are expected in the cementitious near field of L/ILW and ILW repositories (WIELAND 2014). However, the only overall significant effect is isotopic dilution of $^{36}Cl^-$ by inactive Cl^- always available in any pore water. Last but not least, the calculated concentration of activated ^{36}Cl might be overestimated by orders of magnitude because it depends on very few measurements and several (conservative) assumptions about ^{35}Cl trace concentrations in nuclear fuel, reactor steel and other metallic compounds.

4.2.2 Temporal evolution of the chemical conditions in specific waste sorts

Low- and intermediate-level waste (L/ILW) will be disposed of in a deep geological repository with a cementitious near field. The aim of this project is to investigate the temporal evolution of heterogeneities in the near field. In 2016 thermodynamic modelling was performed with the aim of assessing the chemical conditions in selected waste sorts to be disposed of in a L/ILW repository. The results obtained for one of the cement-stabilized waste sorts (denoted as BA-M-H) containing large amounts of spent ion exchange resins are shown in Fig. 4.2.

The initial inventory of this waste sort is as follows: 236.1 kg cement paste including pore solution, 3 kg gravel (quartz), 2.5 kg low-molecular-weight (LMW) organics, 62.7 kg polystyrene (spent ion exchange resin), 35.9 kg steel, 0.04 kg zinc and 5.7 kg magnetite.

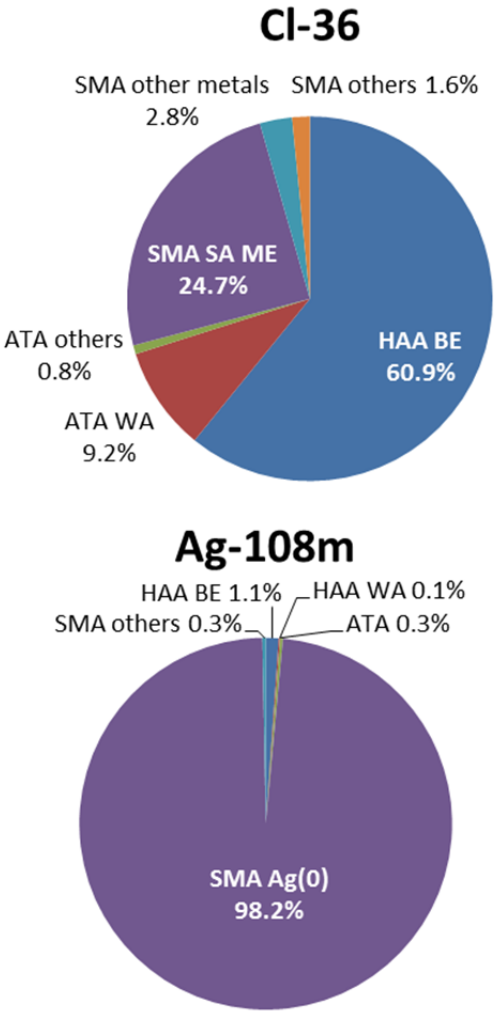

Fig. 4.1: Distribution of ^{36}Cl and ^{108m}Ag in different waste forms in mole percent according to MIRAM 14 (NAGRA 2014). The abbreviations in capitals, taken from MIRAM 14, are HAA BE: high-level waste comprising Spent nuclear Fuel assemblies (SF), HAA WA: vitrified High-Level Waste from reprocessing of spent fuel (HLW), ATA: Alpha-Toxic Waste (ATW, formerly called long-lived Intermediate-Level Waste, ILW), ATA WA: alpha-toxic waste from reprocessing (compacted hulls and ends, vitrified sludges), SMA: Low- and Intermediate-Level Waste (L/ILW), SA ME: decommissioning waste in form of stainless steel from reactor internals.

Other high-molecular-weight organics are present at much lower amounts, such as plastic materials and rubber (total < 0.15 kg). The waste materials are conditioned in cement and cast in 200 L drums.

Thermodynamic modelling of the temporal evolution of the waste sorts was carried out using the GEM-Selektor v3.3 code (KULIK et al. 2013) in the following set-up:

- The basic thermodynamic properties of the cementitious systems were considered as reported in the Nagra/PSI thermodynamic database 12/07 (THOENEN et al. 2014) and the Cemdata 14.01 database (LOTHENBACH et al. 2012a);
- Uptake of alkalis by C-S-H was modelled based on an ideal solid solution model between jennite, tobermorite, $[(KOH)_{2.5}SiO_2H_2O]_{0.2}$ and $[(NaOH)_{2.5}SiO_2H_2O]_{0.2}$ as proposed by KULIK et al. (2007) and using the thermodynamic data reported by LOTHENBACH (2011) and LOTHENBACH et al. (2012b);
- Thermodynamic properties of zeolites were taken from the Thermoddem database (BLANC et al. 2015);
- Thermodynamic data for the Zn and Cu species were taken as given in the SUPCRT database (HELGESON et al. 1978);
- Thermodynamic data of chloride-containing minerals were considered as reported in the SUPCRT database (halite, sylvite) and according to ROBIE & HEMINGWAY (1995) (chloromagnesite, hydrophilite and laurencite).

The degradation of organic materials (i.e. LMW organics and polystyrene in the BA-M-H waste sort), the corrosion of metals (i.e. iron and zinc in the BA-M-H waste sort), and the dissolution of gravel (quartz used as surrogate) were considered according to the reaction rates previously deduced on the basis of literature data. The degradation of organics results in deformation of gaseous compounds: CH_4 and CO_2. The metal corrosion leads to the release of H_2. The dissolution of gravel gives rise to the release of SiO_2. (WIELAND et al. 2016). Hydrogen was considered to be a non-reactive product which is not subjected to further chemical reactions. As a consequence the H_2 volume produced over time and predicted based on thermodynamic modelling was comparable with predictions made on the basis of simple mass balance calculations by considering metal corrosion over those time periods where pH was ≥ 10.5. The other reaction products were equilibrated with the cementitious system. It should further be noted that the degradation of organics, the dissolution of quartz and metal corrosion are water-consuming reactions while carbonation of portlandite and C-S-H are water-releasing reactions.

After each time step the system was equilibrated and the inventory of water and the main waste components, i.e. metallic materials, quartz and organic compounds, the mineral assemblage of the cementitious barrier and the main solution parameters (pH, Eh, most important cations (Na, K, Ca) and anions (total carbonate, Cl^-, SO_4^{2-}, HS^-, total silica)) were determined (Fig. 4.2). Note that the formation of celestite, strontianite, barite and witherite was also observed in addition to the minerals and cement phases listed in Fig. 4.2b. Nevertheless, the inventories of these minerals were found to be very low due to the low Sr and Ba contents of the cements and therefore, these minerals are not displayed in Fig. 4.2b.

Thermodynamic modelling of the initial stage of the cemented BA-M-H waste sort, i.e. prior to the onset of the degradation of organics and gravel as well as metal corrosion, shows that the composition of the solidifying cement paste corresponds to that of a typical cement paste made from ordinary Portland cement, i.e. containing portlandite, C-S-H phases (Ca/Si ratio = 1.55), Al/Fe-containing siliceous hydrogarnet, ettringite, hydrotalcite and calcite. The pH was calculated to be relatively low (12.73) due to the initially high water content of this waste sort and the low alkali content of the HTS cement that was used for conditioning. Note that silica fume (17.7 kg "Micropoz") and 7.9 kg clinoptilolite was added to make the solidifying cement paste. Several modelling scenarios were considered in which the formation of zeolites was either allowed or suppressed in order to assess the effect of zeolites on the long-term chemical conditions in the waste packages. Fig. 4.2 shows the results from calculations performed on the assumption that zeolites are not formed. Furthermore, the modelling was carried out on the assumption that waste packages are closed systems, i.e. no external ingress of water was enabled. One of the main conclusions of the study was that the degradation and corrosion reactions in waste sorts are limited by the availability of water in all waste sorts, except for BA-M-H. In the BA-M-H waste sort the initial water content was high and the temporal evolution of this waste sort was not limited by the water inventory.

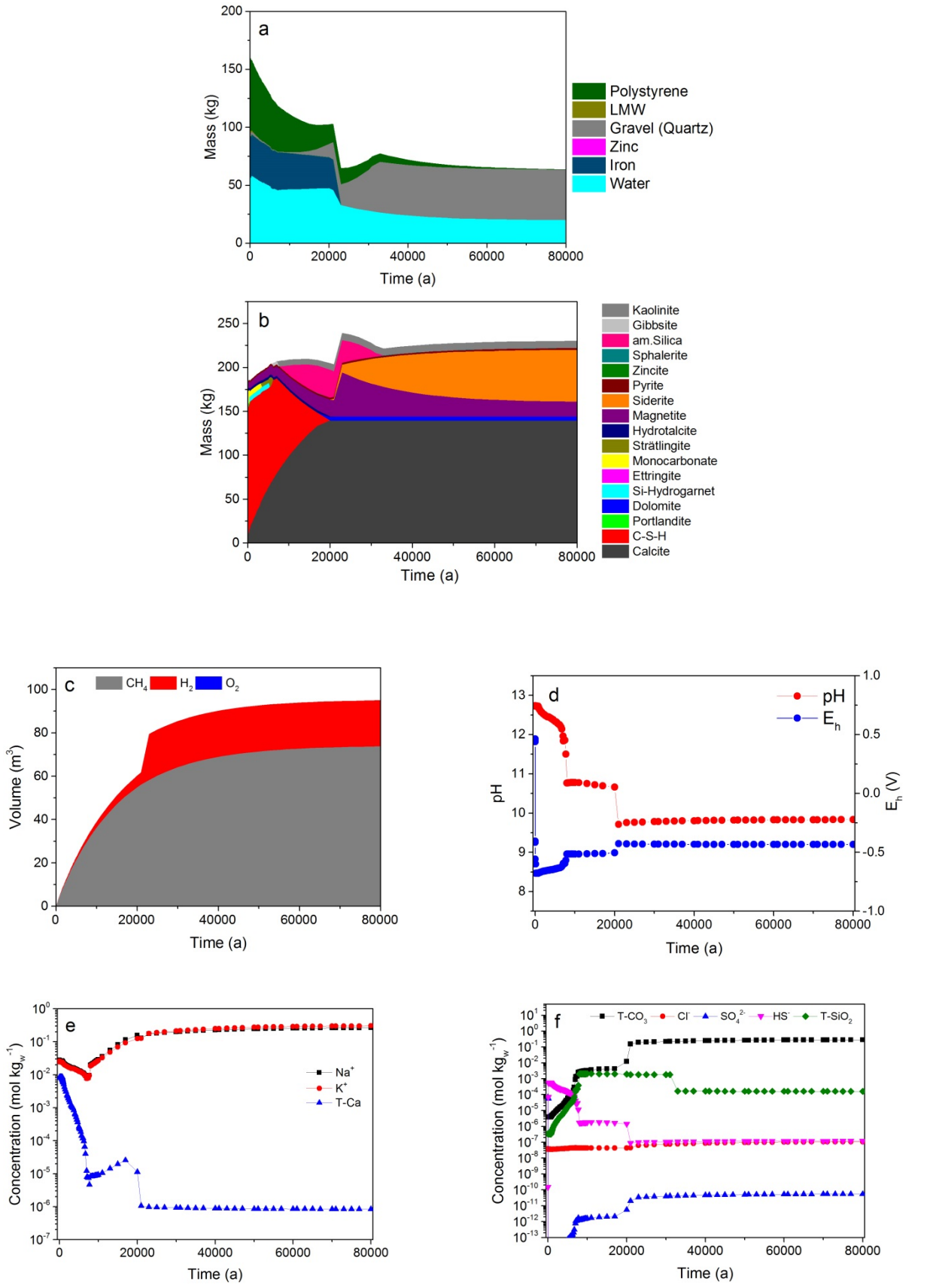

Fig. 4.2: Time-dependent evolution of waste sort BA-M-H with unlimited water availability and absence of zeolites, a) waste materials, b) cement phases and minerals, c) gas production, d) pH and E_h, e) major cations, f) major anions. T-CO_3 and T-SiO_2 are the total aqueous concentrations of carbon and silica species, respectively.

Fig. 4.2a reveals that the evolution of the chemical conditions is mainly controlled by the slow degradation of polystyrene and, as a consequence, continuous production of CH_4 and CO_2. The released CO_2 reacts with C-S-H to form calcite and amorphous silica (Fig. 4.2b). Portlandite, which is present in the initial mix, is converted into C-S-H phases due to continuous reaction with a silica source, i.e. gravel (quartz). In the early ageing phase of this waste sort, i.e. up to ~ 8000 years, the phase assemblage of the cement matrix is composed of C-S-H phases, Al/Fe-Si hydrogarnet, ettringite, monocarbonate, strätlingite and hydrotalcite (Fig. 4.2b). In the long run, however, the cement phases are thermodynamically unstable and calcite, dolomite, magnetite, siderite, pyrite and, in the absence of zeolites, kaolinite and gibbsite are formed. The pH value of the porewater is controlled by the evolution of C-S-H phases, which are the main sink for the alkalis in the system. Simulations predict that pH drops below 10.5 after ~ 20'000 years (Fig. 4.2d). In the early phase the porewater composition of the waste sort corresponds to an alkaline (Na/K)OH solution while in the long-term HCO_3^- is the main charge-balancing anion (Figs. 4.2e and f).

Methane is the main gaseous compound which is continuously produced over the simulated time span (Fig. 4.2c). The production of H_2 is small compared to CH_4 production and is limited by the inventory of metals and slow corrosion at pH ≥ 10.5. However, H_2 production accelerates dramatically in the time period after ~ 20'000 years due to the significantly enhanced corrosion rate of steel at pH < 10.5, i.e. by a factor of 100 compared to the rate at pH ≥ 10.5. As a consequence, the amount of remaining steel and iron is completely corroding within less than 2000 years at pH < 10.5. This acceleration of corrosion is indicated by a sharp increase in the H_2 production rate. Note that the very small amount of O_2 present in the waste package (and therefore not visible in Fig. 4.2c), attributed to air initially entrapped, is consumed by the reaction with metals in the very early stage of the temporal evolution of the waste package (< 0.1 year). The redox potential drops from ~ 0.43 V in the initial matrix to values ranging between -0.5 and -0.7 V due to O_2 consumption already in the early stage of this waste sort.

Thermodynamic modelling allows the behaviour and reactivity of the various waste sorts of interest to be predicted over the entire service life of the repository. The simulations reveal a very different behaviour of the various waste sorts which strongly depends on the type and amount of materials in the waste sort and the type and amount of materials used to make the solidifying concrete. The simulations further suggest that the main factors controlling the reactions progress and the reaction rates are the water content and the *in situ* pH condition. The current simulation setup assumes a homogeneous distribution of waste materials within the waste packages and a fast inter-mixing of the reaction products. These assumptions may not hold locally in a real heterogeneous system resulting in local acceleration or deceleration of the reaction progress.

4.3 Speciation and fate of organic compounds in the cementitious near field

4.3.1 ^{14}C project

^{14}C, possibly carried by small organic compounds resulting from steel corrosion under reducing conditions in a cementitious near field, is a potentially major contributor to the long-term activity release rate (mSv per year) from the cement-based repositories into the far field. To date the chemical form of the ^{14}C-bearing compounds produced during the anoxic corrosion of activated steel is only poorly known. The ^{14}C project in LES aims at filling this knowledge-gap. The experimental studies comprise a corrosion experiment with activated steel and subsequent identification and quantification of the ^{14}C-bearing compounds in the gas and liquid phase using compound-specific ^{14}C accelerator mass spectrometry (^{14}C AMS). In 2016, further development of the GC system was undertaken with the aim of developing and testing the experimental setup for gas phase sampling for further compound-specific ^{14}C AMS. Furthermore, a series of batch-type corrosion experiments with non-irradiated steel powders in hyper-alkaline NaOH solution were completed to check earlier results on the speciation of carbon in cement-type solution and eventually, the compound-specific ^{14}C AMS technique was successfully applied for the identification and quantification of aqueous ^{14}C-bearing species.

4.3.1.1 Development of gas chromatography (GC) for use in compound-specific ^{14}C AMS

The GC system currently in operation in the hot laboratory has to be further modified for the preparation of gaseous samples for compound-specific ^{14}C AMS. The device required for ^{14}C AMS will consist of a GC for the separation of the gaseous, organic compounds coupled to a combustion reactor which oxidizes organic compounds to CO_2, and a CO_2 sampling system (WIELAND & CVETKOVIĆ 2016). The developments require CO_2 to be monitored and quantified after being produced in the combustion reactor from the oxidation of alkanes and alkenes. To this end, thermal conductivity detection (TCD) was installed in the GC system in 2016.

The TCD allows the non-destructive analysis of gaseous compounds of interest, in particular CO_2, and thus opens up the possibility of collecting the target analytes in the fraction sampling system after CO_2 detection by the TCD. The analytical procedure was optimized and tested to determine linearity and capacity of the detector for the analytes of interest. Note that the addition of a significant amount of carbon (20 µg carbon-12 per target analyte) as carrier is required for the preparation of the ^{14}C AMS samples. Therefore, the capacity of the chromatographic column and the TCD had to be determined to verify that no saturation effect of the two devices for CO_2 and organic analytes (in particular methane and ethane) occurred. The tests showed that it is possible to prepare AMS samples with 20 µg carbon per target analyte using a procedure consisting of the separation of the gaseous compounds with the Restek Rt®-Msieve 5A column in combination with TCD detection of the compounds. The next step towards compound-specific ^{14}C AMS for gaseous species will involve installation and testing of the oxidation reactor in combination with the fraction sampling system.

4.3.1.2 Identification and quantification of organics released during iron corrosion

In previous studies with non-irradiated iron powders we were able to identify a total of 20 low-molecular-weight organic molecules that are formed during anoxic corrosion in alkaline, $Ca(OH)_2$ saturated artificial cement porewater (ACW-II) (LES PROGRESS REPORT 2014). In 2016 we carried out a series of corrosion experiments using the same iron powders as in the previous study. However, NaOH solution was used instead of a saturated $Ca(OH)_2$ solution. The organic compounds produced in the course of the corrosion of the iron powders in NaOH solutions (pH = 11 and 12.5) were determined using the improved analytical techniques on the basis of high performance ion exclusion chromatography (HPIEC) and mass spectrometry (MS) detection (HPIEC-MS) for the aqueous species and GC-MS for the gaseous species (LES PROGRESS REPORT 2015).

We were able to identify all compounds during iron corrosion in NaOH that had previously been identified in ACW-II (Table 4.1). Carboxylic acids were identified in the liquid phase (Fig. 4.3) and hydrocarbons in the gas phase as the predominant corrosion products. However, the measured concentrations of the gaseous compounds were significantly higher in NaOH compared to the previously conducted short-term experiments in Ca-bearing ACW-II (Table 4.1). For example, the methane concentration in NaOH (pH 12.5, Fig. 4.3b) was > 4 µM in contrast to ~ 2 µM measured in ACW-II at the same pH (see Table 4.1). Note that the concentrations of the carboxylic acids were found to be comparable in NaOH solution and Ca-containing ACW-II.

The corrosion experiments in NaOH further revealed the presence of larger gaseous compounds with up to seven carbon atoms (C7). A ZEBRON™ ZB-624 column (60 m × 0.25 mm with 1.4 µm film) was used for the separation of these compounds.

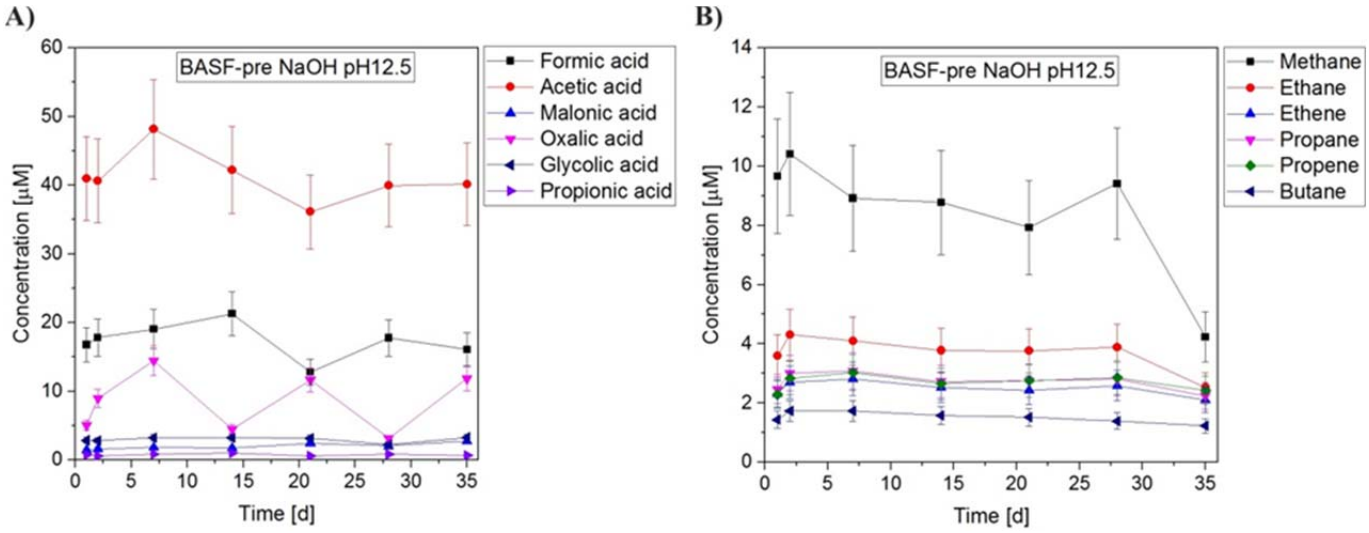

Fig. 4.3: Time-dependent concentrations of carboxylic acids (A) and hydrocarbons (B) formed during the anoxic corrosion of iron powders in NaOH (pH 12.5).

Table 4.1: Comparison of the concentrations of organic corrosion products observed after 28 days in ACW-I/NaOH (pH 11) and ACW-II/NaOH (pH 12.5). ACW-I corresponds to a solution in equilibrium with a C-S-H phase with Ca/Si ratio = 0.8 while ACW-II corresponds to a $Ca(OH)_2$ saturated cement porewater. n.d.: not detectable.

Compound	Concentration [µM]			
	pH 11		pH 12.5	
	ACW-I	NaOH	ACW-II	NaOH
Formic acid	12 ± 2	16 ± 2	15 ± 3	18 ± 3
Acetic acid	36 ± 6	38 ± 6	40 ± 7	40 ± 6
Malonic acid	n.d.	0.6 ± 0.1	n.d.	2.0 ± 0.3
Oxalic acid	0.2 ± 0.1	0.6 ± 0.1	0.8 ± 0.1	3.1 ± 0.5
Glycolic acid	n.d.	1.4 ± 0.2	n.d.	2.2 ± 0.3
Propionic acid	n.d.	0.7 ± 0.1	n.d.	0.8 ± 0.1
Methane	5.2 ± 1.0	52.7 ± 8.7	1.9 ± 0.4	9.4 ± 1.9
Ethane	1.4 ± 0.2	47.7 ± 9.5	0.8 ± 0.1	3.9 ± 0.8
Ethene	1.9 ± 0.4	7.8 ± 1.6	0.8 ± 0.2	2.6 ± 0.5
Propane	1.1 ± 0.1	28.8 ± 5.8	0.7 ± 0.1	2.8 ± 0.6
Propene	1.7 ± 0.3	24.3 ± 4.9	0.7 ± 0.1	2.9 ± 0.6
Butane	0.4 ± 0.1	10.8 ± 2.2	0.3 ± 0.1	1.4 ± 0.3

A large number of unidentified peaks were detected upon analysis of the organic corrosion products formed in NaOH (Fig. 4.4). A library search using the identified masses of the unknown compounds indicated that most of the gaseous compounds are hydrocarbons with a chain length > C3 (Table 4.2). Additional measurements with standards (butane, pentane, 1-hexene, hexane, heptane) enabled us to identify hydrocarbons up to C7 (Fig. 4.4b; chromatograms in blue and red). Note that the latter compounds are present at much lower concentrations and could only be detected as a result of the higher corrosion rate of iron in NaOH.

The batch-type corrosion studies in Ca-bearing ACW-II and in NaOH demonstrate that the same organic compounds are formed, thus suggesting that the speciation is not determined by the composition of the solution. The higher concentration of hydrocarbons in NaOH solution is due to the enhanced corrosion rate. Note, however, that the long-term corrosion rates were found to be similar in both media (KREIS 1991). By contrast, the concentrations of carboxylic acids are similar in both media, thus supporting the idea that carboxylic acids are released instantaneously at the very beginning of the corrosion process.

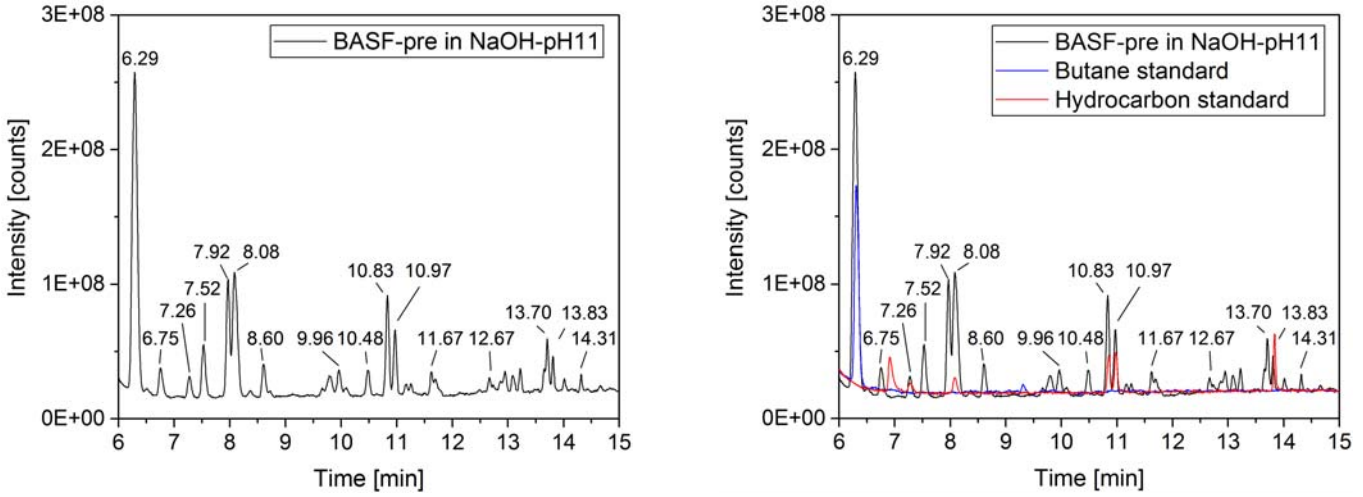

Fig. 4.4: A) MS chromatogram of BASF iron powder corroded in NaOH (pH 11) for 14 days, B) Chromatogram of the same sample including measurements with standards, i.e. butane (blue) and a mixture of several hydrocarbons (pentane, 1-hexene, hexane, heptane) (red).

Table 4.2: Carbon species produced during corrosion of iron powders in NaOH (bold: confirmed by standards, regular: confirmed by mass spectrometry library search).

Retention time [min]	Compound	Formula
6.29	**butane**	**C_4H_{10}**
6.75	2-butene	C_4H_8
7.26	2-pentene	C_5H_{10}
7.52	pentene/2-methylbutane	C_5H_{12}
7.92	1-pentene	C_5H_{10}
8.08	**n-pentane**	**C_5H_{12}**
8.6	2-pentene/3-methyle-2-butane	C_5H_{10}
9.96	2-methylpentane	C_6H_{14}
10.48	3-methylpentane	C_6H_{14}
10.83	1-hexene	C_6H_{12}
10.97	**n-hexane**	**C_6H_{14}**
11.67	2/3-hexene	C_6H_{12}
12.66	3-methyl-hexene	C_7H_{14}
13.7	1-heptene	C_7H_{14}
13.83	**n-heptane**	**C_7H_{16}**
14.31	2/3-heptene	C_7H_{14}

4.3.1.3 Application of compound-specific ^{14}C AMS analysis to liquid samples

The compound-specific ^{14}C AMS method was applied to determine the ^{14}C-containing carboxylic acids in ACW-II in contact with activated steel. An activated steel nut segment (1 g) had been immersed in 30 mL ACW-II (pH 12.5) in a closed container and was allowed to leach over a period of approximately 3 years. The container was stored in a hot cell under atmospheric conditions. Thus, the leach solution was not fully protected against ingress of $^{14}CO_2$. The leachate was analysed using the compound-specific ^{14}C AMS method developed earlier (LES PROGRESS REPORT 2015) based on the separation of the individual compounds by HPIEC and subsequent detection of the activity by ^{14}C AMS. In addition, the total ^{14}C activity was determined by ^{14}C AMS.

Table 4.3 shows that the activity after separation ranges between 0.14 and 0.40 Bq/L or between 36 and 201 µBq/fraction (fraction of 250 µL), respectively, for the different carboxylic acids. Thus, the measured ^{14}C activity of each single compound is clearly below the limit of detection (LOD) of liquid scintillation counting (LSC) (LOD: 10.000 µBq) commonly used for ^{14}C radioanalysis. Note that analysing the solution with LSC would require collection of more than 50 fractions in order to be able to quantify ^{14}C above the LOD of LSC. The results further show that acetate and formate are the main ^{14}C-containing carboxylic acids present in the leach solution. This finding is in line with the results obtained from the corrosion experiments with non-activated iron powders in ACW.

The total ^{14}C activity of the leach solution was estimated from the ^{14}C activities of the four analysed compounds to be 38 ± 15 Bq/L taking into account dilution in the course of chromatographic separation. Direct measurement of the ^{14}C activity in the leach solution by ^{14}C AMS resulted in a ^{14}C activity of 21 ± 5 Bq/L. Thus, the two values agree indicating that $^{14}CO_3^{2-}$ is only a minor species in the leach solution. This first application clearly demonstrates that ^{14}C-bearing species can be detected accurately at very low concentrations using the in-house developed compound-specific ^{14}C AMS method for dissolved species.

4.3.1.4 Start of the corrosion experiment with activated steel

In May 2016 the corrosion experiment was started with two 1 g segments of an activated steel nut. For this experiment the previously developed reactor (LES PROGRESS REPORT 2015) was loaded with two segments of the well characterized activated steel nut

(LES PROGRESS REPORT 2013) (Fig. 4.5a). After closing the reactor, the oxygen was removed by N_2 purge and filled with 300 mL ACW-II (pH 12.5). To ensure anoxic conditions an overpressure of 5 bar N_2 inside the reactor was applied. Temperature, pressure and the dissolved oxygen content are being recorded throughout the experiment (Fig. 4.5b).

Samples have been collected after 1, 15, 29, 93 days reaction time since May. During the sampling, 50 mL gas phase and 7 mL liquid phase were withdrawn from the reactor followed by a re-adjustment of the liquid volume by injecting 7 mL of O_2-free ACW-II and a readjustment of the N_2 overpressure. As expected, Fig. 4.5b shows a drop in pressure during the sampling. The temperature inside the reactor varied between 23.1 and 24.4 °C (average: 23.6 ± 0.3 °C) while the average pressure (excluding the sampling period) was estimated to be 5.03 ± 0.05 bar. Measurements of dissolved oxygen presumably correspond to the detection limit of the sensor. Throughout the experiment dissolved O_2 concentration was below 70 ppb. Note that ground water is often considered to be anoxic at dissolved oxygen content < 500 ppb. Thus, we believe that conditions in the reactor are anoxic and the O_2 concentration is as low as is technically achievable.

The samples were analysed to determine short chain carboxylic acids by HPIEC-MS, hydrocarbons by GC-MS and total organic carbon (TOC of all ^{12}C compounds). Additionally, the ^{14}C activity of the liquid samples was determined by LSC and accelerator mass spectrometry (^{14}C AMS). Note that both ^{12}C- and ^{14}C-bearing compounds can be analysed using the variety of methods listed above. Up to now, however both the concentrations of the ^{12}C- and ^{14}C-bearing compounds are still below or, at best, close to the detection limit of the available analytical techniques. In particular, the concentrations of the ^{14}C-containing carboxylic acids are still below the detection limit of the compound-specific ^{14}C AMS method.

Table 4.3: Activities determined in a leachate of an activated steel nut segment immersed in ACW-II (pH 12.5) in oxic conditions. Activities of the single compounds were determined by compound-specific ^{14}C AMS. [$F^{14}C$] denotes the fraction of modern carbon (1 $F^{14}C = {}^{14}C/({}^{12}C \times 1.18 \cdot 10^{-12})$). A liquid fraction has a volume of 250 µL.

Sample	AMS [$F^{14}C$]	AMS Activity [Bq/L]	AMS Activity [µBq/fraction]
Acetate	0.85 ± 0.35	0.38 ± 0.16	192 ± 78
Formate	0.59 ± 0.23	0.26 ± 0.11	132 ± 53
Malonate	0.34 ± 0.23	0.15 ± 0.10	38 ± 26
Oxalate	0.32 ± 0.11	0.14 ± 0.05	36 ± 12
Total carbon-14	Σ:	0.96 ± 0.40	
	Σ (dilution corrected):	38 ± 15	
	Direct measurement:	21 ± 5	

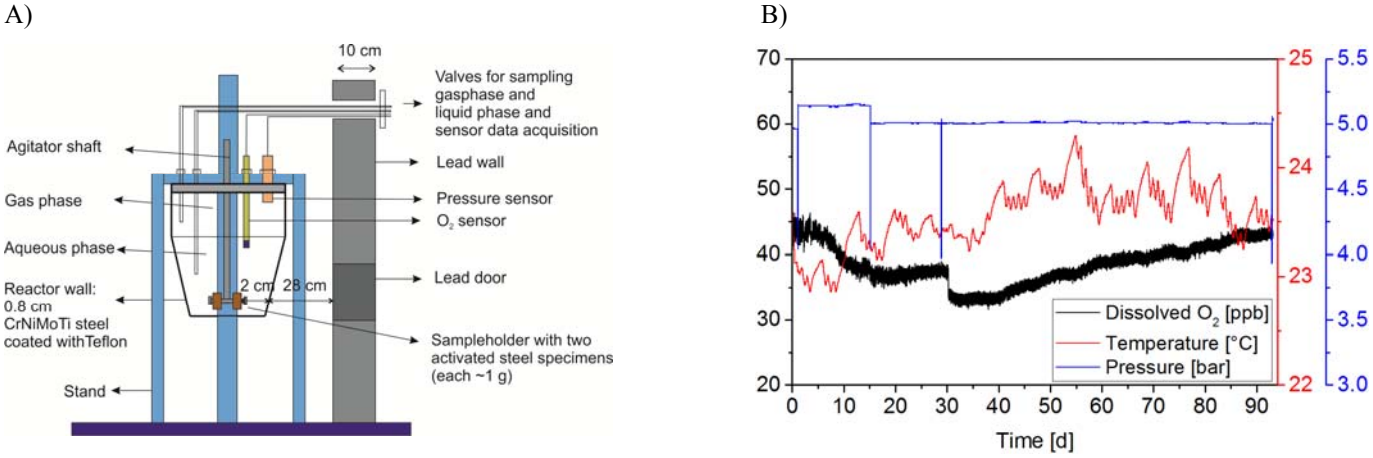

Fig. 4.5: A) Schematic presentation of the corrosion reactor; B) Record of monitored temperature, pressure and dissolved O_2 in the corrosion experiment with activated steel.

4.3.2 Chemical stability of organic compounds under hyperalkaline conditions

Thermodynamic modelling revealed that the ^{14}C-containing LMW organic molecules released during the corrosion of activated steel may not be chemically stable under the hyperalkaline, reducing conditions of a cement-based repository in case of complete thermodynamic equilibrium (WIELAND & HUMMEL 2015). They should eventually decompose into the thermodynamically most stable species $CO_2(g)$, HCO_3^-, CO_3^{2-} and CH_4. Note, however, that complete thermodynamic equilibrium is rarely achieved in the C-H-O system at moderate temperatures. In case of partial thermodynamic equilibrium, it is still unclear what kind of organic compounds might predominate in the repository. In an ongoing experimental study attempts are being made to explore the chemical stability of Na-acetate and Na-formate in hyperalkaline, anoxic conditions relevant to a cement-based repository and to determine whether further degradation takes place to obtain a better insight into the redox kinetics of LMW organics.

The decomposition of carboxylic acids is mainly governed by decarboxylation reactions in anoxic conditions. Such reactions involve breaking of C-C bonds which is inhibited due to high activation energies (e.g., BELL et al. 1994; ONWUDILI & WILLIAMS 2010; PALMER & DRUMMOND 1986). This explains the high resistance of most aliphatic carboxylic acids to decomposition at temperatures below 300°C. Only formic acid is decomposed at lower temperatures due to the absence of a C-C bond. Literature further suggests that the chemical stability of small aliphatic carboxylic acids increases significantly with increasing pH (e.g., BELL & PALMER 1994; MCCOLLOM & SEEWALD 2003). By contrast, the presence of catalyst surfaces such as stainless steel, montmorillonite, hematite, etc. appears to significantly enhance the decomposition. For example, it was stated that "the projected half-life of a 1 M acetic acid solution at 100°C in an (inert) titanium vessel is ±1 billion years, while in a stainless steel vessel the projected half-life is ± 12 year" (MCCOLLOM & SEEWALD 2003). Eventually it was observed that, in reducing conditions and at elevated temperature (175°C) and high pressure (350 bar), the presence of CO_2 and H_2 in solution, resulting from the decomposition of aliphatic carboxylic acids, may lead to the formation of new organic compounds such as long-chain linear alkanes, alkanols and alkanoic acids via Fischer-Tropsch synthesis (e.g., MCCOLLOM & SEEWALD 2007).

Most of the experimental studies on organic acid decomposition published in the literature were performed under acidic or neutral pH conditions at high temperature (> 250°C) and high pressure (> 200 bar). The aim of the present project is to explore the stability of LMW organic molecules under conditions representing the cementitious near field of a repository for radioactive waste, i.e., alkaline conditions (0.01 M $Ca(OH)_2$, pH = 12.5), room temperature and moderate pressure. In the past, decomposition experiments were carried out with Na-acetate in air-tight overpressure reactors at room temperature, moderate overpressure (4 bar) and in anoxic conditions (N_2 atmosphere). The reactor walls in contact with the liquid phase were covered with an inert Teflon® liner. The stability experiments were performed over time periods up to 8 months and the resulting data from gas and liquid phase analysis showed that this small carboxylic acid is indeed stable under these conditions as expected on the basis of the literature survey.

In 2016, a stability test was performed with 300 µM Na-acetate in the presence of stainless steel (the reactor walls) and iron wire (Ø=0.5 mm, L = 1.0 m) as catalysts. The experiment was run at room temperature under anoxic conditions at 4 bar N_2 overpressure. The overpressure in the reactor remained constant over a period of 4 months indicating that the production of H_2 due to Fe corrosion was negligible. HPIEC-MS analysis showed constant acetate concentrations over a period of 4 months indicating that this carboxylic acid was stable over this time period in alkaline conditions and that the presence of Fe as a catalyst did not increase the decomposition rate at room temperature. Note that total organic carbon was found to be systematically higher than the concentration of carboxylic acid initially added. As the source of this contamination could not be eliminated, we carried out the following experiments with formic acid using ^{13}C labelled molecules ($H^{13}COONa$) which enabled us to track the source of carbon in organic reaction products.

The stability tests with ^{13}C labelled Na-formate were performed in Milli-Q water at moderately elevated temperatures (150°C – 200°C) to verify decomposition rates published in the literature. Formate was shown to decompose to CO_2 and H_2 in acid to neutral pH conditions at temperatures above 150°C (MCCOLLOM et al. 1999). Two decomposition experiments were started using Na-formate dissolved in Milli-Q water (300 µM and 50 µM) in the overpressure reactor and anoxic conditions (1 bar N_2) at a temperature of 150 °C. The final overpressure at 150°C in the experiment was 5.5 bar. These experiments are still running. Data from samples taken between 1 day and 2 weeks reaction time do not yet show decomposition of formate suggesting that

the molecule is more stable than expected on the basis of literature data.

The in-house experimental studies carried out up to date indicate that complete thermodynamic equilibrium is not achieved in the C-H-O system under conditions relevant to a cement-based repository.

4.4 Retention of selenium by cementitious materials in anoxic and reducing conditions

^{79}Se (half-life $3.27 \cdot 10^5$ years) is an important redox-sensitive, dose-determining radionuclide in a L/ILW repository (NAGRA 2002). The selenium speciation under oxidizing conditions is dominated by SeO_4^{2-} and SeO_3^{2-} (OLIN et al. 2005, THOENEN et al. 2014) while in alkaline, reducing conditions, i.e. 10.0<pH<13.5 and -750mV<E_h<-230mV, Se(0), HSe^- and poly-selenide species exist along with SeO_3^{2-}. Sorption data for Se(-II) in a cementitious environment are still lacking (WIELAND 2014).

A postdoc project carried out in the framework of the German collaborative project "Immorad" enabled us to gain valuable insight into Se(-II) retention in cementitious systems. Batch sorption experiments with HSe^- onto various cement phases in the presence of hydrazine (N_2H_4) as a reducing agent showed that the anionic HSe^- species sorbs preferentially onto AFm phases, a group of Ca,Al layered double hydroxides consisting of Ca octahedral sheets in which 1/3 of the Ca^{2+} ions are replaced by Al^{3+} ions. The positive structural permanent charge is neutralized by anions, such as Se(-II), intercalated in the interlayer of AFm phases. The study showed that the affinity of the AFm phases for HSe^- is strongly dependent on the type of interlayer anions. For example, HSe^- was strongly retained by monosulfate (AFm-SO_4) and hemicarbonate (AFm-OH-CO_3) while weak retention was observed on Friedel's salt (AFm-Cl_2) and moncarbonate (AFm-CO_3) (ROJO et al. 2016). X-ray absorption spectroscopy (XAS) investigations further revealed that sorbed HSe^- was mainly intercalated in the AFm interlayers upon sorption onto AFm-OH-CO_3 whereas HSe^- sorbed onto AFm-CO_3 was bound mainly on the positively charged sites of the outer surfaces (ROJO et al. 2016).

The postdoc project also showed that a Se(-II) solution at high concentrations is stable but that low concentrations of aqueous Se(-II) are prone to oxidation due to presence of residual oxygen in solution. The presence of strongly reducing N_2H_4 thus was not capable of stabilizing the -II redox state. Therefore, partial oxidation of Se(-II) at low concentrations as observed in the sorption tests with strongly sorbing AFm-OH-CO_3 did not allow sound R_d values for HSe^- sorption to be determined. A new experimental approach was developed in 2016 allowing the Se redox state to be controlled electrochemically in the sorption experiments. To this end, the electrochemical cell developed and described by SOLTERMANNN et al. (2014) was adopted for sorption experiments in highly alkaline conditions. The modified set up enabled us to perform batch sorption studies with Se(-II) for at least 18 days without significant oxidation of Se(-II) in the aqueous phase (Fig. 4.6b). The R_d values determined at these conditions were found to be up to two orders of magnitude lower than those determined previously in the presence of N_2H_4. The higher R_d values are explained by the partial oxidation of HSe^- in solution to SeO_3^{2-} which is known to sorb more strongly onto AFm phases (BAUR & JOHNSON 2003; BONHOURE et al. 2006). The new sorption data confirm our previous observations that HSe^- sorption onto AFm-OH-CO_3 is stronger than on AFm-CO_3.

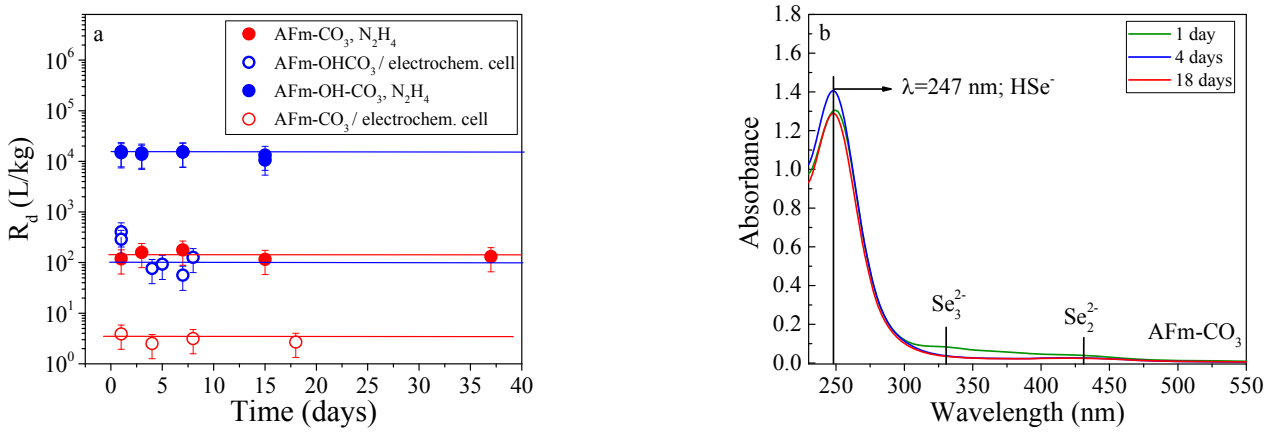

Fig. 4.6: HSe^- sorption kinetics onto AFm-CO_3 and AFm-OH-CO_3. Comparison of experiments performed in the presence of N_2H_4 as a reducing agent and experiments performed in an electrochemical cell at a fixed redox potential of -1.0 V. a) R_d values, b) UV-Vis spectra of supernatant solutions of the sorption experiment with AFm-CO_3.

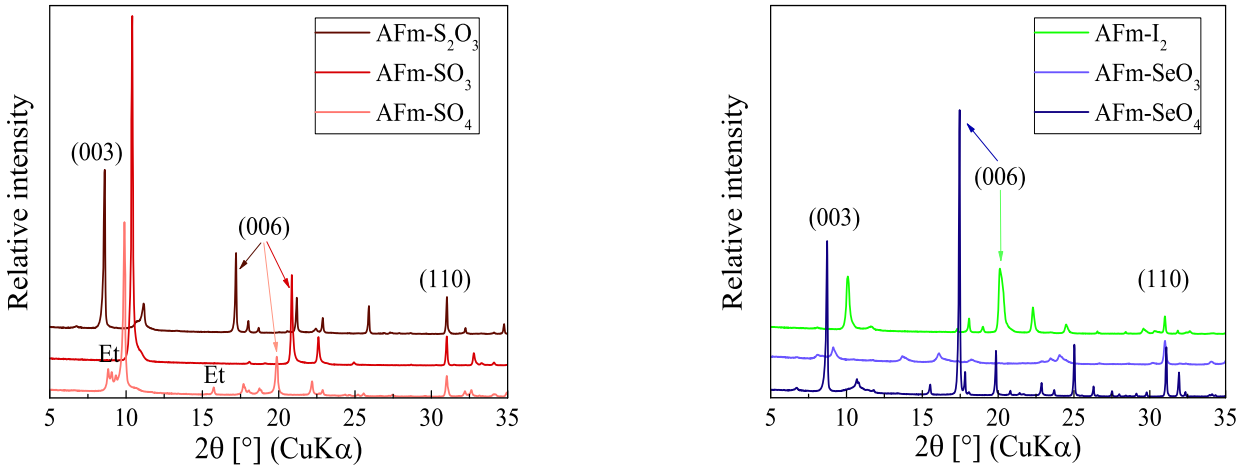

Fig. 4.7: XRD pattern of synthesized AFm phases with Se, S and I in various redox states.

In January 2016 a PhD project was started in the framework of the Horizon-2020 EU project "CEBAM" as a follow-up of the "Immorad" project. In this PhD project the thermodynamic stability of AFm phases containing Se, S and I in various redox states and the formation of solid solutions of Se, S and I bearing AFm endmembers with AFm-CO_3 and AFm-OH-CO_3 will be explored. The aim is to develop thermodynamic solid solution models capable of simulating the uptake of Se(IV), Se(-II) and I(-I) by AFm phases. In 2016, AFm phases with Se, S and I in various redox states were synthesized and characterized using powder X-ray diffraction (XRD), thermogravimetry, infrared and Raman spectroscopy. The XRD pattern show that all AFm phases have the same structure of the main layer (hkl 110 reflections were detected at identical positions), but varying basal spacings (hkl 003 and 006) (Fig. 4.7). This indicates intercalation of Se, S and I anions in the AFm interlayer

4.5 References

BAUR I., JOHNSON C.A. (2003)
Sorption of selenite and selenate to cement materials. Environ. Sci. Technol. 37, 3442-3447.

BELL J.L.S., PALMER D.A. (1994)
Experimental studies of organic acid decomposition, in: Pitman, E.D. & Lewan, M.D. (Eds.), Organic acids in geological processes. Springer Verlag, Berlin.

BELL J.L.S., PALMER D.A., BARNES H.L., DRUMMOND S.E. (1994)
Thermal decomposition of acetate: III. Catalysis by mineral surfaces. Geochim. Cosmochim. Acta 58, 4155 - 4177.

BLANC P., VIEILLARD P., GAILHANOU H., GABOREAU S., MARTY N., CLARET F., MADÉ B., GIFFAULT E. (2015)
ThermoChimie database developments in the framework of cement/clay interactions. Appl. Geochem. 55, 95 - 107.

BONHOURE I., BAUR I., WIELAND E., JOHNSON C.A., SCHEIDEGGER A.M. (2006)
Uptake of Se(IV/VI) oxyanions by hardened cement paste and cement minerals: An X-ray absorption spectroscopy study. Cem. Concr. Res. 36, 91-98.

HELGESON H.C., DELANY J.M., NESBITT H.W., BIRD D.K. (1978)
Summary and critique of the thermodynamic properties of rock-forming minerals. Amer. J. Sci. 278-A, 225p.

KOZLOV V.K., KHODAKOVSKIY I.L. (1983)
The thermodynamic parameters of atomic silver in aqueous solution at 25-280°C. Geochem. Int. 20, 118-130.

KREIS P. (1991)
Hydrogen evolution from corrosion of iron and steel in low/intermediate level waste repositories. Nagra Technical Report NTB 91-21, Nagra, Wettingen, Switzerland.

KULIK D.A., TITS J., WIELAND E. (2007)
Aqueous-solid solution model of strontium uptake in C-S-H phases. Geochim. Cosmochim. Acta 71, A356.

KULIK D.A., WAGNER T., DMYTRIEVA S.V., KOSAKOWSKI G., HINGERL F.F., CHUDNENKO K.V., BERNER U. (2013)
GEM-Selektor geochemical modelling package: revised algorithm and GEMS3K numerical kernel for coupled simulation codes. Computat. Geosci. 17, 1-24.

LOTHENBACH B. (2011)
CI experiment: Thermodynamic modelling of the hydration of ordinary Portland cement and low-pH cements. Technical note TN 2009-33, Empa, Dübendorf, Switzerland.

LOTHENBACH B., PELLETIER-CHAIGNAT L., WINNEFELD F. (2012a)
Stability in the system $CaO-Al_2O_3-H_2O$. Cem. Conc. Res. 42, 1621-1634.

LOTHENBACH B., LE SAOUT G., BEN HAHA M., FIGI R., WIELAND E. (2012b)
Hydration of a low-alkali CEMIII/B-SiO_2 cement (LAC). Cem. Conc. Res. 42, 410-423.

MCCOLLOM T.M., RITTER G., SIMONEIT B.R.T. (1999)
Lipid synthesis under hydrothermal conditions by Fischer-Tropsch-type reactions. Origins Life Evol. B. 29, 153 - 166.

MCCOLLOM T.M., SEEWALD J.S. (2003)
Experimental constraints on the hydrothermal reactivity of organic acids and acid anions: I. Formic acid and formate. Geochim. Cosmochim. Acta 67, 3625 - 3644.

MCCOLLOM T.M., SEEWALD J.S. (2007)
Abiotic synthesis of organic compounds in deep-sea hydrothermal environments. Chem. Rev. 107, 382 - 401.

NAGRA (2002)
Project Opalinus Clay. Safety report. Demonstration of disposal feasibility for spent fuel, vitrified high-level waste and long-lived intermediate level waste (Entsorgungsnachweis). Nagra Technical Report NTB 02-05, Nagra, Wettingen, Switzerland.

NAGRA (2014)
Modellhaftes Inventar für radioaktive Materialien MIRAM 14. Nagra Technical Report NTB 14-04, Nagra, Wettingen, Switzerland.

OLIN Å., NOLÄNG B., OSADCHII E.G., ÖHMAN L.O., ROSÉN E. (2005)
Chemical thermodynamics of Selenium. Elsevier, Amsterdam.

ONWUDILI J.A., WILLIAMS P. (2010)
Hydrothermal reactions of sodium formate and sodium acetate as model intermediate products of the sodium hydroxide-promoted hydrothermal gasification of biomass. Green Chem. 12, 2214 - 2224.

PALMER D.A., DRUMMOND S.E. (1986)
Thermal decarboxylation of acetate. Part I. The kinetics and mechanism of reaction in aqueous solution. Geochim. Cosmochim. Acta 50, 813 - 823.

ROBIE R.A., HEMINGWAY B.S. (1995)
Thermodynamic properties of minerals and related substances at 298.15 K and 1 bar (10^5 Pascals) pressure and at higher temperatures. US Geological Survey Bulletin 2131.

ROJO H., SCHEINOST A., LOTHENBACH B., LAUBE A., WIELAND E., TITS J. (2016)
Retention of selenium by calcium aluminate hydrate (AFm) phases under strongly reducing conditions. Environ. Sci. Technol. (submitted).

SOLTERMANN D., BAEYENS B., BRADBURY M.H., MARQUES FERNANDEZ M. (2014)
Fe(II) uptake on natural montmorillonites. II. Surface complexation modelling. Environ. Sci. Technol. 48, 8698-8705.

THOENEN T., HUMMEL W., BERNER U., CURTI E. (2014)
The PSI/Nagra Chemical Thermodynamic Database 12/07. PSI Bericht Nr. 14-04, ISSN 1019-0643.

WIELAND E. (2014)
Sorption data base for the cementitious near field of L/ILW and ILW repositories for provisional safety analyses for SGT-E2. Nagra Technical Report NTB 14-08, Nagra, Wettingen, Switzerland.

WIELAND E., CVETKOVIĆ B.Z. (2016)
Development of a compound-specific carbon-14 AMS technique for the detection of carbon-14 labelled organic compounds. EU Project "CAST" report D 2.3.

WIELAND E., HUMMEL W. (2015)
Formation and stability of carbon-14 containing organic compounds in alkaline iron-water-systems: Preliminary assessment based on a literature survey and thermodynamic modelling. Mineral. Mag. 79, 1275-1286.

WIELAND E., KOSAKOWSKI G., LOTHENBACH B., KULIK D.A. (2016)
Preliminary assessment of the temporal evolution of waste packages in the near field of an L/ILW repository. Nagra Working Report NAB (in prep.).

5 DIFFUSION PROCESSES

L.R. Van Loon, M.A. Glaus, S. Frick, P. Bunic, Y. Chen (PhD student), C. Wigger (PhD student), Y. Fukatsu (visiting PhD student), Y. Zhao (Guest scientist)

5.1 Introduction

The "Diffusion Processes" group aims at improving the mechanistic understanding of diffusion and sorption processes of cations, anions and neutral species in compacted clay materials. This knowledge is needed to allow a better evaluation of the long-term migration behaviour of radionuclides in technical barrier systems (e.g. bentonite) and in clay-rich sedimentary host rocks (e.g. Opalinus Clay). The following projects are currently ongoing:

- TRAPHICCS: this project deals with fundamental diffusion processes. The current focus is on the diffusive transport of strongly sorbing radionuclides in single phase clay minerals with different physico-chemical properties (illite, montmorillonite), and on multicomponent diffusion through uncharged and charged membranes. The latter allows to develop models that accurately describe multicomponent diffusion in charged porous media and to verify the applicability of the sorption models developed based on batch experiments to compacted systems
- PRECIP: this project deals with dissolution and precipitation reactions at interfaces with strong chemical gradients. Currently precipitation reactions in illite and their effect on porosity and diffusive transport are being studied.
- ROLOC: a PhD project related to the migration behaviour of small organic molecules in compacted clay systems such as illite, kaolinite, and in clay formations such as Opalinus Clay. The focus is on resolving retardation mechanisms of ^{14}C-containing organic molecules in clays and clay stones.
- ANPOR: a PhD project focussing on a better understanding of anion exclusion effects in clay-rich sedimentary rocks with different mineral compositions and physicochemical properties. The focus is on identifying the most reliable model for describing anion exclusion in consolidated clay stones.

5.2 TRAPHICS: Transport phenomena in compacted clay systems and membranes

The recent work has been devoted to the investigation of the coupled diffusion of charged species in argillaceous media. In the presence of surfaces with permanent electrical charges, the diffusive ion transport is governed by different driving forces, viz. the concentration gradients of the species in the different pore domains and gradients of electrostatic potential maintaining the charge neutrality in the system. The interaction between these driving forces and the magnitude of the resulting fluxes in compacted clay systems is not *a priori* clear from theory. It was demonstrated that the fluxes of Na^+ tracer ions in compacted smectites can be reduced for simplicity to a description based on concentration gradients (GLAUS et al. 2013).

As a first step the coupled ion transport across an uncharged diffusion barrier was investigated using commercial polymeric filtration membranes. Regenerated cellulose acetate was found to be a suitable material for these purposes. The experiment was based on an exemplary computational simulation proposed by LICHTNER (1995), which was later on used as a benchmark case for the comparison of different computer codes (RASOULI et al. 2015). A gradient of HNO_3 concentrations was superimposed to two adjacent gel domains containing the same initial concentrations of a background electrolyte (e.g. NaCl). The subsequent diffusive flux of HNO_3 and the different mobilities of the ions involved (H^+, NO_3^-) induce local changes of the concentrations of the background electrolyte. In contrast to the experiments performed in GLAUS et al. (2013), the present background electrolyte fluxes can be seen as true uphill processes, i.e. diffusion against a concentration gradient. In order to keep the experimental efforts at a manageable level and to maintain a well-defined boundary condition for the modelling, a porous membrane representing the transport media was placed between two homogeneously stirred solutions with initially different pH (cf. Fig. 5.1). The dynamics of this system is thus characterised by time dependent changes of total concentrations in well-mixed gradient free reservoirs which define boundary conditions for diffusion through the membrane. Fig. 5.2 shows the results from two independent experiments together with simulations obtained using the multicomponent transport module of the PHREEQC code (APPELO & WERSIN 2007), which enables the use of species-specific diffusion coefficients with the constraint that overall charge balance is maintained. The only adjustable parameter used for the simulation was the geometry factor of the membrane, which was optimised according to the diffusion data of HTO (data not shown). No diffusion data are available so far for the proton. The reason is the leakage of Cl^-

ions from the electrolyte solution of combined glass electrodes. Efforts are currently taken to realise online pH measurements and also monitoring the diffusion potential across the membrane. The results demonstrate that the system behaviour can well be described using a Nernst-Planck formalism. To the best knowledge of the authors no experimental verification of the simulations of the "Lichtner-Benchmark" (LICHTNER 1995) has been available from the literature so far. The results will further be used as a test case for the development of coupled codes in the 'Transport Mechanisms' group.

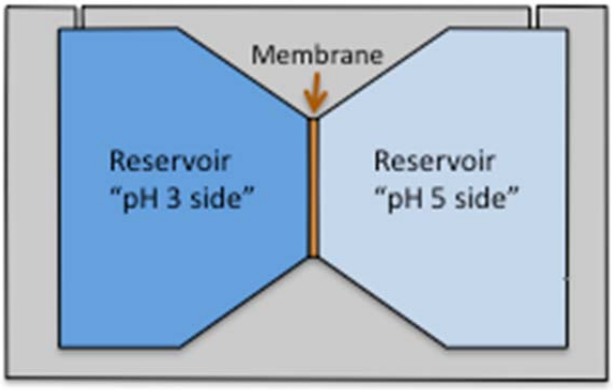

Fig. 5.1: Schematic representation of the layout of the "uphill" experiment. Two solutions separated by a porous membrane and containing the same concentrations of KCl are spiked with different concentrations of HNO_3 resulting in pH 3 and pH 5 after dilution.

The sorption-competition measurement in compacted smectites remains to be an unresolved technical challenge. The membrane-confined type of diffusion cell (MCDC) in its original form (GLAUS et al. 2015) has turned out to be inappropriate for experiments with montmorillonite compacted to bulk-dry densities larger than 1000 kg m^{-3}. The swelling pressures involved lead to rupture of the membrane. Two strategies were followed to find a remedy: (i) the use of a mechanical support for the membrane and (ii) the use of synthetic smectites exhibiting less swelling properties. For the former option, a thin perforated titanium plate has been added in the setup of the MCDC. Test experiments using Co^{2+} in-diffusion in compacted illite demonstrated that the same results were obtained as in setups without the titanium plate. However, the titanium plate added a further diffusive resistance, which lead to increased uncertainties in the determination of capacity factors from in-diffusion experiments. A limited applicability of this setup has thus to be accepted.

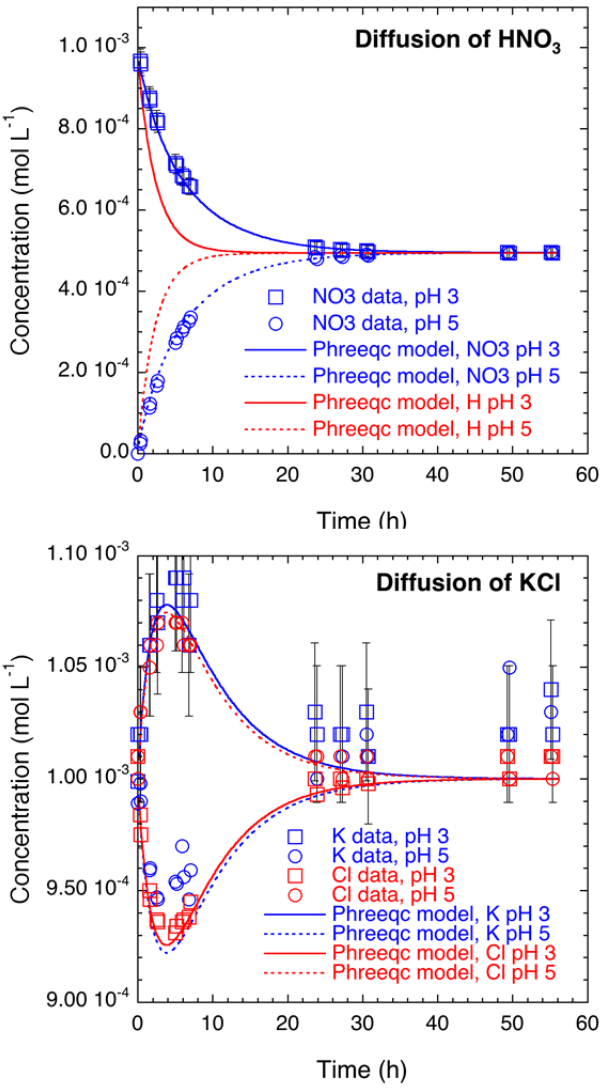

Fig. 5.2: Evolution of species concentrations with time in the "uphill" experiments.

For the second option two different synthetic clays from the smectite group are currently under investigation: (i) Barasym SSM-100 Syn-1 available from the Clay Minerals Society, which is characterised by having mostly tetrahedral charges (thus having rather properties of a Beidellite), and (ii) a synthetic iron-free montmorillonite (REINHOLDT et al. 2001; REINHOLDT et al. 2005) having mostly octahedral charges.

Both clays showed clearly less swelling than Milos montmorillonite. Through-diffusion experiments using simultaneously HTO, $^{22}Na^{+}$ and $^{36}Cl^{-}$ as tracers were carried out at different concentrations of the background electrolyte ($NaClO_4$), in order to clarify whether these clays exhibit similar surface diffusion properties towards cations and exclusion properties towards anions as Milos montmorillonite. The results showed a clear dependence of the effective diffusion coefficients of the charged tracers on the concentrations of the background electrolyte, while

these remained unaffected in the case of HTO. Although some significant nuances between the various synthetic clays and Milos montmorillonite can be ascertained, the further use of these clays appears to be a promising option.

Furthermore, the combined sorption and diffusion studies using strongly sorbing elements such as Eu(III) and Th(IV) were continued. One of the key questions to be resolved in the scope of these experiments is whether the pH dependence of sorption ("sorption edge") in compacted clay minerals is the same as obtained from measurements in dilute suspensions. While this question could be positively answered for Co(II) (MONTOYA et al. 2017), increased experimental difficulties were encountered in the case of Eu(III) and Th(IV). In particular, incomplete mass recoveries upon tracer profile measurements observed at pH values where metal hydrolysis starts, severely impaired the evaluation of the experimental data. Currently it is tested whether the use of weak organic ligands may resolve this issue. No results can be reported at present because these experiments are still running.

Finally a comprehensive series of anion diffusion experiments in compacted montmorillonite (bulk-dry densities between 1300 and 1900 kg m^{-3}) carried out at background electrolyte concentrations between 1 and 5 M were terminated. The results of these experiments may be used for discriminating various models to assess the anion accessible porosity in smectites (TOURNASSAT & APPELO 2011). It has been clearly shown in these experiments that the anion-accessible porosity is less than the total accessible water porosity across the entire range of background electrolyte concentrations. This observation is in direct contradiction to the description of smectite porosity as a single porous medium in which anion exclusion is governed by a Donnan type of equilibrium (BIRGERSSON & KARNLAND 2009).

5.3 PRECIP: Precipitation reactions in porous media

Dissolution-precipitation reactions occurring at interfaces with strong chemical gradients (e.g. cement-clay) can result in porosity changes and changes in the transport properties of solutes and gases. A visiting PhD student (Yuta Fukatsu) from the Tokyo Institute of Technology studied the effect of precipitation reactions on porosity changes in compacted illite. Precipitation of $SrSO_4$ was induced by counter diffusion of Sr^{2+} and SO_4^{2-} in compacted illite as described in CHAGNEAU et al. (2015). To this end, special designed mini diffusion cells loaded with compacted illite at a bulk dry density 1600 kg/m^3 were used. After ca. 2 months, the precipitate was studied using micro X-ray tomography, micro X-ray fluorescence and micro X-ray diffraction.

A precipitate could be observed under a conventional optical microscope (Fig. 5.4). X-ray fluorescence clearly revealed that the precipitate was composed of strontium and sulphur, which can be interpreted as $SrSO_4$.

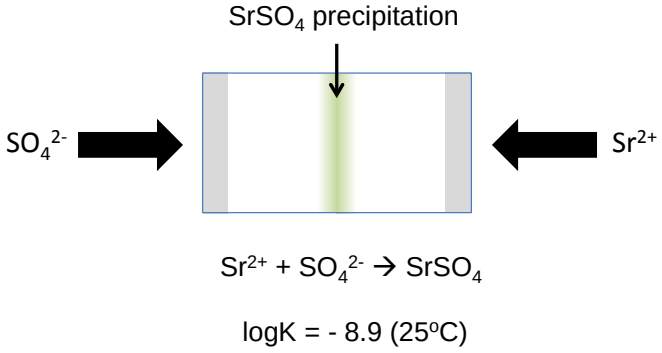

Fig. 5.3: Experimental setup for inducing precipitation reactions in compacted clay systems.

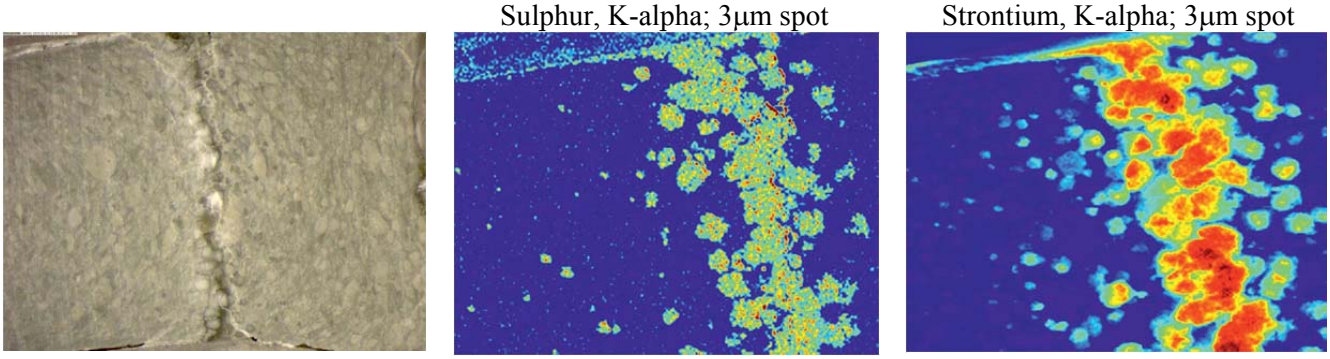

Fig. 5.4: Precipitation zone of $SrSO_4$ in illite as observed with an optical microscope (left) and X-ray fluorescence (middle and right). The $SrSO_4$ precipitate clearly shows a mushroom type of pattern (Courtesy of D. Grolimund).

A large spatial "mushroom" of precipitation clusters resulting in a "mushroom" type pattern was observed (Fig. 5.4). Micro X-ray diffraction analysis showed that the precipitate was microcrystalline. The nano-crystals showed a preferred orientation in individual precipitation clusters. The nanocrystallinity indicates that precipitation was induced by homogeneous nucleation in the pore space (POONOOSAMY et al. 2016). Interpretation of the data is ongoing.

5.4 ROLOC: Transport of small organic molecules in dense clay systems

Carbon-14 is an important contributor to the annual radioactive dose predicted in performance assessment of low- and intermediate-level radioactive waste repository in Switzerland. ^{14}C is assumed to be mainly released to the biosphere in form of low molecular weight organic compounds, yielding from the anoxic corrosion of activated steel (NAGRA 2008; see also CEMENT SYSTEMS). To date, performance assessment is based on the assumption that the transport of organic compounds is unretarded. However, if a weak retardation can be robustly demonstrated, this would lead to a larger extent of decay of ^{14}C within the barriers and to a significant reduction of its maximum dose. Possible interactions of the organic model compounds with clay are still poorly known, and are presumed to be rather weak. The main tasks of this project are: (i) to investigate the transport behaviour of model organic compounds with different composing minerals of argillaceous rocks, and (ii) to derive the quantitative relationships (SCHWARZENBACH et al. 2006) between the sorption properties and structural elements of organic compounds.

In 2016 the focus was on the transport behaviour of selected organic molecules in Opalinus Clay and in artificial systems composed of illite and kaolinite (mimicking Opalinus Clay). Accompanying experiments with HTO and $^{36}Cl^-$ were used to characterise the porosity and the geometric properties of the media. The idea behind the use of mineral mixtures was to check whether the component additivity approach can be applied to predict the retardation in a composite material (R), based on the retardation behaviour in the pure components. The predicted R for mixed clay systems was calculated by:

$$R = R_{ill} \cdot w_{ill} + R_{kao} \cdot w_{kao}$$

where R_{ill} is the tracer retardation in a pure Na-illite sample, and R_{kao} is the tracer retardation in a pure kaolinite sample. w_{ill} and w_{kao} represent the weight percentage of each component in the mixture. This component additivity approach could be successfully applied for all mixed clay samples and Opalinus Clay in the case of anionic tracers such as $^{36}Cl^-$ and aliphatic carboxylates, as well as for all tested alcohols. The calculated R values were identical to the measured ones within the experimental uncertainties (Fig. 5.5). In the case of the hydroxylated carboxylates with relatively strong retardation, the agreement was less good, i.e. the predicted R values were much larger than the measured ones (Fig. 5.5).

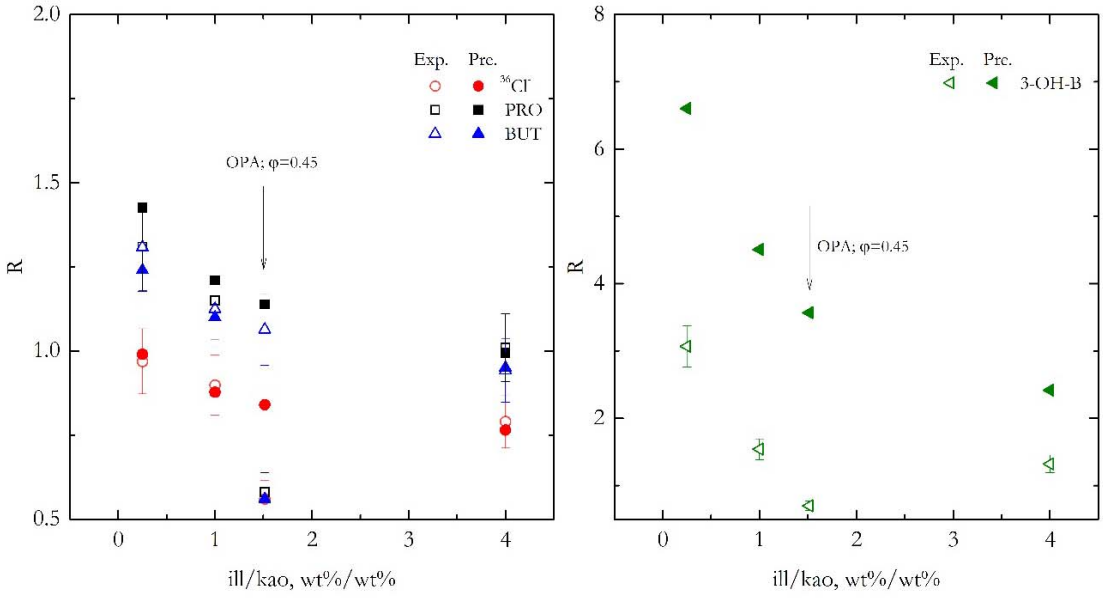

Fig. 5.5: Comparison of measured R values in OPA samples and mixed clay samples (with varying illite/kaolinite ratios) and predicted R values using the component additivity approach (±10% error bars). PRO: propanoic acid, BUT: butanoic acid and 3-OH-B: 3-hydroxy butanoic acid.

5.5 ANPOR: Anion exclusion phenomena in low porosity clay rocks

Argillaceous rocks consist to a large part of clay particles composed by TOT-layers. They are negatively charged and these negative charges are compensated by cations in the interlayer pore space and the external pore space forming so called diffuse double layer. Anions are repelled by the negative charges of the clay minerals and are excluded from the diffuse double layer. The latter phenomenon is well known as anion exclusion and has been observed in soils, clay rocks and in compacted bentonite. For neutral and positively charged chemical species, the whole porosity of a clay rock (ε_{tot}) is available for transport. Anions, however, are partially excluded from the near surface domains and the corresponding transport porosity, i.e. the anion accessible porosity (ε_{an}), is smaller than the total porosity. Earlier studies on compacted bentonite showed that the composition of the pore water had an effect on the diffusion accessible porosity of anions (VAN LOON et al. 2007). Increasing the ionic strength of the pore solution (NaCl) led to an increase in the anion accessible porosity. A similar dependence was observed for clay stones such as Opalinus Clay and Helvetic Marl (WIGGER & VAN LOON 2016). Identical experiments with $CaCl_2$ and CsCl instead of NaCl showed the same effect, but shifted towards lower ionic strength values (Fig. 5.6). Ca^{2+} and Cs^{+} are thus more effective in shielding the electric charge than Na^{+}. The diffences between OPA and Helvetic Marl are due to a difference in the clay composition and not due to a difference in the clay content of the samples.

Measurements on two clay stone samples from Canada were also performed. A similar behaviour as observed for the Swiss clay stones was observed. Interpretation of the results and an extensive modelling is currently ongoing. Different models are being evaluated. The model from BIRGERSSON & KARNLAND (2009) describes the whole pore space as a Donnan space, accessible for both anions and cations. This model, however, does not predict a plateau value of the anion accessible porosity at higher ionic strength values and is therefore not appropriate to describe the anion behaviour in clay-rich sedimentary rocks. More promising is a dual-porosity model where the porosity is sub-divided in an interlayer or interlayer equivalent pore space devoid of anions, and a Donnan space accessible for anions (TOURNASSAT & APPELO 2011).

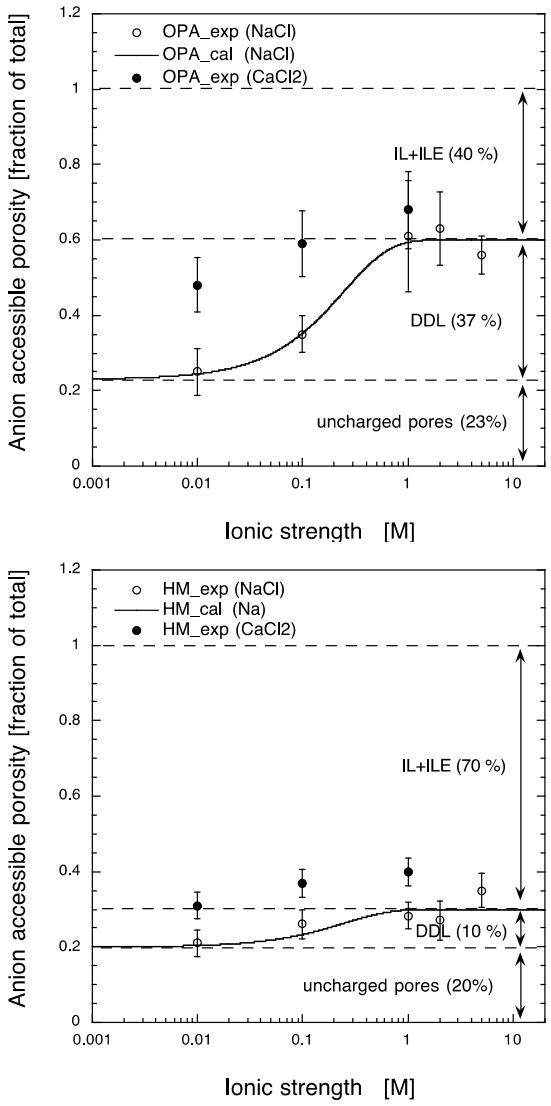

Fig. 5.6: Anion accessible porosity in Opalinus Clay (OPA Schlattingen borehole) and Helvetic Marl (HM Wellenberg) as a function of the ionic strength of the pore solution. The accessible porosity is given as a fraction of the total porosity as measured with tritiated water (HTO). $CaCl_2$ has a larger effect on the anion exclusion then NaCl.

5.6 References

APPELO C.A.J., WERSIN P. (2007)
Multicomponent diffusion modelling in clay systems with application to the diffusion of tritium, iodide, and sodium in Opalinus Clay. Environ. Sci. Technol. 41, 5002-5007.

BIRGERSSON M., KARNLAND O. (2009)
Ion equilibrium between montmorillonite interlayer space and an external solution – consequences for diffusional transport. Geochim. Cosmochim. Acta 73, 1908–1923.

CHAGNEAU A., TOURNASSAT C., STEEFEL C., BOURG I.C., GABOREAU S., ESTEVE I., KUPCIK T., CLARET F., SCHÄFER T. (2015)
Complete restriction of $^{36}Cl^-$ diffusion by celestite precipitation in densely compacted illite. Environ. Sci. Technol. 2, 139-143.

GLAUS M.A., BIRGERSSON M., KARNLAND O., VAN LOON L.R. (2013)
Seeming steady-state uphill diffusion of $^{22}Na^+$ in compacted montmorillonite. Environ. Sci. Technol. 47, 11522-11527.

GLAUS M.A., AERTSENS M., APPELO C.A.J., KUPCIK T., MAES N., VAN LAER L., VAN LOON L.R. (2015)
Cation diffusion in the electrical double layer enhaces the mass transfer rates for Sr^{2+}, Co^{2+} and Zn^{2+} in compacted illite. Geochim. Cosmochim. Acta 165, 376-388.

LICHTNER P.C. (1995).
Principles and practice of reactive transport modelling, in: Murakami, T., Ewing, R.C. (Eds.), Scientific Basis for Nuclear Waste Management XVIII, Pts 1 and 2, pp. 117-130.

MONTOYA V., KUPCIK T., VAN LAER L., MARQUES FERNANDES M., BAEYENS B., GLAUS M.A., BRUGGEMAN C., MAES N., TOURNASSAT C., SCHÄFER T. (2017)
Sr^{2+}, Co^{2+} and Zn^{2+} sorption onto Na-illite: Batch sorption studies and modelling. In preparation.

POONOOSAMY J., CURTI E., KOSAKOWSKI G., GROLIMUND D., VAN LOON L.R., MÄDER U. (2016)
Barite precipitation following celestite dissolution in a porous medium: A SEM/BSE and μ-XRD/XRF study. Geochim. Cosmochim. Acta 182, 131-144.

RASOULI P., STEEFEL C.I., MAYER K.U., ROLLE M. (2015)
Benchmarks for multicomponent diffusion and electrochemical migration. Comput. Geosci. 19, 523-533.

REINHOLDT M., MIEHÉ-BRENDLÉ J., DELMOTTE L., TUILIER M.-H., LE DRED R., CORTES R., FLANK A.M. (2001)
Fluorine route synthesis of montmorillonites containing Mg or Zn and characterization by XRD, thermal analysis, MAS NMR, and EXAFS spectroscopy. Eur. J. Inorg. Chem., 2831-2841.

REINHOLDT M., MIEHÉ-BRENDLÉ J., DELMOTTE L., LE DRED R., TUILIER M.-H. (2005)
Synthesis and characterization of montmorillonite-type phyllosilicates in a fluoride medium. Clay Miner. 40, 177-190.

SCHWARZENBACH R.P., ESCHER B.I., FENNER K., HOFSTETTER T.B., JOHNSON C.A., VON GUNTEN U., WEHRLI B. (2006)
The challenge of micropollutants in aquatic systems. Science 313, 1072-1077.

TOURNASSAT C., APPELO C.A.J. (2011)
Modelling approaches for anion-exclusion in compacted Na-bentonite. Geochim. Cosmochim. Acta 75, 3698–3710.

VAN LOON L.R., GLAUS M.A., MÜLLER W. (2007)
Anion exclusion effects in compacted bentonites: Towards a better understanding of anion diffusion. Appl. Geochem. 22, 2536-2552.

WIGGER C., VAN LOON L.R. (2016)
The importance of interlayer equivalent pores for anion diffusion in clay-rich sedimentary rocks. Submitted for publication in Environ. Sci. Technol.

6 PUBLICATIONS

6.1 Peer reviewed journals

Chollet M., Martin P., Degueldre C., Poonoosamy J., Belin R.C., Hennig C. (2016)
Neptunium characterization in uranium dioxide fuel: Combining a XAFS and a thermodynamic approach. J. Alloys Compd. 662, 448-454.

Dähn R., Arakcheeva A., Schaub Ph., Pattison P., Chapuis G., Grolimund D., Wieland E., Leemann A. (2016)
Application of micro X-ray diffraction to investigate the reaction products formed by the alkali-silica reaction in concrete structures. Cem. Concr. Res. 79, 49-56.

Fowler S., Kosakowski G., Driesner T., Kulik D.A., Wagner T., Wilhelm S., Masset O. (2016)
Numerical simulation of reactive fluid flow on unstructured meshes. Transport Porous Med. 112(1), 283-312.

Grolimund D., Wang H.A.O., Van Loon L.R., Marone F., Diaz N., Kaestner A., Jakob A. (2016)
Microscopic chemical imaging: a key to understand ion mobility in tight formations. CMS Workshop Lectures, Series, 21(9), 105-128.

Kéri A., Osán J., Fábián M., Dähn R., Török S. (2016)
Combined X-ray microanalytical study of the Nd uptake capability of argillaceous rocks. X-ray Spectrom. 45, 54-62.

Leal A.M.M., Kulik D.A., Kosakowski G. (2016)
Computational methods for reactive transport modelling: A Gibbs energy minimization approach for multiphase equilibrium calculations. Adv. Water Res. 88, 231-240.

Leal A.M.M., Kulik D.A., Kosakowski G., Saar M.O. (2016)
Computational methods for reactive transport modelling: An extended law of mass-action, xLMA, method for multiphase equilibrium calculations. Adv. Water Res. 96, 405-422.

Leal A.M.M., Kulik D.A., Saar M.O. (2016)
Enabling Gibbs energy minimization algorithms to use equilibrium constants of reactions in multiphase equilibrium calculations. Chem. Geol. 437, 170-181.

L'Hôpital E., Lothenbach B., Scrivener K., Kulik D.A. (2016)
Influence of calcium to silica ratio on aluminium uptake in calcium silicate hydrate. Cem. Concr. Res. 85, 111-121.

L'Hôpital E., Lothenbach B., Scrivener K., Kulik D.A. (2016)
Alkali uptake in calcium alumina silicate hydrate (C-A-S-H) Cem. Concr. Res. 85, 122-136.

Miron G.D., Wagner T., Kulik D.A., Heinrich C.A. (2016)
Internally consistent thermodynamic data for aqueous species in the system Na-K-Al-Si-O-H-Cl. Geochim. Cosmochim. Acta 187, 41-78.

Marques Fernandes M., Scheinost A., Baeyens B. (2016)
Sorption of trivalent lanthanides and actinides onto montmorillonite: Macroscopic, thermodynamic and structural evidence for ternary hydroxo and carbonato surface complexes on multiple sorption sites. Water Res. 99, 74-82.

Poonoosamy J., Curti E., Kosakowski G., Grolimund D., Van Loon L.R., Mäder U. (2016)
Barite precipitation following celestite dissolution in a porous medium: A SEM/BSE and μ-XRD/XRF study. Geochim. Cosmochim. Acta 182, 131-144.

Sui R., Prasianakis N.I, Mantzaras J., Mallya N., Theile J., Lagrange D., Friess M. (2016)
An experimental and numerical investigation of the combustion and heat transfer characteristics of hydrogen-fueled catalytic microreactors. Chem. Eng. Sci. 141, 214-230.

Wieland E., Jakob A., Tits J., Lothenbach B., Kunz D. (2016)
Sorption and diffusion studies with low molecular weight organic compounds in cementitious systems, Appl. Geochem. 67, 101-117.

Wu T., Li Q., Wang Z., Zheng Q., Li J., Van Loon L.R. (2016)
Re(VII) diffusion in montmorillonite: Effect of organic compounds, pH and temperature. Appl. Clay Sci. 127, 10-16.

6.2 Books contributions

Churakov S.V. (2016)
Ab initio simulations of mineral surfaces: Recent advances in numerical methods and selected applications, In "Highlights in Mineralogical Crystallography", Eds. Armbruster Th. and Danisi R., p. 75-108. De Gruyter, 210 pp.

He W., Poonoosamy J., Kosakowski G., Van Loon L.R., Mäder U., Kalbacher T. (2016)
Reactive Transport in "Thermo-Hydro-Mechanical-Chemical Processes in Fractured Porous Media: Modelling and Benchmarking" Springer International Publishing Switzerland , 179-197.

6.3 Conferences/workshops/presentations

Alt-Epping P., Gimmi T., Wersin P., Jenni A.
Implementing an explicit diffuse layer in reactive transport simulations by using the Nernst-Planck equation. 26th Goldschmidt Conference, Yokohama, Japan, June 26 – July 1, 2016.

Chen Y., Glaus M.A., Van Loon L.R., Mäder U.K.
Migration behavior of carboxylic acids in compacted illite, kaolinite and Opalinus Clay. 26th Goldschmidt Conference, Yokohama, Japan, June 26 – July 1, 2016.

Churakov S.V., Labbez C., Pegado L.
C-A-S-H-ion interactions from ab initio simulations. 4th International Workshop on "Mechanisms and Modelling of Waste/Cement Interactions", Murten, Switzerland, May 22-25, 2016.

Cvetković B.Z., Wieland E., Kunz D., Salazar G., Szidat S.
Analytical strategy for the identification of carbon-14 containing organics released during anoxic corrosion of activated steel in alkaline conditions. MRS Fall Meeting, Boston, USA, November 28 - December 2, 2016.

Dähn R.
Micro X-ray diffraction investigation of the reaction products formed by the alkali-silica reaction in concrete structures. 4th International Workshop on "Mechanisms and Modelling of Waste/Cement Interactions", Murten, Switzerland, May 22-25, 2016.

Fernández J., Pfingsten W., Samper J., Montenegro L.
Benchmarking of caesium migration through Opalinus Clay calculated by a single-species model using a measured non-linear sorption isotherm and a multi-species transport model. Subsurface Environmental Simulation Benchmarking Workshop V. A Coruna, Spain, October 13-15, 2016.

Francois B., Phil M., Wasselin-Trupin V., Pfingsten W., Smidts O., Miksova J., Tokaresvski O.
The ETSON study on treatment processes for the sustainable management of radioactive waste. International Conference on the Safety of Radioactive Waste Management. IAEA, Vienna, Austria November 21-25, 2016.

Hax Damiani L., Kosakowski G.
Status and work plan for PSI's contribution to WP3, CEBAMA Workshop, Barcelona, Spain, May 11-13, 2016.

Huang Y., Kosakowski G., Kolditz O., Shao H.
Modelling long-term gas production process in waste containing drums, 67. Berg- und Hüttenmännischer Tag, Freiberg, Germany, June 10, 2016.

Huang Y., Kosakowski G., Kolditz O., Shao H.A.
Numerical investigation on the influence of the water availability on the temporal evolution of the waste package. Subsurface Environmental Simulation Benchmarking Workshop V, A Coruña, Spain, October 13-15, 2016.

Jenny A., Alt-Epping P., Gimmi T., Mäder U.
Reactive transport across concrete - clay interfaces. Mont Terri CI meeting, St. Ursanne, Switzerland, February 12, 2016.

Kéri A., Dähn R., Krack, M., Churakov S.V.
Combined ab initio and EXAFS spectroscopy study on the characteristics of iron uptake by clay minerals. Second European Mineralogical Conference, Rimini, Italy, September 11-15, 2016.

Kosakowski G.
Evolution of material interfaces in deep geological repositories: models and experiments. 67. Berg- und Hüttenmännischer Tag, Freiberg, Germany, June 10, 2016.

Kosakowski G.
Reactive transport modelling of cement/clay interactions. 4th International Workshop on "Mechanisms and Modelling of Waste/Cement Interactions", Murten, Switzerland, May 22-25, 2016.

Kulik D.A., Kosakowski G.
Coupling "rich" thermodynamic models (GEM) into reactive transport simulations. International Workshop "Predictive geosciences for georesources, exploration/ management and environmental issue", BRGM Orleans, October 25-26, 2016.

Kulik D.A., Lothenbach B., Miron G.D.
Thermodynamic dataset for modelling CASHNK aqueous-solid solution systems. 4th International Workshop on "Mechanisms and Modelling of Waste/Cement Interactions", Murten, Switzerland, May 22-25, 2016.

Kurganskaya I., Fischer C., Arvidson R.S., Luttge A., Churakov S.V.
A computational study of carbonate dissolution kinetics: Grand Canonical and Kinetic Monte Carlo approaches. Second European Mineralogical Conference, Rimini, Italy, September 11-15, 2016.

Kurganskaya I., Fischer C., Arvidson R.S., Luttge A., Churakov S.V.
Monte Carlo approaches to study mineral-water interface structure and reactivity. EMPG XV, ETH Zurich, Switzerland, June 5-8, 2016.

Labbez C., Churakov S.V., Pegado L., Nonat A.
A microscopic model for equilibria of phases and at interfaces in the SiO_2-CaO-H_2O system: Application of the reactive ensemble. 4th International Workshop on "Mechanisms and Modelling of Waste/Cement Interactions", Murten, Switzerland, May 22-25, 2016.

Leupin O.X., Van Loon L.R., Gimmi T.
Review of diffusion and retention experiments at the rock laboratory of Mont Terri: lessons learned and impact on safety. Mont Terri Technical Meeting TM-34, St. Ursanne, Switzerland, February 10-11, 2016.

Marques Fernandes M., Scheinost A.C., Baeyens B.
Sorption of trivalent actinides onto montmorillonite: Macroscopic, thermodynamic and structural evidence for ternary hydroxo and carbonato surface complexes on multiple sorption sites. 46ieme Journées des actinides, Alpes d'Huez, France, March 16-20, 2016.

Miron G.D., Wagner T., Kulik D.A., Heinrich C.A.
Internally consistent thermodynamic data for aqueous species in the Na-K-Al-Si-O-H-Cl system. Goldschmidt Conference, Yokohama, Japan, June 26 – July 1, 2016.

Miron G.D., Wagner T., Kulik D.A., Heinrich C.A.
Internally consistent thermodynamic data for hydrothermal mineral solubility equilibria in the system Ca-Mg-Na-K-Al-Si-O-H-C-Cl, ISSP17, Geneva, Switzerland, July 24-29, 2016.

Miron G.D., Wagner T., Kulik D.A., Lothenbach, B.
Internally consistent thermodynamic data for hydrothermal mineral solubility equilibria in the system Ca-Mg-Na-K-Al-Si-O-H-C-Cl. Second European Mineralogical Conference, Rimini, Italy, September 11-15, 2016.

Mon A., Kosakowski G., Samper J., Montenegro L.
Non-isothermal benchmark of interactions of concrete, bentonite and clay. Subsurface Environmental Simulation Benchmarking Workshop V. A Coruña, Spain, October 13-15, 2016.

Mueth J., Pfingsten W.
Management of irradiated graphite from decommissioning. ETSON International Workshop on "Treatment processes for the sustainable management of radioactive waste including innovative techniques", Vienna, July 4-6, 2016.

Nedyalkova L., Lothenbach B., Tits J., Wieland E., Mäder U.K.
Uptake of sulfur, selenium and iodine in AFm phases. 4th International Workshop on "Mechanisms and Modelling of Waste/Cement Interactions", Murten, Switzerland, May 22-25, 2016.

Poonoosamy J., Kosakowski G., Wanner C., Alt-Epping P., Aguila J., Samper J., Montenegro L., Mäder U., Van Loon L.R.
Benchmarking of reactive transport codes for a 2D setup with mineral dissolution/precipitation reactions and feedback on transport parameters, Subsurface Environmental Simulation Benchmarking Workshop V. A Coruña, Spain, October 13-15, 2016.

Prasianakis N.I.
Perspectives of reactive transport simulations at pore scale (Lattice Boltzmann + chemical processes). International Workshop "Predictive geosciences for georesources, exploration/management and environmental issue", BRGM Orleans, October 25-26, 2016.

Shafizadeh A., Gimmi T., Van Loon L.R., Churakov S.V., Kaestner A.P., Lehmann E., Mäder U.K.
Porosity changes during cement-clay interactions and their effect on transport. 4th International Workshop on "Mechanisms and Modelling of Waste/Cement Interactions", Murten, Switzerland, May 22-25, 2016.

Szidat S., Salazar G., Agrios K., Espic C., Uglietti C., Cvetković B. Z., Wieland E.
Advanced approaches of compound-specific radiocarbon analysis (CSRA) of environmental and radiolabeled materials. 9th International Conference on Nuclear and Radiochemistry (NRC9), Helsinki, Finland, August 29 - September 2, 2016.

Tits J., Rojo H., Scheinost A.C., Lothenbach B., Wieland E.
Assessing the role of AFm phases in the immobilization of selenium by cement under oxidizing and reducing conditions. 4th International Workshop on "Mechanisms and Modelling of Waste/Cement Interactions", Murten, Switzerland, May 22-25, 2016

Van Loon L.R., Fetz E., Hummel W., Plötze M.
Modified montmorillonite as tool for exploring diffusion pathways for anions and cations. 26th Goldschmidt Conference, Yokohama, Japan June 26 – July 1, 2016.

Wick S., Baeyens B., Marques Fernandes M., Voegelin A.
Thallium sorption to illite and its implication for Tl in soils. 14th Swiss Geoscience Meeting, Geneva, Switzerland, November 18-19, 2016.

Wieland E., Jakob A., Tits J., Lothenbach B., Kunz D.
Interaction of low molecular weight organic compounds with hardened cement paste. 4th International Workshop on "Mechanisms and Modelling of Waste/Cement Interactions", Murten, Switzerland, May 22-25, 2016.

Wigger C., Van Loon L.R.
Anion accessibility in low porosity argillaceous rocks – Canadian samples. NWMO Annual Geotechnical Meeting, June 7-8, 2016, Toronto, Canada

Wigger C., Van Loon L.R., Gimmi T.
Anion diffusion (^{36}Cl) in clay rocks with different cations (Na, Ca & Cs). 26th Goldschmidt Conference, Yokohama, Japan, June 26 – July 1, 2016.

Yapparova A., Gabellone T., Whitaker F., Kulik D.A., Matthai S.K.
Reactive transport modelling of hydrothermal dolomitisation using the CSMP++GEM coupled code, Dolomieu Conference on Carbonate Platforms and Dolomite, Selva di Val Gardena, Italy, October 3-7, 2016.

Yapparova A., Kulik D.A., Driesner T.
Reactive transport modelling of two-phase geothermal systems, SCCER-SoE Annual Conference 2016, Sion, Switzerland, September 13, 2016.

6.4 Invited talks

Churakov S.V.
Computer assisted modelling (*ab initio*, molecular dynamics and Monte Carlo). (Key Note Lecture). ISSP17, Geneva, Switzerland, July 24-29, 2016.

Hummel W.
Long-term behaviour of waste materials, ISSP17, Geneva, Switzerland, July 24-29, 2016.

Wieland E.
Mechanisms and modelling of radionuclide uptake by cementitious materials. MRS Fall Meeting, Boston, USA, November 28 - December 2, 2016.

6.5 Teaching

Churakov S.V.
Bachelor Course: Crystallography I + II, Institute for Geological Sciences, University of Bern.

Churakov S.V.
Bachelor Course: Crystall-optics, Institute for Geological Sciences, University of Bern.

Gimmi T.
Lecture and examinations 'Fluids in the Crust' (with other lecturers), Master Course in Environmental and Resource Geochemistry, University of Bern, Fall Semester 2016/17.

Hummel W., Plötze L.M.
Master Course: Landfilling, Contaminated Sites and Radioactive Waste Repositories, ETH Zürich.

Kulik D.A., Miron G.D.
Invited GEMS training, ERDW, ETH Zürich, 10-13 October 2016. Pre -ThermAc3 Workshop GEMS Training, HZDR, November 28-30, 2016.

Pfingsten W.
Modelling of Processes in Soils and Aquifers (701-1334-00L) Department for Environmental Sciences, ETH Zurich, Spring Semester 2016.

Prasser H.-M., Günther-Leopold I., Hummel W., Zuidema P. K., Hirschberg S.
Master Course: Nuclear Energy Systems, ETH Zürich.

Van Loon L.R.
Diffusion and sorption data bases for safety analyses based on a mechanistic understanding of key geo-chemical processes. 26th DoJo Seminar on Radiation Waste Disposal, Tokyo Institute of Technology, Tokyo, November 29, 2016.

6.6 Other

Baeyens B., Marques Fernandes M.
Examination PhD thesis of Vanessa dos Santos Guimarães, Faculdade de Ciências, Universidade do Porto, Porto, July 15, 2016.

Churakov S.V.
Examination PhD thesis of Maxime Pouvreau
Laboratoire Subatech, UMR 6457, Nante France, December 13, 2016.

Churakov S.V., Glaus M., Kosakowski G., Van Loon L.R.
Examination PhD thesis of Jenna Poonoosamy, University of Bern, Bern, February 18, 2016.

Curti E.
Literaturstudie zum Einfluss von Zement auf die Stabilität der Abfallmatrix (Glass, Brennstoff) im HAA/BE Tiefenlager. Aktennotiz AN 16-448, Nagra, Wettingen.

Curti E.
The chemical state of ^{79}Se in spent nuclear fuel. Scientific Highlights 2016, Nuclear Energy and Safety Division (NES), Paul Scherrer Institut.

Gimmi T.
Associate Editor of the Applied Geochemistry Journal.

Hummel W.
Co-organizer of the IUPAC 17th International Symposium on Solubility Phenomena and Related Equilibrium Processes (ISSP17), Geneva, Switzerland, July 24-29, 2016.

Kosakowski G.
Head of committee at the PhD defense of Carme Chaparro at University of Barcelona, March 4, 2016

Kulik D.A.
Associate editor of the Applied Geochemistry Journal.

Kulik D.A.
Prepared memorandum on cooperation between PSI NES LES and ETHZ IG GEG regarding development of numerical simulators for geochemical, thermo-dynamic, and reactive transport processes (Reaktoro and GEMS), signed in August 2016.

Meng S., Pfingsten W. (2016)
Multispecies random walk simulations in radial symmetry: model concept, benchmark, and application to HTO, ^{22}Na and ^{36}Cl diffusion in clay. Geological Society, London, Special Publications, SP443.15.

Van Loon L.R.
Examination PhD thesis of Yuta Fukatsu, Tokyo Institute of Technology, Tokyo, November 28, 2016.

Wieland E., Gschwend B.
Co-organizers of the 4th International Workshop on "Mechanisms and Modelling of Waste/Cement Interaction", Murten, Switzerland, May 22-25, 2016.

Wieland E.
Executive Guest Editor, Special issue on "Mechanisms and Modelling of Waste/Cement Interactions", Journal of Physics and Chemistry of the Earth.

Wieland E., Cvetković, B.Z. (2016)
Development of a compound-specific Carbon-14 AMS Technique for the Detection of Carbon-14 Labelled Organic Compounds. EU Project "CAST" report D 2.3.

6.7 PhD thesis defenses

Poonoosamy J.
Dissolution-precipitation in porous media: experiments and modelling, PhD defense, University of Bern, Bern, February 18, 2016.

Paul Scherrer Institut :: 5232 Villigen PSI :: Switzerland :: Tel. +41 56 310 21 11 :: Fax +41 56 310 21 99 :: www.psi.ch